The origin and development of the cellular endosperm and the aleurone layer in the seed of *Brassica napus* L. cv. Regent

by
Edwin P. Groot
M.Sc. candidate

A thesis
submitted in partial fulfillment
of the requirements for the degree of
Master of Science
in the Department of Botany
The University of Manitoba
August 1992

ISBN 0-315-77847-4

THE ORIGIN AND DEVELOPMENT OF THE CELLULAR ENDOSPERM AND THE ALEURONE LAYER IN THE SEED OF *Brassica napus* L. cv. REGENT

BY

EDWIN P. GROOT

A Thesis submitted to the Faculty of Graduate Studies of the University of Manitoba in partial fulfillment of the requirements for the degree of

MASTER OF SCIENCE

TABLE OF CONTENTS

LIST OF FIGURES

Page

ABBREVIATIONS

Ab	abaxial
ABA	abscisic acid
Ad	adaxial
AL	aleurone layer
aP	amyloplast
BB	basal body
CE	cellular endosperm
Ch	chalaza
Cot	cotyledon
cP	chloroplast
Cr	crista(e)
CV	central vacuole
CW	cell wall
DNA	deoxyribonucleic acid
DNPH	dinitrophenylhydrazine
DPP	days post pollination
dS	dictyosome
DV	dictyosome vacuole
eD	epidermis
ER	endoplasmic reticulum
eS	endosperm
ESW	embryo sac wall
F	funiculus
FNE	free nuclear endosperm
G_1	gap one phase of cell cycle
G_2	gap two phase of cell cycle
GA	gibberellic acid
Gr	granum
II	inner integument
LD	lipid droplet
mB	microbody
M	mitochondria
Mi	micropyle
N	nucleus
Nl	nucleolus
OI	outer integument
P	plastid
PB	protein body
pD	plasmodesma(ta)
PalL	palisade layer
PAS	periodic acid-Schiff's
phP	cell plate
PigL	pigment layer

RER	rough endoplasmic reticulum
RNA	ribonucleic acid
S	synthesis phase of cell cycle
S	suspensor
seD	subepidermis
SG	starch grain
T	testa
UeS	underlying endosperm
UV	ultra violet
V	vacuole

ACKNOWLEDGEMENTS

I wish to acknowledge those who participated in the fulfillment of my degree. Towards this end, I extend sincere thanks:

to Dr. Lawrence Van Caeseele, my supervisor and mentor, for his recognition, acceptance, encouragement, and timely manuscript suggestions;

to Drs. William Remphrey and Michael Sumner, my advisory committee members, for their ideas and wise counsel;

to the University of Manitoba Botany department, for technical facilities, and the opportunity to pursue my calling;

to the students and staff of the Botany department, for their friendly academic and social environment;

to Mr. Garry Burgess, EM technician extraordinaire, for his time and teaching;

to Mr. Richard Martin, the one who came after, for his admiration, amusing diversions, and energy;

to Mr. André Dufresne, M.Sc., the one who went before, for his friendship, experience, and initiative;

and thanks to all for sharing the best years of my life.

ABSTRACT

Light microscopy and microfluorometry reveals that the aleurone layer differentiates from the outermost layer of cellular endosperm. At approximately 14 days after pollination, free nuclear endosperm lines the interior of the embryo sac, which is appressed to the innermost layer of the inner integument. At 16 days, cellularization of the endosperm initially results in one to two cell layers and an innermost free nuclear layer. Further cellularization and cell division fills the majority of the embryo sac, and radial files of cells are observed at the periphery of the endosperm. Starch grains and lipid droplets accumulate in the endosperm cells in a gradient that increases from the inner layers towards the outer layers. By 18 days after pollination the cells of the inner integument begin to plasmolyze and collapse, and at 22 days, the incipient aleurone layer is distinguishable as the outermost cell layer of the endosperm. The underlying endosperm degenerates and collapses as the aleurone layer attains a dense accumulation of storage bodies. Rapid thickening of the aleurone cell walls commences at 30 days after pollination, and protein bodies appear within the aleurone cells by 34 days. In the mature seed, the inner integument is reduced to a layer of cell wall material and a layer of intact cells called the pigment layer. Only the aleurone layer remains of the endosperm. Small lipid droplets line the plasmalemma and the protein bodies of the aleurone cells. The plastids are round, lack starch and internal membranes, and contain electron-dense globules. Microfluorometry and computerized image analysis of isolated aleurone nuclei indicates a ploidy of three; therefore, the aleurone layer is derived from the triploid endosperm rather than from the diploid inner integument.

INTRODUCTION

The archetypical aleurone layer is found in caryopses of the Gramineae; e.g., barley and corn. In such species, it is derived from the outermost layer of the endosperm, and it surrounds the starchy endosperm and embryo. At maturity, the protoplasmic contents of these cuboidal cells are dominated by aleurone grains (a specialized type of protein body) in a matrix of tiny lipid droplets (Morrison *et al.* 1975). The cell walls are considerably thickened. During germination, this layer secretes enzymes that digest the starchy endosperm, releasing nutrients for the emerging seedling (Bewley and Black 1978, pages 183-188). An aleurone layer is reported to be in the seeds of several species of the Dicotyledons, because it resembles the structure of that in the Gramineae (Bergfeld and Schopfer 1986). The majority of such species belong to the Brassicaceae, an agronomically important family (Bouman 1975). Seeds of the Brassicaceae are exalbuminous, and as a result, the aleurone layer in *Sinapis arvensis* envelops the embryo without any intervening endosperm (Edwards 1968). In the mature seed of *Sinapis alba*, the aleurone cells are thick-walled and they contain protein bodies and lipid droplets (Bergfeld and Schopfer 1986). The function of the aleurone layer in the Brassicaceae has not been systematically studied, but in the albuminous seed of *Trigonella foenum-graecum* (Fabaceae), the aleurone layer secretes enzymes that digest the galactomannan reserves of the underlying endosperm, and the cotyledons of the seedling absorb the released sugars (Reid and Meier 1972, 1973). The aleurone layer of Brassicaceae seeds cannot have such a function because the seed is exalbuminous, and the seed coat, along with the aleurone layer, is discarded once the photosynthetic cotyledons emerge from the ground.

The histogenesis of the aleurone layer in the Gramineae has been well established through many investigations of endosperm development (Morrison *et al.* 1975). On the other hand, studies in the seed development of the Brassicaceae, dating from Guignard (1893), show no consensus on the origin of the aleurone layer. Guignard (1893) interpreted an endospermal origin of the aleurone layer in the Brassicaceae, but subsequent researchers have reported its origin from various seed tissues, ranging from the nucellus (Thompson 1933), to the endosperm (Edwards 1968), and to the inner integument (Bergfeld and Schopfer 1986). The latest and most detailed account of the development of the aleurone layer in the Brassicaceae is provided by Bergfeld and Schopfer (1986) in *Sinapis alba*, a species that is quite similar to *Brassica napus* in morphology and economic importance.

This study was undertaken to begin the examination of the thesis that the origin, structure, and fate of the aleurone layer in *Brassica napus* is sufficiently different from that in the Gramineae to question its classification as an aleurone layer. In addition, with the established use of DNA-specific fluorescent dyes and of computerized image analysis to measure ploidy, it was felt that the controversy over the origin of the aleurone layer in the Brassicaceae could be resolved.

LITERATURE REVIEW

Survey of Species

An aleurone layer, by definition, is the specialized, outermost cell layer or layers of the endosperm in certain seeds. It is rich in both protein and oil reserves, but contains little or no starch. It has been reported in isolated families of dicots and monocots studied to date. The largest number of anatomical studies of dicot seeds that note the presence of such a layer is in the Brassicaceae, or mustard family. The earliest such report is on mature *Capsella bursa-pastoris* seeds by Strasburger in 1884 (Bouman 1975). Guignard (1893) described an aleurone layer in many Brassicaceae species in his treatise of seed coat development, and named it "la couche à aleurone". In the Brassicaceae, other researchers have described an aleurone layer in *Capsella bursa-pastoris* (shepherd's purse) (Bouman 1975; Bergfeld and Schopfer 1986), *Brassica nigra* (black mustard) (Bouman 1975), *Brassica oleracea capitata* L. (cabbage) (Thompson 1933), *Sinapis alba* (white mustard) (Bergfeld and Schopfer 1986; Bouman 1975), *Sinapis arvensis* L. (charlock) (Edwards 1968), and *Lunaria annua* (moneywort) (Bouman 1975).

Reports of an aleurone layer in species of other dicot families are comparatively fewer. Marquez-Guzman and Laguna-Hernandez (1982) described an aleurone layer in *Turbina corymbosa* (Convolvulaceae) seeds, while other researchers have reported such a layer in *Cuscuta pedicellata* (dodder, Cuscutaceae) (Lyshede 1984), and in the tribe Trifolieae of the Fabaceae:*Trigonella foenum-graecum* L. (fenugreek), *Trifolium incarnatum* L. (crimson clover), and *Medicago sativa* L. (alfalfa) (Reid and Meier 1972). In spite of these few reports, there are probably more representatives yet to be

described. An analysis of the survey of oilseed structure by Vaughan (1970) reveals that about 35% of the seeds described possess an aleurone-like layer. For the purposes of the analysis, an aleurone layer is defined as a tissue between the testa and the embryo, having one to several specialized cell layers, containing oil droplets and aleurone grains (protein bodies), and having varying degrees of cell wall thickening. The remaining representatives in the survey either were endospermless, or had no specialized layers of endosperm tissue.

In the monocots, anatomical studies of the aleurone layer concentrate on the Gramineae (grass family). Some of the representative species having such a layer are *Avena fatua* (wild oats) (Raju and Walther 1988), *Avena sativa* (oats) (Bechtel and Pomeranz 1981), *Oryza sativa* (rice) (Bechtel and Pomeranz 1977), *Hordeum vulgare* (barley) (Jacobsen *et al.* 1971), *Triticum aestivum* (Wheat) (Morrison *et al.* 1975), *Tripsacum dactyloides* (eastern gama grass) (Bates *et al.* 1981), and *Zea mays* (corn) (Randolph 1936). The aleurone layer in the monocots is not restricted to the Gramineae. In the review of seed anatomy by Netolitzky (1926), other monocot families are reported to have aleurone layers. Some of the representatives include the Cyperaceae, Araceae, Bromeliaceae, Pontederiaceae, Juncaceae, and Musaceae families. About 50 families among the monocot and dicot families combined possess an aleurone-like layer.

Location

The dicot aleurone layer is typically found at the boundary between the embryo and the innermost layer of the testa (Edwards 1968; Bouman 1975; Marquez-Guzman and Laguna-Hernandez 1982). In those dicots that are

albuminous, the aleurone is the outermost layer of the endosperm and borders the innermost layer of the testa (Reid and Meier 1972). In the Gramineae, the aleurone is the outermost layer of the starchy endosperm, and it borders the nucellar remains and the testa (Esau 1977, page 436; Raju and Walther 1988; Bechtel and Pomeranz 1977). If one studies the mature seed only and not its development, the aleurone layer can be mistakenly termed as the innermost layer of the testa, because it is often attached to the seed coat when the testa is removed. For example, in the milling of wheat, the aleurone layer is removed attached to the bran (Brenchley 1909).

Function

The function of the Gramineae aleurone layer had been a matter of conjecture until the 1960s when molecular biological techniques enabled the elucidation of the action of hormones and enzyme synthesis during germination (Cutter 1978, pages 42-43). The Gramineae aleurone layer had been interpreted as having a protective function, preventing microbial invasion (Raju and Walther 1988), and Roberts (1964) discovered that dormancy in some rice species is due to high activity of certain oxidases in the aleurone layer. The most significant function of the Gramineae aleurone layer is the gibberellin-activated production of hydrolytic enzymes that digest the starchy endosperm during germination (Cutter 1978, pages 42-43). In addition, Raju and Walther (1988) recognize that the aleurone layer in wild oats is divided into three regions, which are named on the basis of location in the caryopsis: endosperm, groove, and embryo. Each region has a distinct morphological subtype of cells, and each region behaves differently with respect to water uptake regulation. Endosperm aleurone cell walls are

hygroscopic and may be a major route of water uptake during caryopsis imbibition. Embryo aleurone cell walls however, are rather hydrophobic, which might inhibit premature germination by delaying imbibition of the embryo tissue.

Direct studies of aleurone layer function in the Brassicaceae are lacking. Edwards (1968) points to the aleurone as the unit of dormancy in charlock, based on the various functions of the Gramineae aleurone layer. Surgical experiments had ruled-out the possibility of mechanical obstruction and water or oxygen unavailability, with respect to dormancy. Bergfeld and Schopfer (1986) reported that the mustard aleurone layer underwent marked changes during germination, but could only speculate on functions such as nutrient storage, germination assistance, and water uptake regulation.

In another dicot family, Reid and Meier (1972) showed that the aleurone layer of several species of the Fabaceae digest the galactomannan reserves of the underlying endosperm during germination, and that the embryo absorbs the released carbohydrates. This function is quite similar to that in the Gramineae, but the embryo in the Fabaceae is not responsible for the initiation of this action. The mobilization of galactomannan can also proceed without significant RNA synthesis in the aleurone layer (another difference to the Gramineae).

Origin

In the case of the Brassicaceae, the origin of the aleurone layer has been a matter of controversy. The groundbreaking treatise by Guignard (1893) established an endospermal origin of the aleurone layer but further

developmental studies attributed the aleurone layer to the: a)nucellus (Thompson 1933), b)inner integument (Bergfeld and Schopfer 1986), and c)endosperm (Bouman 1975; Edwards 1968). There have been no other developmental studies of the aleurone layer in other dicot families.

Bergfeld and Schopfer (1986) have contributed the most comprehensive study of the progenitor of the Brassicaceae aleurone layer to date, using *Sinapis alba* as a model. They reported that the seed coat of the mature ovule did not undergo any cell divisions and that the nucellus degenerated soon after fertilization. The free nuclear endosperm never cellularized, and it disappeared within about three weeks. During this period, the inner integument differentiated to the aleurone layer. The inner layer of the inner integument and the adjacent 5-7 cell layers lysed, and the outer layer of the inner integument and the adjacent 1-2 cell layers plasmolyzed and eventually collapsed to a thin layer of cell wall debris. The remaining 4-5 middle layers developed thick walls, and by 14 days post-pollination the outermost layer began to differentiate into the aleurone layer. The incipient aleurone layer had a denser protoplasm than the underlying cell layers. In another species, *Capsella bursa-pastoris*, Bergfeld and Schopfer (1986, unpublshed results) found that the aleurone layer differentiated from the inner epidermis of the inner integument.

Edwards (1968) studied seed development in a similar species, *Sinapis arvensis*, but concluded that the aleurone originated from the endosperm. Soon after fertilization, the free nuclear endosperm absorbed the adjacent nucellus, and during the heart stage embryo, it rapidly cellularized to a layer of cells that lined the interior of the embryo sac. Repeated divisions of the layer formed files of cells extending inwards. After cessation of

"meristematic" activity the outermost endosperm cells enlarged and acquired a dense granular cytoplasm, becoming recognizable as the aleurone layer. This mode of aleurone development is similar to that in the Gramineae.

In the developmental study of *Brassica oleraceae capitata* by Thompson (1933), the progenitor of the aleurone layer was indirectly attributed to the nucellus. Early in embryo development the free nuclear endosperm lined the interior of the embryo sac and cellularized throughout it, except at the chalazal end. The elongating embryo soon absorbed the endosperm, but the nucellus persisted, in part, leaving a layer or two to surround the embryo. The nucellar remnant is not labelled as the aleurone layer in his diagrams, but its location within the seed implied its identity as the aleurone layer.

There are no reports that are contrary to the belief that the Gramineae aleurone is endospermal. Brenchley (1909) noted that the nucellar outer epidermis of wheat did proliferate and persist after absorption of the remainder of the nucellus, but their contents emptied and the cells collapsed as the aleurone layer differentiated from the endosperm. Evers (1970) studied the development of wheat endosperm in detail. After cellularization of the free nuclear endosperm, the outermost endosperm layer repeatedly divided periclinally to form radial columns of endosperm cells. Some anticlinal divisions also occurred. Around 16 days post anthesis the cells of the outermost layer of the endosperm differentiated into the aleurone layer by developing thick cells walls, large nuclei, and dense granular contents. The remaining endosperm cells differentiated to the starchy endosperm through the process of cell enlargement and starch accumulation.

Structure Of The Dicot Aleurone Layer

Mature seed

The aleurone cells of mature dicot seeds have been described in white mustard (Bergfeld and Schopfer 1986), *Turbina corymbosa* (Laguna-Hernandez *et al.* 1984), dodder (Lyshede 1984), and in *Trigonella foenum-graecum* L. (Reid and Meier 1972). Mustard and *Turbina* are exalbuminous seeds; therefore, the aleurone layer is separated from the embryo only by cell wall debris. The other two species have several to many cell layers of endosperm tissue which separate the aleurone layer from the embryo. All seeds have an aleurone layer that is one cell layer thick, except that in *Turbina*, which may vary from one to four cell layers. The cells are isodiametric but, in *Turbina*, deposits between the plasmalemma and the cell wall give the protoplasts an irregular shape. The aleurone cells of *Turbina* are interconnected by plasmodesmata. In all of the species the protoplasts are dominated by lipid droplets and protein bodies. There are no starch grains, except for a few in *Turbina*.

The protein bodies vary depending on the species. In *Turbina* they range in size from 0.3 μm spheres to 2.5 μm irregular masses. The protein matrix is granular or fibrillar, and some protein bodies contain vesicles, and electron-dense structures similar to globoid inclusions. There are many aleurone grains (protein bodies) in *Trigonella*, but they seldom contain electron-dense globoid inclusions. The lipid droplets in *Trigonella* are found both along the plasmalemma and among the protein bodies. Other organelles include many free ribosomes, mitochondria, and a large nucleus in both *Turbina* and *Trigonella*. In addition, microbodies were found in *Trigonella*. The nuclei in *Turbina* consist of a large and compact nucleolus, and granular,

fibrillar, and randomly dispersed chromatin. Laguna-Hernandez *et al.* (1984) report the lack of ER and dictyosomes in *Turbina*, but Reid and Meier (1972) report the presence of a few dictyosomes and sparse ER in *Trigonella*. The mitochondria in *Turbina* have few cristae, and the mitochondria of *Trigonella* contain darkly-staining globules. The few plastids found in *Trigonella* have osmiophilic globules.

Developing seed

The development of dicot aleurone tissue has been discussed in detail only for white mustard (Bergfeld and Schopfer 1986). The cells of the incipient aleurone layer had relatively thin walls and dense protoplasmic contents. As the cell walls thickened, the chloroplasts with starch grains became amyloplasts, and then small proplastids without thylakoid membranes. The ongoing, protein body and oleosome accumulation continued and eventually filled the cells. The several layers of thick walled cells beneath the aleurone layer lost their storage bodies and became compressed by the expanding embryo.

The mode of protein and lipid accumulation in both the aleurone cells and the embryo storage cells in mustard is reported to be similar (Bergfeld and Schopfer 1986), but has only been discussed for the mesophyll cotyledon cells of the embryo (Rest and Vaughan 1972; Bergfeld *et al.* 1978, 1980). In those cells, protein bodies began as vacuoles lined with osmiophilic material (Bergfeld *et al.* 1980). As the deposits enlarged and merged to form a continuous layer, crystalloid particles were visible at their inner surface. Dictyosome vesicles may contribute to the filling process because they contained a structurally indistinguishable material from that of the vacuoles.

The vacuoles eventually became filled with the storage protein, and inclusions were present. Oil bodies showed no evidence of being ER-derived (Rest and Vaughan 1972; Bergfeld *et al.* 1978). They arose from the cytoplasm alongside plastids, and had no distinct border (Bergfeld *et al.* 1978). As their number increased, the RER proliferated and RER cisternae became intimately associated with the lipid body periphery. The lipid bodies acquired a thin osmiophilic coat, detached from the ER, and migrated to the periphery of the cell. In spite of their tight packing, they did not fuse. Rest and Vaughan (1972) noted that they gradually became electron-transparent towards maturity.

Germinating seed

The aleurone cells of dicots resume activity during germination and are considered viable because the vital dye, tetrazolium chloride stains them red (Bergfeld and Schopfer 1986; and Reid and Meier 1972). Bergfeld and Schopfer (1986) noted the parallel in germination behavior between the aleurone cells and the cotyledon storage cells of white mustard. After 12 h of imbibition, when germination commenced, storage protein depleted and their vacuoles coalesced into a large central vacuole 12 h later. Concurrently, the oleosomes disappeared. The cytoplasm appeared active and contained a nucleus, mitochondria, plastids, microbodies, and ER.

The aleurone cells of *Trigonella* exhibited anatomical evidence of secretion during germination (Reid and Meier 1972). After 12 h of germination, membrane-associated polysomes proliferated. As the number of spherosomes decreased, the mitochondria proliferated, and starch accumulated in the plastids. The plasmalemma became indented. The endosperm galactomannan began to break down after 24 h, and this was

paralleled by proliferation of RER, exceptional indentation of the plasmalemma, and corrosion of the cell walls. As galactomannan digestion continued, autophagy of the aleurone grains resulted in a large central vacuole. The RER distended to form large sacs and the plasmalemma profile became smooth once again. By 48 h after germination began, galactomannan breakdown was complete.

Structure Of The Monocot Aleurone Layer

Mature seed

In the mature caryopsis of the Gramineae, the aleurone is a single cell layer that encloses the endosperm tissue; however, in barley, Jacobsen *et al* (1971) note that the aleurone layer is usually 3 cell layers thick. Others have noted that some areas of the aleurone are more than one cell layer (Bechtel and Pomeranz 1977, 1981; Ogawa *et al.* 1979; Morrison *et al.* 1975). In rice, Oparka and Gates (1981) state that the aleurone may be up to 5 cell layers in the region of the vascular bundle. The aleurone cells are viable in the mature seed, and their nuclei are intact (Brenchley 1909). In contrast, the nuclei of the starchy endosperm are disorganized, reticulate, and stain lightly. They are assumed to be inviable at maturity.

The aleurone layer of mature caryopses has been described in many species of the Gramineae; e.g., wheat (Brenchley 1909; Morrison *et al.* 1975), oats (Bechtel and Pomeranz 1981; Peterson *et al.* 1985), barley (Jacobsen *et al.* 1971), and rice (Bechtel and Pomeranz 1977). The aleurone cells are cuboidal, and the cell walls are thickened and sometimes bilayered (Morrison *et al.* 1975). Bechtel and Pomeranz (1977) found many plasmodesmata interconnecting rice aleurone cells.

The aleurone cytoplasm contains a large central nucleus, and densely packed aleurone grains (the protein body of the Gramineae aleurone layer) surrounded by lipid droplets. Morphometric analysis of wheat aleurone cytoplasm yield total organelle volume fractions of 50-60% for aleurone grains, 30% for lipid droplets, 5% for mitochondria, 1.5% for leucoplasts, and 0.5% for microbodies (Buckhout *et al.* 1981). The aleurone grains are bound by a unit membrane, but not the lipid droplets (Jacobsen *et al.* 1971). In rice, the lipid droplets sometimes fuse into large masses, indicating the lack of a unit membrane. The remaining organelles are free ribosomes, mitochondria, plastids without starch, and some RER. In addition, microbodies were found in rice. In oat aleurone cells Bechtel and Pomeranz (1981) found plastids with osmiophilic globules and phytoferritin; the mitochondria contained only osmiophilic globules. The plastids of rice aleurone had osmiophilic globules and invaginations of cytoplasm, but no grana. In wheat, the mitochondria have indistinct cristae, and the aleurone grains consist of a proteinaceous matrix with both type I and type II inclusions (Morrison *et al.* 1975). In other Gramineae species the inclusions are termed phytin globoids and protein-carbohydrate bodies (protein crystalloids) respectively (Jacobsen *et al.* 1971; Peterson *et al.* 1985). The number of inclusions per aleurone grain varies among species. In barley, there are one to several globoids and about one protein-carbohydrate body per aleurone grain. The globoids contain phytin which causes them to be electron-opaque in glutaraldehyde-OsO_4 - fixed tissue, and they usually shatter during sectioning (Jacobsen *et al.* 1971). The crystalloids stain for both protein and carbohydrate, and they appear granular, electron-dense, and they do not shatter during sectioning. In fresh sections stained with toluidine blue at pH 5.0, metachromasia causes the globoids to stain red and the protein-carbohydrate bodies to stain green. In oat aleurone

grains, the protein-carbohydrate bodies are electron-dense and and in turn contain an electron-lucent inclusion with electron-dense structures and a transparent area (Bechtel and Pomeranz 1981).

Developing seed

There are comprehensive studies of Gramineae aleurone cell development in both wheat (Morrison *et al.* 1975) and oats (Peterson *et al.* 1985). During the proliferation of endosperm tissue, the aleurone cells were localized as the cells of the outermost layer of the endosperm that were dividing periclinally. At this stage, the cuboidal aleurone cells had thin cell walls, large nuclei, and several vacuoles that contained the beginnings of phytin globoid inclusions. In wheat, plasmodesmata interconnected incipient aleurone cells. There were many free ribosomes, but sparse ER membranes. Mitochondria, lipid droplets, and plastids with starch grains were also present. Vacuoles became smaller and more numerous as phytin globoid inclusions enlarged, and amyloplasts and some dictyosomes were evident. Peterson *et al.* (1985) noted the presence of internal membranes in some of the vacuoles, and Morrison *et al.* (1975) noted an intense autofluorescence in the cell walls of wheat. The fluorescence was due to ferulic acid-carbohydrate complexes in the cell wall, which was thought to prevent cell wall autodigestion during the enzyme secretion phase of germination. After this stage, Morrison *et al.* (1975) noted an abundance of ER and mitochondria in wheat. In oats, phytin globoid accumulation was nearly complete. Lipid droplets increased in number, but no ER connections to them were evident (Peterson *et al.* 1985). The next stage was a rapid thickening of the cell walls. In wheat and barley the cell wall was bilayered with respect to toluidine blue

staining, but it was still uniformly autofluorescent (Morrison *et al.* 1975). The aleurone grains (protein bodies) became filled with protein-carbohydrate bodies and a proteinaceous matrix. As desiccation commenced, lipid droplets began to line the plasmalemma and the aleurone grains. Starch grains and also dictyosomes gradually disappeared; however, Peterson *et al.* (1985) noted that RER and ribosomes were still present towards maturity. In wheat, several phytin globoid inclusions were visible in each aleurone grain, and in barley there was usually one globoid and one or more protein-carbohydrate inclusions present. As the aleurone cells approached a mature state, the lipid droplets completely surrounded the aleurone grains, and protein deposition in the aleurone grains ceased.

Germinating seed

The major function of the Gramineae aleurone is well known. It is the secretion of hydrolases that release nutrients from the endosperm for the emerging seedling. The hydrolases are synthesized de novo in response to GA (gibberellic acid) secreted by the embryo (Cutter 1978, pages 42-43). A comprehensive study of the changes in barley aleurone layer ultrastructure in response to GA_3 was conducted by Jones (1969a, 1969b) and by Jones and Price (1970). In the lag phase (2-10 h after GA application) the aleurone grains lost their sphericity and swelled, displacing other organelles, but the spherosomes remained associated with them. The amount of RER increased and stacked ER membranes appeared, but there were no changes in the mitochondria, dictyosomes, microbodies, and leucoplasts. Endoplasmic reticulum continued to proliferate from 10-22 h, the enzyme synthesis phase. The globoid inclusions of the aleurone grains began to degenerate, and the secondary cell

wall lost its fibrillar appearance and became digested. The ER cisternae became distended and later, vesicles proliferated from both the ER and the dictyosomes. Concomitantly, the aleurone grains decreased in size and the number of spherosomes decreased, but the number of plastids and microbodies increased in number. Near the end of the synthesis phase the amount of ER and its vesicles decreased. The aleurone grains became vacuolate and the vacuoles began to enlarge. In the final phase (24-36 h), the phase of ribonuclease release, spherosomes, dictyosomes, microbodies, and mitochondria were still present. Microbodies were considerably reduced in number, but the number of mitochondria were not affected. RER stacks were associated with the nuclear membrane, and there was a renewed proliferation of dictyosome vesicles. The aleurone grain vacuoles coalesced into one large central vacuole that contained many membrane-like fragments.

Other researchers have found similar ultrastructural changes occurring in barley aleurone cells during germination (Obata 1979). After 8 h of GA treatment, lipid droplets that had surrounded the aleurone grains dispersed into the cytoplasm. Free ribosomes and some RER were observed. Enzyme secretion began after 24 h of GA treatment. Stacks of RER often surrounded the perimeter of amoeboid-shaped nuclei and mitochondria, and the RER stacks also stretched towards the plasmalemma. Stacked ER was also found in wheat that had been treated with GA_3 for 6-10 h (Buckhout *et al.* 1981); however, ER stacks were associated only with nuclei and with aleurone grain-lipid body complexes. After 48 h, synthesis of enzymes had abated, but secretion continued. A large central vacuole was present, and the RER stacks became smaller and fewer. No evidence of ER-derived secretory vesicles was found (Obata 1979; Jones 1969b).

Ploidy determination

Ploidy level is the number of haploid sets of chromosomes in a genome. In this study it is used to determine whether the aleurone layer in canola seed is a triploid or a diploid tissue. Ploidy can be measured directly by counting condensed chromosomes, or indirectly by photometry of stained nuclei. Chromosome counting is limited to regions of active cell division, such as meiotic cells in flower buds and mitotic cells in root tips (Jones and Luchsinger 1986, pages 180-182). Photometry is the commonly used method to determine ploidy because it can be applied to sections and squashes of all tissues of the plant. In quantitative measurements, c is the amount of DNA per haploid set of chromosomes, and it varies, depending on phases of the cell cycle (Gahan 1984, pages 22-23). In diploid (2n) tissue, anaphase, telophase, and early interphase (G_1) nuclei have 2c DNA, prophase, metaphase, and late interphase (G_2) nuclei have 4c DNA, and interphase nuclei during the S phase will have between 2c and 4c DNA. A histogram of c in such a population of nuclei results in two peaks: one at 2c, and the other at 4c. The ploidy of the tissue is the lowest c value of the pair of peaks, or 2n.

Determination of ploidy by photometry makes use of DNA-specific stains. The Feulgen reaction has been used to determine seasonal variations in DNA content of balsam fir cambia (Mellerowicz *et al.* 1989), and to assess polyploidy in the cotyledons of developing canola embryos (Silcock *et al.* 1990). The fluorescent stain Hoechst dye #33258 enabled the microfluorometric determination of ploidy in Mitchell petunia protoplasts (Kamo and Griesbach 1989), and Hoechst dye #33342 was used to determine ploidy of isolated carrot nuclei by flow cytometry (Coutos-Thevenot *et al.*

1990). The use of fluorescent stains usually results in a higher signal to noise ratio than with absorptive (e.g., Feulgen reaction) stains (Gahan 1984, page 155). The Feulgen reaction takes longer than fluorescent staining and it requires a carefully-controlled DNA hydrolysis step. The high lipid content of canola seeds absorbs Schiff's reagent, interfering with the Feulgen reaction (Silcock *et al.* 1990). The Hoechst dyes do not bind to either single-stranded DNA or to RNA, so that specific hydrolyzations of these need not be undertaken as controls (Arndt-Jovin and Jovin 1989, page 427). The tissue to be stained with Hoechst is fixed in acetic acid-ethanol, rather than in an aldehyde, because aldehyde fixation could impede dye binding (Huebner, E personal communication).

Several photometric methods exist to measure the intensity of stained nuclei. For absolute measurements, an internal standard, such as chicken erythrocyte nuclei is needed for calibration (Berlyn and Miksche 1976, page 262). Relative measurements can use nuclei of known ploidy as an external standard for the basis of ploidy comparisons. Microspectrophotometry, the oldest method of measurement, detects absorption at a wavelength by fitting a monochromator and a photomultiplier tube to a light microscope (Gahan 1984, page 139). The absorbance of several small fields of view, or "plugs", delimited by a measuring diaphragm of a nucleus is averaged, and the volume of the nucleus is estimated to provide a measure of the staining of the nuclei. This technique suffers from distributional error, which can be overcome in a more sophisticated scanning integrating system (Gahan 1984, page 142). The use of fluorescent stains is an advantage because microfluorometry does not suffer from distributional error; therefore, the image does not need to be scanned, and a single measurement, enclosing the

nucleus by a measuring diaphragm, can be used (Gahan 1984, page 155). This advantage has also enabled the rapid ploidy determination of a large population of nuclei by fluorescence flow cytometry (Arndt-Jovin and Jovin 1989, page 426).

Nuclei or other objects of an arbitrary shape cannot be measured by a microdensitometer, but they can be measured by computerized image analysis. A computerized image analysis system stores digitized data of a specimen, which can be subsequently operated on by numerical methods (Bradbury 1989, page 213). These systems can either be dedicated machines, or a personal computer with additional hardware. Digitized data is obtained by either tracing micrographs on a digitizing tablet connected to a computer, or from a frame grabber, which digitizes an image from a video camera attached to the microscope. A digitized image is an array of numbers, each representing the optical density at a particular x-y co-ordinate in the array. The digitized image can be stored on magnetic media, processed numerically, or displayed on a video monitor by converting each number in the array to a pixel of corresponding brightness or colour. For example, grey levels are commonly represented by a number ranging from 0, corresponding to black, to 255, corresponding to white (Bradbury 1989, page 213). The resolution of the digitized image is hardware dependent and subject to continuous improvement. On a Leica Quantimet 500 it is 752 X 512 pixels (Leica 1992, page 7). Computerized image analysis systems have an immense number of functions to process an image for analysis and their applications are explained in the accompanying technical manuals. Those functions relevant to image analysis are subtraction of background images, elimination of irrelevant detail, delimiting the nuclear outlines, report of total brightness/absorbance

of each nucleus, and calculation of ploidy. The major advantages of a computerized image analysis system is the rapidity of analysis from automation of tasks, and the flexibility to accommodate various types of measurements and analyses. The field of image analysis advances rapidly, so detailed descriptions of hardware and software capabilities is not informative.

MATERIALS AND METHODS

Plant material

Brassica napus L. cv. Regent was seeded in 20 cm pots and placed in a Conviron model E15 chamber (Controlled Environments Ltd., Winnipeg, Manitoba) with an 8 h photoperiod. Day and night temperatures were 19°C and 15°C respectively. When a rosette of 7 leaves had formed (approximately 5 weeks after seeding), they were transferred to a long day chamber with an 18 h photoperiod and day and night temperatures of 22° and 17° respectively. Bolting commenced approximately 7 weeks after seeding. Flowers on the main axis that had anthesed during the morning were marked and pollinated by hand.

Specimen preparation

Pods were harvested 5 to 40 days post pollination (DPP) at intervals ranging from one to 2 days. Seeds were removed from the pod for fixation. Developing seeds from 5-9 DPP were fixed whole while 10-22 DPP seeds were slit with a razor blade to enhance infiltration and 24-40 DPP seeds were slit with a razor blade and de-embryonated before fixation.

Fixation and infiltration

Harvested seeds were fixed in 3% glutaraldehyde in 0.75 M potassium phosphate buffer, pH 6.8 for 6 h at room temperature, then overnight at 4°. They were washed 4 times for a total of 1 h in 0.75 M potassium phosphate buffer, pH 6.8, and postfixed in 2% OsO4 in 0.75 M potassium phosphate

buffer, pH 6.8 for 4 h at room temperature. After washing 4 times for a total of 1 h in 0.75 M potassium phosphate buffer, pH 6.8, the seeds were dehydrated in an ethanol series: 15 min each in 10, 20, 30, 50, 70, 85, 95% ethanol, and 3 times in absolute ethanol. Infiltration was begun with 100% propylene oxide for 1 h, propylene oxide:Spurr's resin (2:1) for 1 h, propylene oxide:Spurr's resin (1:1) for 1 h, and propylene oxide:Spurr's resin (1:2) overnight on a rotator. Infiltration was continued for 4 more days by rotating in a fresh change of 100% Spurr's resin each day. The seeds were then poured in 44 mm aluminum weighing dishes (Fisher Scientific), covered with fresh Spurr's resin and polymerized at 70° overnight.

A methacrylate, Historesin (LKB, Bromma, Sweden), was used as an embedding medium for fluorescent staining of sections. Harvested seeds were fixed in 2.5% glutaraldehyde in 0.025 M potassium phosphate buffer, pH 6.8 for 16 h at room temperature. After washing 6 times for a total of 3 h in 0.025 M potassium phosphate buffer, pH 6.8, they were dehydrated in an aqueous Historesin series of at least 3 h each in 5, 10, 20, 40, 60, 80, 90, 95, and 100% Historesin at 4° in the dark (adapted from Ashford *et al.* 1972). They were infiltrated in 100% Historesin at 4° in the dark for at least one week. The seeds were then placed in 44 mm aluminum weighing dishes (Fisher Scientific) and covered with Historesin embedding medium. Another weigh dish was nested on the embedding medium to exclude oxygen, and the medium was left to polymerize for 3 h at room temperature.

Sectioning

Survey sections were cut from one to two specimens of each harvest date to determine the representative developmental stages. From each

representative stage, five to ten specimens were sectioned, and the best one to two specimens were retrimmed and sectioned for both light microscopy and electron microscopy.

Epoxy sections for light microscopy were cut 0.5 μm with glass knives using a Sorvall JB-4 microtome. Sections were transferred to a drop of water on a chrome gelatin-coated slide and dried under xylene vapour on a slide warmer at 65°. Gold to silver sections for electron microscopy were cut with a diamond knife using a Reichert-Jung Ultracut ultramicrotome. They were transferred to copper grids. Historesin sections were cut 2 μm with dry glass knives using a Sorvall JB-4 microtome. Sections were transferred to a drop of water on a chrome gelatin-coated slide and dried on a slide warmer at 65°.

Staining

Crystal violet

Crystal violet stain was made by dissolving 2 g crystal violet in 20 mL ethanol and mixing with 0.8 g ammonium oxalate dissolved in 80 mL distilled water (Gerhardt *et al.* 1981, page 24). The stain was filtered twice through Whatman #1 filter paper. The stain was dispensed onto slide-mounted Spurr's resin sections through a 0.45 μm syringe filter, stained 10-30 sec on a slide warmer at 65°, and rinsed under running distilled water to remove excess stain. Slides were dried with a stream of filtered air, and mounted in 70% sucrose.

Sudan black B

Lipid droplets were localized with saturated Sudan black B used according to Bronner (1975) with modifications. A saturated solution (about 0.3%) of Sudan black B in 70% ethanol was warmed at 37° overnight and filtered twice through Whatman #1 filter paper just prior to use. Slides with Spurr's resin sections were preincubated in 70% ethanol for 2 min, and stained in Sudan black B at 55° for 1 h. They were rinsed 1 min in 70% ethanol, and differentiated 15 min in 80% ethanol at room temperature. Slides were rinsed briefly in running distilled water, blown dry with a stream of filtered air, and mounted in 70% sucrose.

Coomassie brilliant blue

Proteins were stained with Coomassie brilliant blue by a method modified from Fisher (1968). A 0.25% solution of Coomassie brilliant blue in 7% aqueous acetic acid was filtered twice though Whatman #1 filter paper prior to use. Spurr's resin sections were stained at 55° for 50 min, rinsed 1 min in 7% acetic acid, then rinsed briefly in running, distilled water. The slides were blown dry with a stream of filtered air and mounted in 5% acetic acid in glycerol.

Periodic acid Schiff's reagent (PAS)

Sections were stained for insoluble polysaccharides according to O'Brien and McCully (1981, page 6.90). The slides with Spurr's resin sections were blocked for endogenous aldehyde by incubating in saturated dinitrophenlyhydrazine (DNPH) for 30 min at room temperature and rinsed

10 min in distilled water. After incubation for 30 min in periodic acid and rinsing 10 min in distilled water they were stained for 20 min in Schiff's reagent (Fisher Scientific). The slides were rinsed 30 min in distilled running water, blown dry with a stream of filtered air, and mounted in 70% sucrose.

Acridine orange

Nuclei stained with acridine orange fluoresce green under blue excitation (O'Brien and McCully 1981, page 2.29). A 0.1% stock solution is stored in the dark. Historesin sections were stained one min with freshly diluted 0.001% acridine orange. The slides were rinsed 1 min in running distilled water, blown dry with a stream of filtered air, and mounted in glycerol.

Hoechst Dye #33342

Hoechst dye #33342 was a gift from Dr. E. Huebner. A 100 µg/mL stock was stored at 4° in the dark. Historesin sections were stained in the dark for 4 min in freshly diluted 10 µg/mL Hoechst dye #33342 in distilled water, and rinsed one min in running distilled water. The slides were dried with a stream of filtered air and mounted in glycerol. Nuclei fluoresce blue white under UV excitation. Condensed chromatin fluoresces especially bright.

Uranyl acetate-lead citrate

Ultrathin sections were stained for general contrast according to Reynolds (1963), with modifications. Saturated uranyl acetate in 50% methanol was dispensed into wells through a 0.2 µm syringe filter. Sections

on copper grids were floated section side down on the stain for 30 min. The grids were dipped briefly in 50% methanol and rinsed 30 min in 50% methanol. The grids were dipped briefly in distilled, ultrafiltered water and rinsed 30 min in distilled, ultrafiltered water. A petri dish was lined with Parafilm and a small dish of wetted KOH was placed inside to absorb carbon dioxide. After 5 min, large drops of lead citrate were dispensed through a 0.2 μm syringe filter onto the Parafilm. Grids were floated section side down on the drops for 10 min. The grids were dipped for 10 sec in degassed water, blotted with filter paper, and laid on a silicone rubber mat to dry overnight.

Microscopy

Thin sections were photographed using a Nikon Optiphot compound microscope. For fluorescence microscopy, the same instrument was fitted with an episcopic attachment containing a 50 W high pressure mercury lamp. For observation under UV excitation, a filter transmitting 330-380 nm, a dichroic mirror DM 400, and a barrier filter transmitting above 420 nm were used. Grids of ultrathin sections were examined in a Hitachi 7000 electron microscope.

Ploidy Determination

Tissue Preparation

Diploid tissue (embryo cotyledon) and aleurone tissue were obtained from mature seeds (approx. 50 DPP). The mature seeds were soaked 5 min in 0.7 M sucrose to soften the seeds. The funicular end and the end opposite the funiculus were cut off, leaving a disc. The disc was cut in half along the

diameter, and the embryo was removed from the seed coat. Both tissues were soaked for 5 min in 0.7 M sucrose. The aleurone layer was peeled from the seed coat using fine forceps. It is a colourless, translucent tissue and contrasts sharply from the red-brown palisade layer. The embryo cotyledon was sliced thinly with a razor blade. The tissues were rinsed 3 times for a total of 5 min in 0.2 M sodium phosphate buffer, pH 7.2, and rinsed 3 times for a total of 5 min in fixative (ethanol:acetic acid, 3:1). Using a 1 cm piece of razor blade, the tissue was minced for 5-10 min in fixative on a depression slide, keeping the tissue irrigated with the fixative. The pulp was washed, using fixative, into a vial, and fixed for 30 min.

Triploid tissue (free nuclear endosperm) was obtained from 12 DPP seeds. Seeds were slit with a fresh razor blade, and the free nuclear endosperm was withdrawn with a micropipettor (Eppendorf 10-100 μL). After a sufficient amount (25 μL) was collected, the free nuclear endosperm was mixed 1:1 with fixative, and fixed for 30 min.

The fixed samples were applied to a cleaned slide a few drops at a time, letting the sample almost dry between applications. The material was fixed on the slide by heating for 2 min on a slide warmer set at 65°. The material was rehydrated for 1 min in 0.2M $NaPO_4$ buffer, pH 7.2, and stained 4 min in the dark in freshly diluted 1 μg/mL Hoechst dye #33342 in 0.2 M $NaPO_4$ buffer, pH 7.2. The slide was washed 2 times for a total of 1 min in 0.2 M $NaPO_4$ buffer, pH 7.2. The slide was dried with a stream of filtered air and the specimen was mounted in glycerol.

Image Analysis

A computerized image analysis system was used to determine the nuclear DNA content. The system consisted of an epifluorescence microscope (Zeiss Photomicroscope I), a high resolution video camera (Dage SIT), a personal computer (Compaq 386) with video acquisition hardware, and the appropriate software to acquire and process video images (Image I, Universal Imaging Corp., Westchester, PA). Under UV excitation, the stained nuclei fluoresced blue-white. The image of each nucleus of interest was acquired and digitized by the computer. Abnormally large nuclei found in the free nuclear endosperm were ignored because they were assumed to be endopolyploid. Each image was corrected for camera background and for specimen mount background. The nuclei of background-corrected images were circumscribed and measured for total fluorescence using National Institute of Health (NIH) Image version 1.43 image analysis software. A t-test of the intensities of known and unknown ploidies, using Data Desk statistical software, categorized the ploidy level of the aleurone cells.

RESULTS

Free nuclear endosperm stage

Up to 14 DPP (days post pollination) the endosperm of a developing canola seed is free nuclear (Fig. 1). The testa consists of the outer integument and the inner integument. The outer integument consists of an epidermis, two cell layers of subepidermis, and an inner layer of palisade cells (Fig. 3). The cells of the palisade layer have thickened radial and inner periclinal walls, and they resemble sclereids. The inner integument consists of an outermost cell layer of relatively large cells that are rectangular in section. The remainder consists of 4 to 7 layers of parenchymatous cells that are ovoid in section. The innermost cell layer is designated the pigment layer because it later accumulates osmiophilic and intensely staining deposits.

The nucellus degenerates shortly after fertilization, so that the embryo sac wall appresses to the inner integument (Fig. 5). Within the embryo sac are an embryo (not shown), free nuclear endosperm, and a large central vacuole (Fig. 1). The embryo at 14 DPP is past the torpedo stage and it is rapidly elongating. The free nuclear endosperm is confined by the central vacuole to a thin layer that lines the embryo sac and fills the chalazal cavity. Its vacuolate symplasm contains large free nuclei that have one or two prominent nucleoli (Fig. 5). Each nucleus is surrounded by chloroplasts aligned tangentially to the testa. The chloroplasts are fusiform in section and appear lens-shaped in fresh specimens. The embryo sac wall appears to have pulled away from the inner integument at some places. The chloroplasts of the testa contain large, multiple starch grains that are smaller in the palisade layer (Fig. 4). Staining

by Sudan black B reveals that lipid droplets are present only in the palisade layer (Fig. 2).

Electron microscopy of the same specimen reveals that the free nuclei are round with a wavy outline, and contain a uniformly granular nucleoplasm (Fig. 6). The chloroplasts range from biconvex to plano-convex in section, and numerous grana separate strands of regularly spaced stroma that contain electron-opaque globules. Mitochondria are abundant and contain saccular cristae appressed to one another (Fig. 7). The profile of most mitochondria is round, but some mitochondria found alongside the embryo sac wall are elongate (Fig. 8). The vacuoles are electron-lucent, and some contain bits of electron-opaque material at the periphery (Fig. 6). Dictyosomes are present, but profiles of RER are short, singular, and infrequent. Free ribosomes are distributed throughout the cytoplasm. There are closely spaced peg-like projections of the embryo sac wall, but there is no apparent initiation of endosperm cell walls (Fig. 9).

The cells of the inner integument appear slightly plasmolyzed, which emphasizes plasmalemma connections to the cell wall (Fig. 10). The nucleus contains several small inclusions of the same density and texture as the nucleolus. The amyloplasts contain few endomembranes. The cells also contain mitochondria, microbodies, ER, and free ribosomes.

Cellularized endosperm

Cellularization of the endosperm occurs at approximately 16 DPP. The process of endosperm cellularization proceeds rapidly, and after completion, the cells fill the embryo sac except for a central region (Fig. 11). Cellularization

initially results in a peripheral cellular layer with convex inner periclinal cell walls, and an inner layer not yet completely enclosed by walls (Fig. 12). The presence of an periclinally oriented phragmoplast in the inner layer (Fig. 13 and 24a), and of radial files of endosperm cells after further cellularization (Fig. 14), suggests that endosperm tissue proliferates by mitosis.

The newly formed cells exhibit a different organellar configuration than that of the free nuclear tissue. A central, astroid-shaped cytoplasm is bounded by several large, peripheral vacuoles (Fig. 12). The central nucleus is surrounded by radially oriented chloroplasts. The cellularization is also accompanied by the appearance of tiny lipid droplets in the endosperm cells (Fig. 15). Near the completion of endosperm cellularization, both starch grains (Fig. 16) and lipid droplets (Fig. 17) are present. The pigment layer commences differentiation from the innermost layer of the inner integument at this stage, and it serves as a marker for the border between the testa and the endosperm (Fig. 18).

The ultrastructure of the endosperm changes slightly during the early stages of cellularization. In the sections observed, starch accumulation is not yet apparent in the nascent cells (Fig. 19). The small lipid droplets that have appeared at this stage are electron-translucent and have no apparent limiting membrane. The mitochondria appear especially concentrated in the cytoplasm adjacent to the embryo sac wall (Fig. 20).

Delicate anticlinal cell walls with free ends extending towards the central vacuole partition the free nuclei of the inner endosperm (Fig. 21). They contain numerous plasmodesmata, and mitochondria are present in the adjacent cytoplasm (Fig. 22). The orientation of the chloroplasts is at an

intermediate state between that of the free nuclear stage and that of cellular endosperm (compare to Figure 13). The mitochondria appear randomly distributed, and lipid droplets are present (Fig. 23). A gradient of increasing vacuolar size is apparent from the nucleus towards the anticlinal partition walls. Many of the vacuoles contain internal membranes, which suggests that the increase in vacuolar size proceeds by coalescence. A cell plate in one of the partitions lies across a spindle profile (Fig. 24a) and microtubules are visible in it (Fig. 24b).

Further endosperm cellularization results in larger and more numerous lipid droplets, and accumulations of starch in the chloroplasts (Fig. 25a; compare to Fig. 19). Most of the vacuoles are lined with a thin layer of electron-opaque material (Fig. 25b). Numerous plasmodesmata interconnect all endosperm cells (Fig. 25b), but there are no cytoplasmic connections evident between the inner integument and the endosperm (Fig. 26). The cells of the pigment layer contain intensely staining grains similar in shape and texture to protein bodies (Fig. 27). The grains are large, rounded, electron-opaque and contain electron-lucent circular areas.

Collapse of the inner integument

At 18 DPP, the cytoplasm of the endosperm cells is no longer distinctly astroid-shaped (Figs. 28 and 30). Cellularization of the endosperm appears to have ceased. The amount of starch in the endosperm appears to have increased since 16 DPP, but the starch grains are still smaller than those of the testa (Figs. 29 and 16). Endosperm lipid content has also increased (Figs. 30 and 17), and the outer cell layers have a greater concentration of lipid and starch than the inner layers (Fig. 28). The cells of the inner layers are larger and

more vacuolate, and they undergo disintegration and breakage in advance of the growing embryo (Fig. 11). The cells of the inner integument, except for the pigment layer and the outermost layer, are noticeably plasmolyzed and compressed (Fig. 28). Denser cytoplasm is evident in the cells of the pigment layer than there was at 16 DPP (Figs. 30 and 12), and there is less starch in the inner integument (Figs. 29 and 16). When Historesin sections are stained with fluorescent DNA stains, mitotic figures are observed in the peripheral layers of the endosperm (Figs. 31a-32b).

Electron micrographs of the endosperm tissue reveal multiple starch grains in the chloroplasts (Fig. 33). An electron-lucent area encloses each starch grain. Long profiles of RER have appeared and they tend to be associated with the periphery of chloroplasts (Fig. 34). The mitochondria contain electron-opaque globules (Fig. 35). Electron-dense particles encircle the boundary of many of the smaller lipid droplets. Large vacuoles are still present, but smaller vacuoles have appeared, each containing an electron-opaque inclusion (Fig. 36). One of these vacuoles appears associated with dictyosomes, suggesting a possible origin (Fig. 37). In another such vacuole, strands of the inclusion extend towards particles that are associated with the tonoplast (Fig. 38). These inclusions are also found within vacuoles of the inner integument cells (Fig. 39).

Inception of the aleurone layer

The aleurone layer has differentiated from the outermost layer of the endosperm by approximately 22 DPP (Fig. 40). At this stage, the embryo has curved completely around the inside of the seed. The aleurone cells contain more lipid droplets (Fig. 41a) and smaller starch grains (Fig. 42a) than the

more vacuolate cells of the underlying endosperm. Many of the lipid droplets appear to contact each other in the aleurone cells. The cotyledon also contains both starch and lipid, but it appears to stain more densely than does the aleurone layer (Figs. 41b and 42b). The protoplasm of the palisade cells has become sudanophilic, but no aggregations of lipid droplets are apparent (Fig 41b). Degeneration is now evident in the outermost cell layer of the inner integument (Fig. 43).

The anticlinal cell walls of the aleurone layer seem especially delicate and are susceptible to breakage during handling of the seed before embedding it (Fig. 45). The aleurone chloroplasts appear smaller, and contain fewer starch grains per plastid than those of the underlying endosperm. A count of 28 plastids in one section yielded an average of 1.6 grains per aleurone plastid and 3.4 grains per underlying endosperm plastid. Electron-dense particles still encircle the border of some lipid droplets in the aleurone layer (Fig. 44), but the electron-opaque inclusions within small vacuoles that were observed at 18 DPP are absent (Fig. 46). In spite of the absence of an apparent coat, most lipid droplets appear not to coalesce where they contact (Fig. 45). Long profiles of RER remain associated with the chloroplasts of the endosperm (Fig. 46). The electron-dense grains of the pigment layer are uniform in density, and the round, electron-lucent areas which were evident at 16 DPP (Fig. 27) are now absent (Fig. 45). The pigment layer lacks starch grains (compare to Fig. 27).

Collapse of the underlying endosperm

After the inception of the aleurone layer, the underlying endosperm cells begin to lose their storage reserves and collapse (Fig. 47a). The number of starch grains in both the testa and the endosperm have decreased from the previous stage (Figs. 47b and 42a), and many of the plastids in the endosperm appear flattened (Fig. 47a). The aleurone cells lack the vacuolation of previous stages, and stain densely with the lipophilic stain, Sudan black B (Fig. 47c). The cells of the inner integument continue to collapse until the pigment layer is the only recognizable component (Fig. 47a). The collapse of the underlying endosperm does not proceed simultaneously in the whole seed, but it proceeds from the adaxial to the abaxial end of the seed (Fig. 73a). The aleurone layer is also discontinuous in the region of the micropyle and the chalaza (Figs. 73a, 73b). The cells of that region lack the dense accumulations of storage material that is characteristic of the aleurone layer.

Plasmolysis is evident in the cells of the underlying endosperm, and it appears to be more advanced in the inner cell layers (Fig. 48). The nuclei of the underlying endosperm have an amoeboid outline. In the aleurone cells, grana are evident in the chloroplasts that are depleted of starch (Fig. 49). The chloroplasts of the aleurone layer are biconvex, but in the underlying endosperm, the chloroplasts intergrade from biconvex in the outermost cell layer to flattened in the innermost cell layer (Fig. 48). Groups of electron-translucent globules appear in the flattened plastids of the inner cell layers of the underlying endosperm (Fig. 50). Dictyosomes are not apparent in the sections that were observed. Endoplasmic reticulum and mitochondria, exhibit little contrast against the dense cytoplasm of the aleurone cells (Fig. 51). On the other hand, the mitochondria of the underlying endosperm are

easily identified (Fig. 50). The outer periclinal cell wall of the aleurone layer is considerably thicker than the wall that separates the aleurone layer from the underlying endosperm (Fig 48). The cell walls of the underlying endosperm are thicker at the vertices. The aleurone protoplast has pulled away from the wall adjacent to the inner integument. This is an artefact of specimen preparation.

Thickening of aleurone walls

By 30 DPP the cell walls of the endosperm are noticeably thickened. The aleurone cells are distinctly rectangular-shaped in section, and plasmolysis of the underlying endosperm cells is evident (Fig 52a). The aleurone protoplast is sudanophilic (Fig 52b), and PAS-positive starch grains are also present (Fig. 52c). Other tissues of the seed coat are devoid of starch and lipid, except for the presence of lipid droplets in the underlying endosperm.

The endosperm cell walls are unevenly thickened, which is analogous to collenchyma tissue (Fig. 53). The nuclei of the underlying endosperm cells become elongate, concomitant with the collapse of the cell (Fig. 54). Starch grains are present only in the aleurone layer (Fig. 53). The chloroplasts of the underlying endosperm cells are flattened and contain electron-translucent globules (Fig. 55). Long profiles of RER are visible in the underlying endosperm, but portions of the cisternae appear to be collapsed and lack ribosomes (Fig. 56). Lipid droplets in the aleurone cells remain discrete where they are closely appressed (Fig. 57). Electron-dense bodies are visible among the lipid droplets, but no apparent limiting membrane is visible (Fig. 58). The texture and electron-density of these bodies appears similar to that of the particles that encircle the border of lipid droplets. Aleurone cells contain

intracellular spaces around breaks of the anticlinal cell walls, and between the protoplast and the outer periclinal cell wall, but these appear to be an artefact of specimen preparation (Fig. 57). Cells of the pigment layer contain irregular, electron-dense grains and a large central vacuole coated with electron-dense material (Fig. 53).

Protein body deposition

Collapse of the underlying endosperm is complete at 34 DPP (Fig. 59a). The aleurone protoplasts are oval due to the uneven cell wall thickening. In addition to starch grains in the aleurone layer (Fig. 59c), protein bodies are present that stain positively with crystal violet and with Coomassie brilliant blue (Figs. 59a and 59b). The majority of the aleurone protoplast is sudanophilic, and the palisade cell walls are weakly sudanophilic, causing them to be tan in colour (Fig. 59d). The anticlinal cell walls of the aleurone are still relatively thin and susceptible to breakage (Fig. 59a).

Electron microscopy of the aleurone cells reveals rounded and electron-dense bodies that appear to correspond to the coomassie brilliant blue-positive protein bodies (Figs. 60 and 59b). The protein bodies are membrane bound and their contents are granular (Fig. 61). The outline of the nucleus is deformed by the bordering lipid droplets (Fig. 62). Electron-dense globules and starch grains are present in the chloroplasts (Fig. 63). Short profiles of RER are evident in the cytoplasm (Fig. 64). High magnifications of the cell wall reveal an electron-dense, fibrillar herringbone pattern that forms concentric bands around the protoplast (Fig. 65).

Near-mature aleurone

The aleurone layer is in a near mature state at 38 DPP. The outer integument consists of an epidermis, two cell layers of subepidermis, and a palisade layer (Fig. 66a). The epidermal cells appear empty, except for a deposit appressed to the inner face of the outer periclinal cell wall. The walls of the palisade layer are weakly sudanophilic (Fig. 66d). The only visible portion of the inner integument are cells of the pigment layer (Fig. 66b). They are lined with a layer of intensely staining deposits, and fragments of similarly staining deposits are found scattered in the cell lumen. The aleurone layer is a single cell layer of ovoid protoplasts with thickened cell walls. The inner periclinal cell wall appears thicker because the cell wall material of the collapsed underlying endosperm is appressed there. Staining with PAS indicates that starch grains are present (Fig. 66c). The amount of sudanophilic material appears to have decreased, while the Coomassie brilliant blue-stainable material appears to have increased, relative to previous stages (Figs. 66d and 66e; and 59b and 59d). The cell walls of the aleurone layer remain distinctly non-sudanophilic (Fig. 66d).

The lipid droplets of the aleurone layer appear more closely appressed to one another than at 34 DPP, resulting in polygonal outlines (Figs. 67 and 60). The borders between lipid droplets are distinct. The lipid droplets that line the cell wall appear smaller than the more centrally located lipid droplets. Protein bodies, chloroplasts with starch grains, and profiles of ER are found between the lipid droplets (Fig. 68). The chloroplasts also contain both electron-dense and electron-translucent globules (Figs. 68 and 69). The cell walls of the aleurone layer appear thicker than at 34 DPP, and the anticlinal

cell walls are intact when submitted to the same isolation and fixation regimes as at 34 DPP (Fig. 67).

Mature aleurone cells

The aleurone layer isolated from mature seeds (about 50 DPP) is a single layer with collapsed remnants of underlying endosperm cells appressed to one face (Fig. 70a). The protoplast lacks PAS-positive inclusions (Fig. 70b), but protein bodies are present, embedded in a matrix of sudanophilic material (Figs. 70c and 70d). Sudanophilic material also lines the periphery of the cell, and in some cells, forms a large globule (Fig. 70c). The cell wall is non-sudanophilic.

Electron microscopy of the mature aleurone cell shows giant central lipid droplets and many small lipid droplets of irregular shape (Fig. 71). The small lipid droplets line the periphery of the cell and surround protein bodies. The protein bodies are round and contain electron-dense and electron-lucent inclusions. Round plastids lacking internal membranes are present, and they contain many electron-dense globules (Fig. 72). Dictyosomes, ER, and mitochondria are not evident in the sections that were surveyed.

Microfluorometry of Hoechst dye #33342-stained nuclei

Isolated nuclei stained by Hoechst dye #33342 fluoresce blue-white under UV excitation. The nuclei of embryo tissue from mature seeds appear polygonal (Fig. 75). The nuclei of free nuclear endosperm tissue collected at 12 DPP are round in outline (Fig. 74). Aleurone nuclei from a mature seed are rounded, but have an irregular outline (Fig. 76). Other cell components

fluoresce, especially cell wall material (not shown), which autofluoresces under UV excitation. The surrounding cytoplasm fluoresces weakly, and in all the nuclear preparations, pinpoints of fluorescence are visible in the surrounding cytoplasm (Figs. 74, 75 and 76). Weakly fluorescent nucleolar regions were present in the embryo nuclei (Fig. 75).

Figure 77 provides a visual comparison of the nuclear fluorescence among the three tissues. The total fluorescence of aleurone nuclei is more similar to that of endosperm free nuclei than to nuclei of diploid tissue. Data from a t-test at a 95% confidence interval show that the total fluorescence of the embryo nuclei is significantly different from that of either endosperm free nuclei or of aleurone nuclei (Table 1). The fluorescence of aleurone nuclei is significantly similar to that of endosperm free nuclei using the same confidence interval.

Table 1. t-test of nuclear fluorescence at 95% confidence.

Test	Degrees of Freedom	p Value	t-Statistic	Result
μ(triploid) - μ(diploid) =0	33	<0.001	9.783	reject
μ(aleurone) - μ(diploid) = 0	21	<0.001	-7.312	reject
μ(aleurone) - μ(triploid) = 0	27	0.06	1.972	fail to reject

FIGURE DESCRIPTIONS

Figure 1. Longitudinal section of a seed at 14 DPP, stained with crystal violet. The funiculus (F) is attached to the abaxial (Ab) end of the seed. The embryo sac central vacuole (CV) confines the free nuclear endosperm (FNE) to the periphery of the embryo sac. The chalaza (Ch) and the basal body (BB) are visible, but the micropyle is out of the plane of the section. Ad adaxial end. 1 cm scale bar = 199μm.

Figure 2. Light micrograph of a portion of the testa at 14 DPP, stained with Sudan black B. Lipid droplets (arrowheads) are visible in the palisade layer. 1 cm scale bar = 9.74μm.

Figure 3. Light micrograph of the testa and free nuclear endosperm at 14 DPP, stained with crystal violet. The testa consists of the outer integument (OI) and the inner integument (II). The outer integument consists of an epidermis (eD), two cell layers of subepidermis (seD), and a palisade layer of sclerenchyma cells (PalL). The inner integument consists of an outermost cell layer of large rectangular cells, several cell layers of smaller, rounded cells, and a pigment layer (PigL). The free nuclear endosperm (FNE) is appressed to the integument by the embryo sac central vacuole (CV). The embryo sac wall has pulled away from the inner integument in one place (large arrow). Enlargement of boxed area is in Figure 5. 1 cm scale bar = 38.9μm.

Figure 4. Light micrograph of the testa and free nuclear endosperm at 14 DPP, stained with PAS: semi-adjacent section to Figure 3. Starch grains (large arrowheads) and cell wall material (small arrowheads) react positively. Note the smaller starch grains in the palisade layer. 1 cm scale bar = 38.9μm.

Figure 5. Light micrograph of the free nuclear endosperm and testa at 14 DPP, stained with crystal violet: higher magnification of Figure 3. The embryo sac wall (ESW) borders the inner integument. The free nuclei (N) contain a prominent nucleolus (Nl), and they are surrounded by chloroplasts (cP). 1 cm scale bar = 9.74μm.

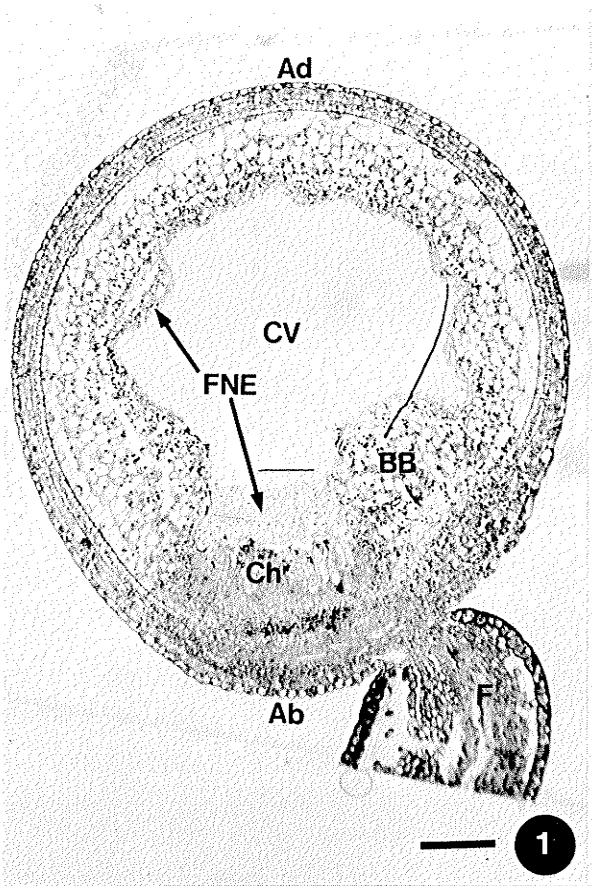

1

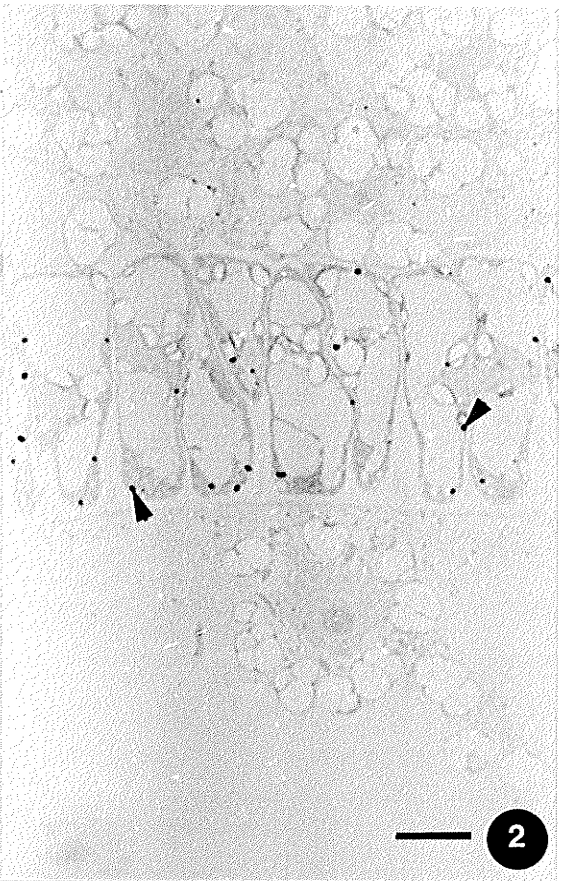

2

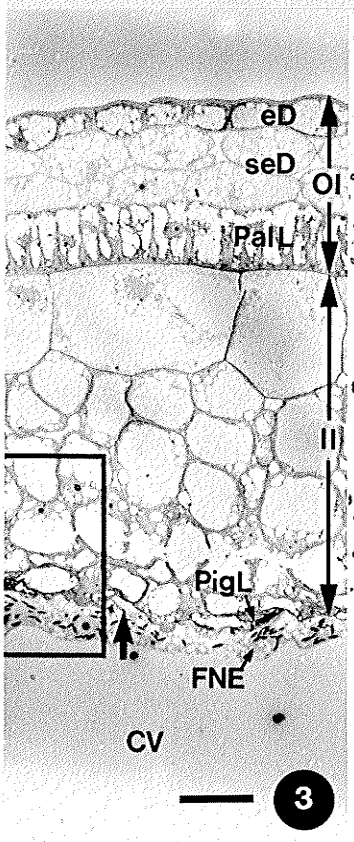

3

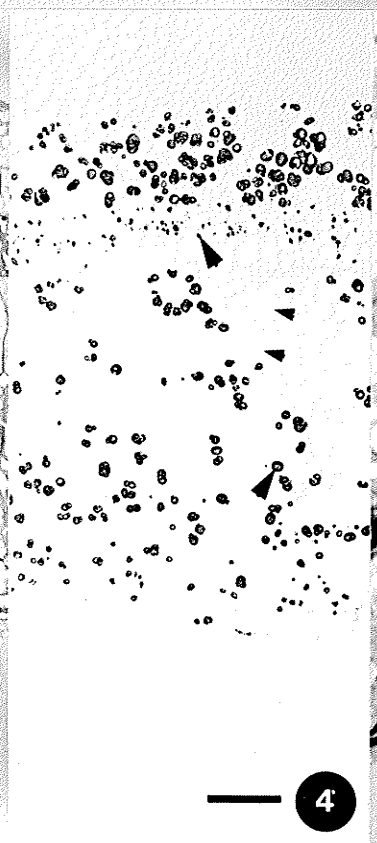

4

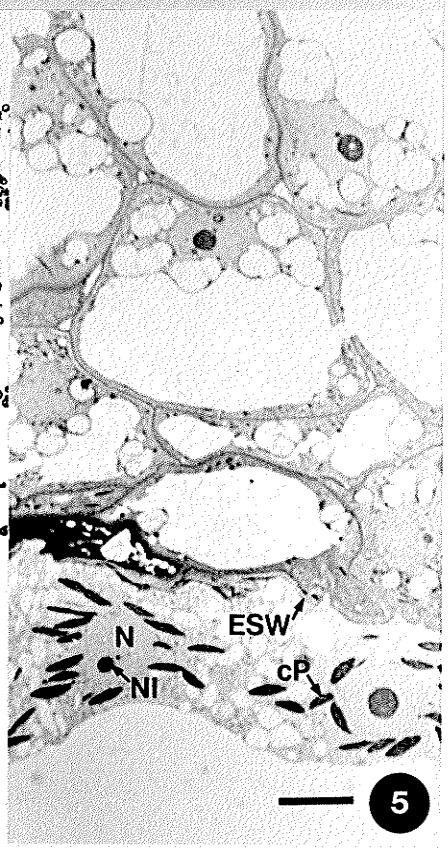

5

Figure 6. Electron micrograph of the free nuclear endosperm at 14 DPP, stained with uranyl acetate-lead citrate. The free nucleus (N) has a wavy outline and a prominent nucleolus (Nl). The chloroplasts (cP) contain well-developed grana (Gr) and electron-opaque globules (arrowheads). The vacuoles (V) are small and numerous, and some are lined with electron-dense deposits (arrows). Mitochondria (M), rough endoplasmic reticulum (RER), and dictyosomes (dS) are also present. The embryo sac central vacuole (CV) defines the inner boundary of the free nuclear endosperm. 1 cm scale bar = 0.985μm.

6

Figure 7. Electron micrograph of mitochondria of the free nuclear endosperm at 14 DPP, stained with uranyl acetate-lead citrate. Mitochondria (M) have a round profile and contain saccular cristae (Cr) appressed to one another. A dictyosome (dS) is found near the embryo sac wall (ESW). The embryo sac wall has pulled away from the inner integument, leaving loosely arranged fibrillar material behind it. 1 cm scale bar = 0.323μm.

Figure 8. Electron micrograph of a mitochondrion of the free nuclear endosperm at 14 DPP, stained with uranyl acetate-lead citrate. The plane of this section has revealed an unusually long profile of a mitochondrion (M) found alongside the embryo sac wall (ESW). 1 cm scale bar = 0.430μm.

Figure 9. Electron micrograph of the embryo sac wall at 14 DPP, stained with uranyl acetate-lead citrate. The embryo sac wall (ESW) in this region has closely spaced, peg-like projections (arrowheads). 1 cm scale bar = 0.430μm.

Figure 10. Electron micrograph of the inner integument at 14 DPP, stained with uranyl acetate-lead citrate. Plasmolysis leaves a space (arrows) between the cell wall (CW) and the protoplast. The nuclei (N) contain nucleoli (Nl) and electron-dense inclusions (arrowheads). Amyloplasts (aP), mitochondria (M), microbodies (mB), and endoplasmic reticulum (ER) are also present. SG starch grain. 1 cm scale bar = 1.08μm.

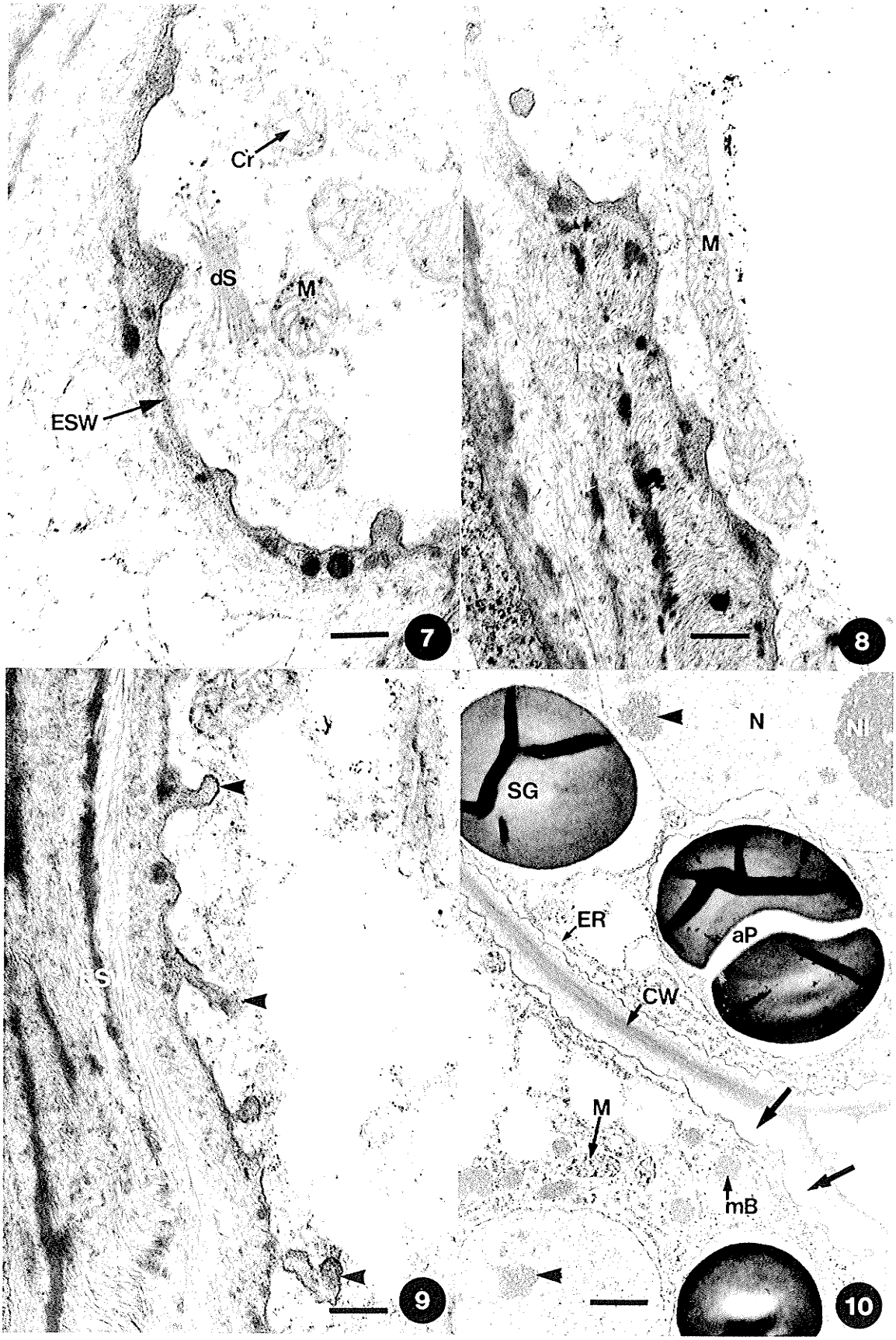
Cr
dS
M
ESW
7
M
8
9
SG
N
NI
ER
aP
CW
M
mB
10

Figure 11. Light micrograph of a seed at 22 DPP, stained with crystal violet. The sagittal section reveals an embryo (E) following the curvature of the seed. The endosperm (eS) fills the embryo sac except for a central region (asterisk). The inner endosperm cells are more vacuolate and lyse (arrows) in advance of the cotyledons (Cot). 1 cm scale bar = 199μm.

Figure 12. Light micrograph of cellularizing endosperm and testa at 16 DPP, stained with crystal violet. The peripheral layers of cellular endosperm (CE) border the pigment layer (PigL) of the inner integument. The astroid cytoplasm of the endosperm cell contains large peripheral vacuoles (V) and a central nucleus (N) with a prominent nucleolus (Nl). Chloroplasts (cP) are arranged radially around the nucleus. The innermost layer of the endosperm (FNE) is still free nuclear. 1 cm scale bar = 9.74μm.

Figure 13. Light micrograph of cellularizing endosperm at 16 DPP, stained with crystal violet. The outer layers of the endosperm are cellular (CE) and the innermost layer is still free nuclear (FNE). The free nuclei are separated by anticlinal cell walls with free ends (CW). A periclinally oriented cell plate (phP) is in the process of partitioning a free nucleus (compare to Figure 24a), but the nuclei are out of the plane of section. The central vacuole of the embryo sac (CV) defines the inner boundary of the free nuclear portion of the endosperm. 1 cm scale bar = 9.74μm.

Figure 14. Light micrograph of cellularizing endosperm and testa at 18 DPP, stained with crystal violet. Radial files of cells (large arrows) are visible in the peripheral endosperm. The pigment layer (PigL) of the inner integument marks the boundary between the endosperm and the testa. 1 cm scale bar = 38.9μm.

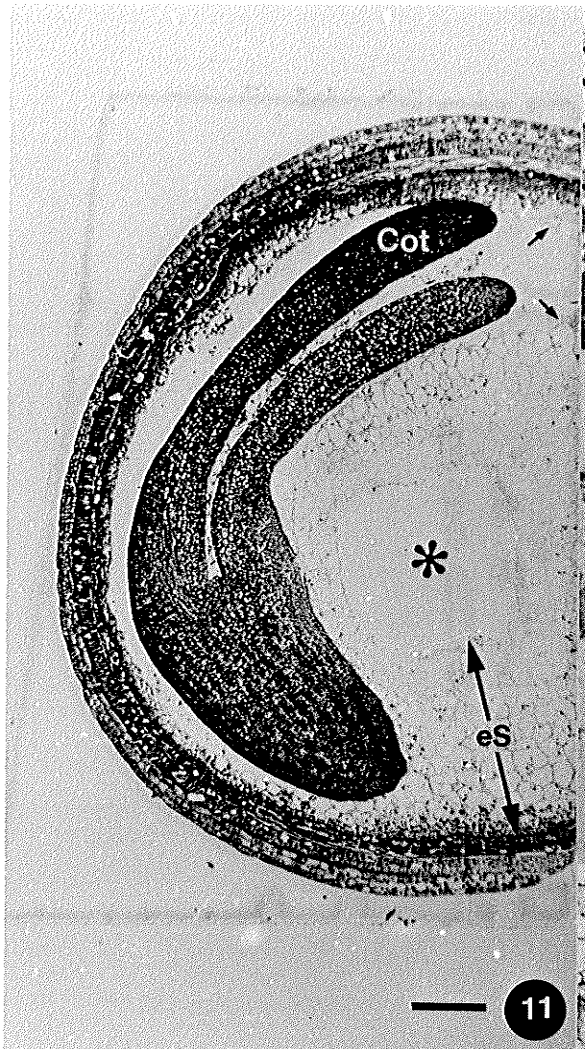

11

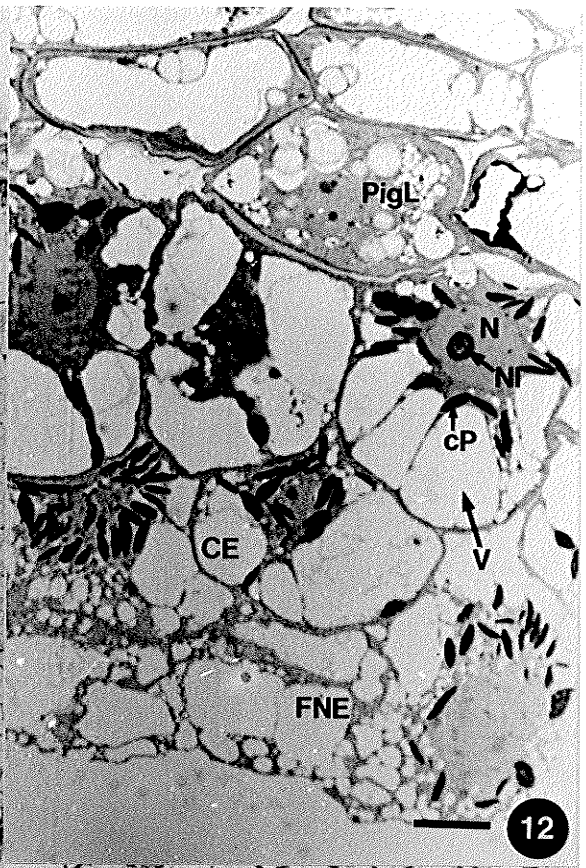

12

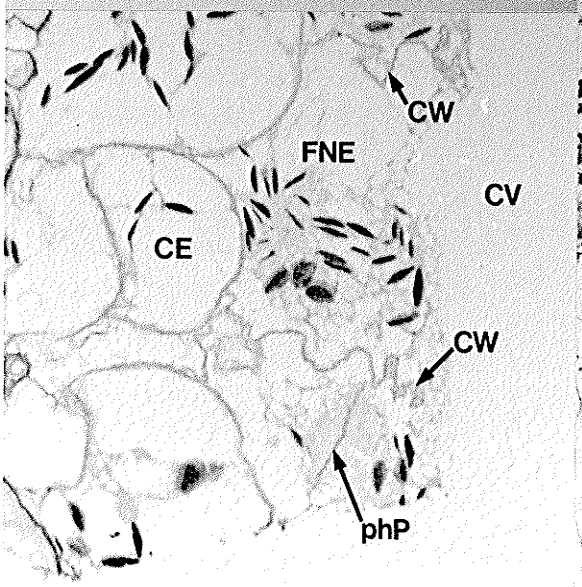

13

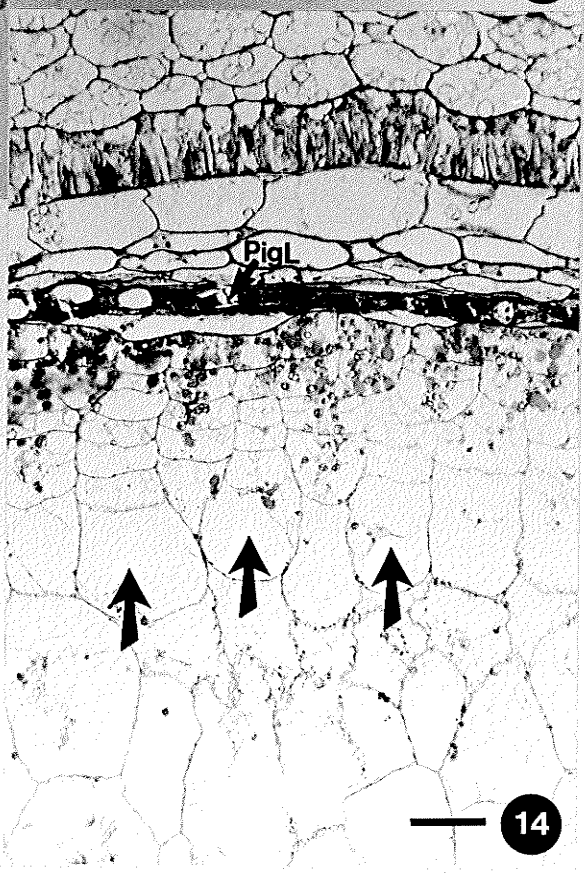

14

Figure 15. Light micrograph of cellularizing endosperm and testa at 16 DPP, stained with Sudan black B: semi-adjacent section to Figure 12. Small lipid droplets (arrowheads) are revealed in the cellular endosperm. Chloroplasts (cP) are also Sudan black B-positive. 1 cm scale bar = 9.74μm.

Figure 16 Light micrograph of further cellularization of the endosperm and testa at 16 DPP, stained with PAS. Starch grains (arrowheads) are larger in the inner integument (II) than in the endosperm (eS). 1 cm scale bar = 9.74μm.

Figure 17. Light micrograph of further cellularization of the endosperm and testa at 16 DPP, stained with Sudan black B. Lipid droplets (arrowheads) are in both the endosperm (eS) and the pigment layer. Starch grains (SG) are unstained by Sudan black B. 1 cm scale bar = 9.74μm.

Figure 18. Light micrograph of further cellularization of the endosperm and testa at 16 DPP, stained with crystal violet. The pigment layer (PigL) marks the boundary between the endosperm (eS) and the testa (T). 1 cm scale bar = 38.9μm.

15

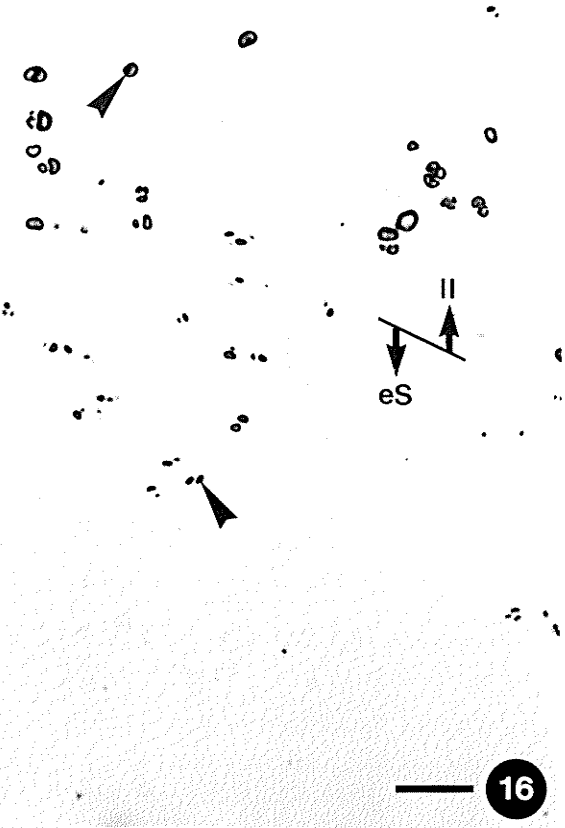

16

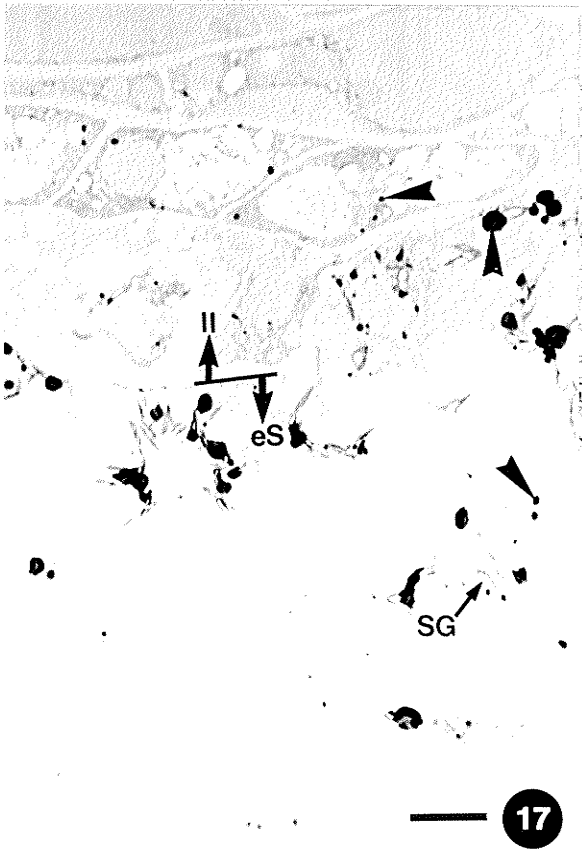

17

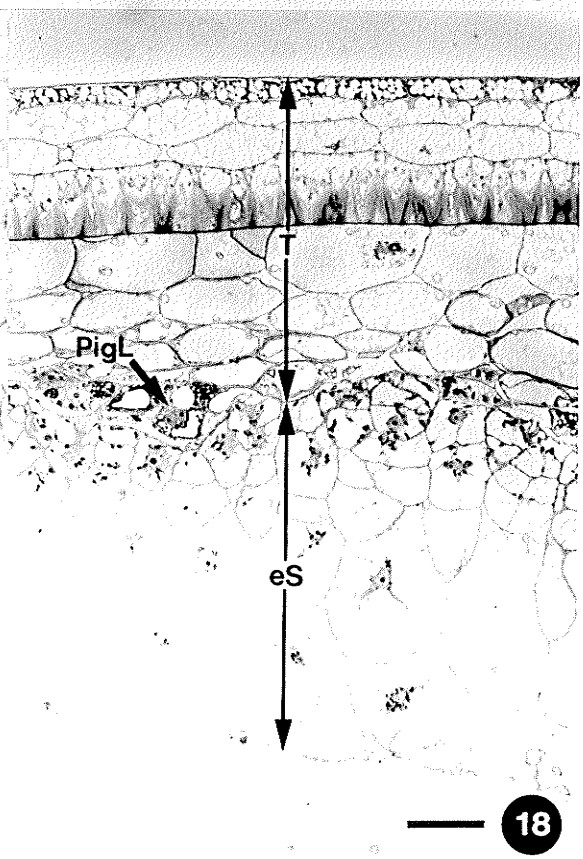

18

Figure 19. Electron micrograph of nascent cellular endosperm at 16 DPP, stained with uranyl acetate-lead citrate. The chloroplasts (cP) lack starch grains. Lipid droplets (LD) are present. 1 cm scale bar = 0.380μm.

Figure 20. Electron micrograph of nascent cellular endosperm at 16 DPP, stained with uranyl acetate-lead citrate. The mitochondria (M) appear concentrated near the embryo sac wall (ESW). Endosperm cell walls are indicated by arrowheads. 1 cm scale bar = 0.538μm.

Figure 21. Electron micrograph of the free nuclear portion of cellularizing endosperm at 16 DPP, stained with uranyl acetate-lead citrate. Anticlinal cell walls (arrowheads) partition the free nucleus (N) which is surrounded by chloroplasts (cP). The open partition has a peripheral array of vacuoles (V). The free nuclear portion of the endosperm is bounded by a peripheral layer of cellular endosperm (CE). 1 cm scale bar = 4.30μm.

Figure 22. Electron micrograph of a nascent cell wall of cellularizing endosperm at 16 DPP, stained with uranyl acetate-lead citrate. The walls that partition the free nuclear portion of cellularizing endosperm contain many plasmodesmata (arrows). Mitochondria (M) are found near the cell wall. 1 cm scale bar = 0.645μm.

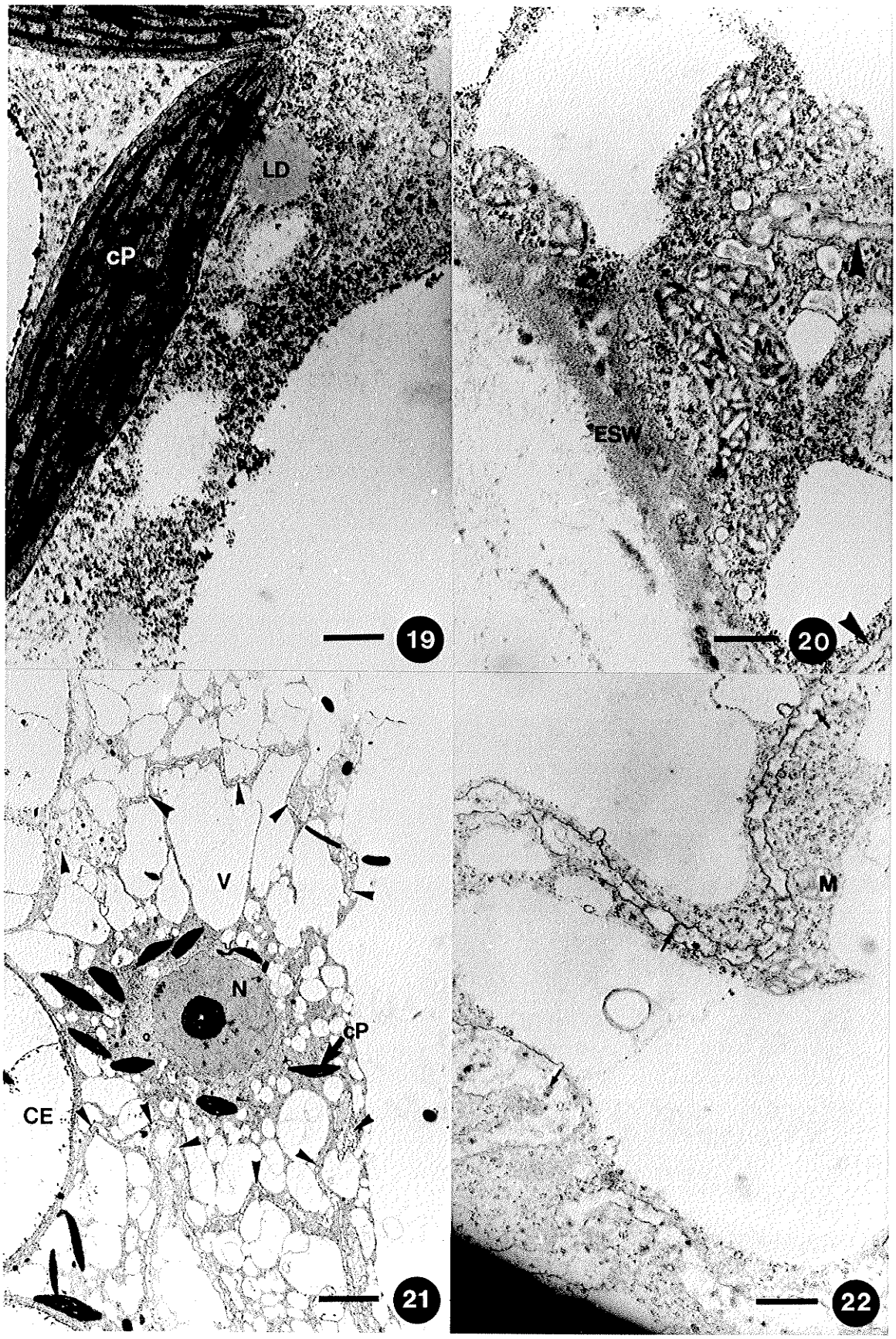
LD
CP
19
M
ESW
20
V
N
CP
CE
21
M
22

Figure 23. Electron micrograph of the free nuclear portion of cellularizing endosperm at 16 DPP, stained with uranyl acetate-lead citrate. The mitochondria (M) appear randomly distributed. Vacuoles (V) contain internal membranes (arrowheads) and appear to be coalescing. Chloroplasts (cP), lipid droplets (LD), endoplasmic reticulum (ER), and dictyosomes (dS) are also present. 1 cm scale bar = 1.32μm.

Figure 24a. Electron micrograph of a cell plate in cellularizing endosperm at 16 DPP, stained with uranyl acetate-lead citrate. The cell plate (phP) separates two nuclei (N), one of which is absent from the plane of section, and it extends towards an anticlinal cell wall (arrowheads). Cellular endosperm (CE) and the embryo sac central vacuole (CV) define the outer and the inner boundaries of this region, respectively (Compare to Figure 13). Enlargement of boxed area is in Figure 24b. 1 cm scale bar = 3.33μm.

Figure 24b. Electron micrograph of a cell plate in cellularizing endosperm at 16 DPP, stained with uranyl acetate-lead citrate: higher magnification of Figure 24a. Microtubules (arrowheads) extending from the cell plate (CP) are visible. 1 cm scale bar = 0.323μm.

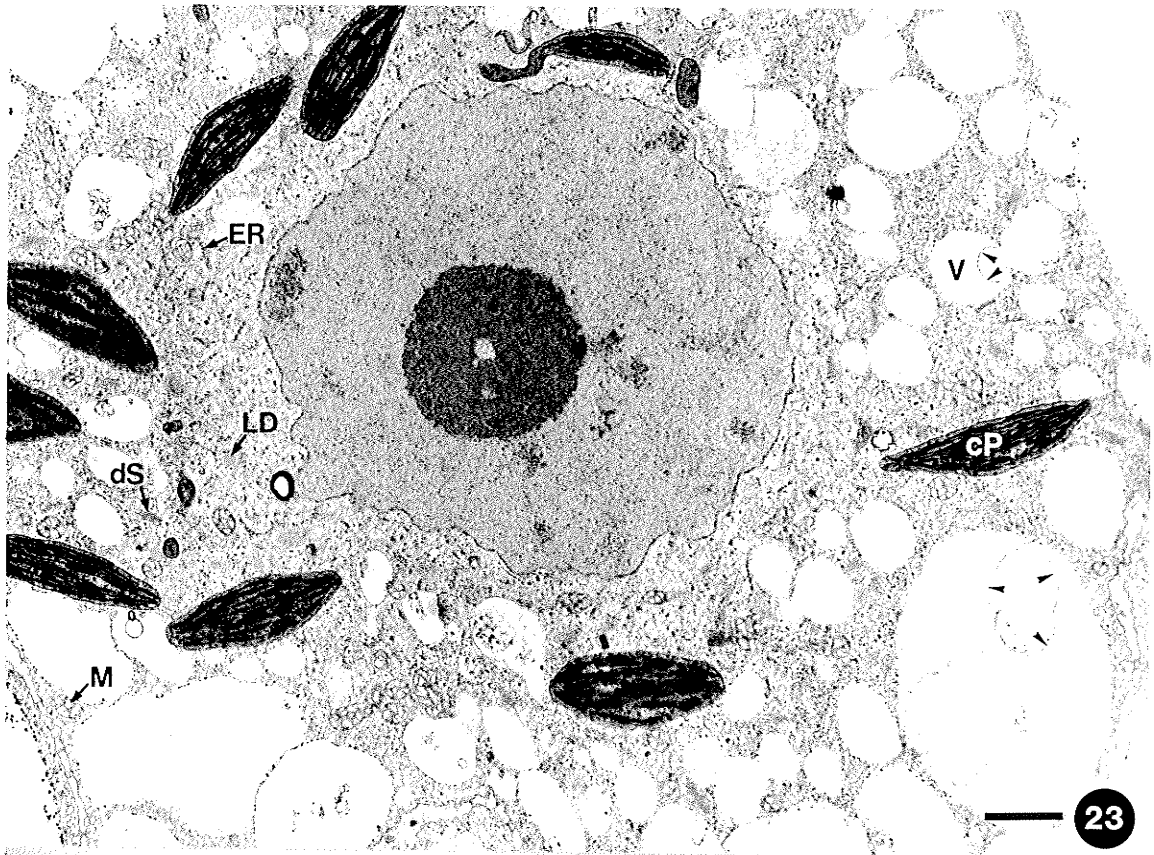
ER
V
LD
dS
cP
M
23

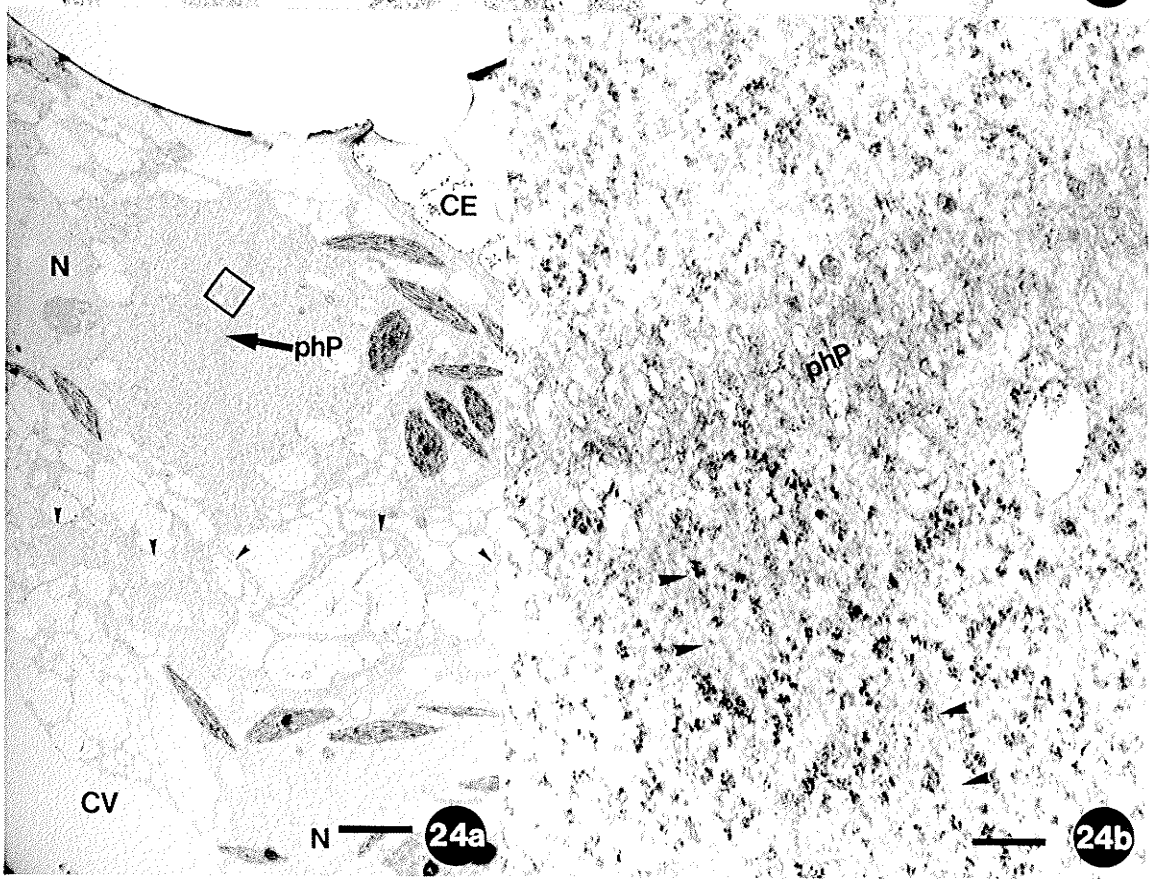
CE
N
phP
phP
CV
N
24a
24b

Figure 25a. Electron micrograph of an endosperm cell at 16 DPP, stained with uranyl acetate-lead citrate. Lipid droplets (LD) are larger than at earlier stages (compare to Figure 19), and chloroplasts (cP) contain starch grains (SG). Enlargement of boxed area is in Figure 25b. 1 cm scale bar = 2.58μm.

Figure 25b. Electron micrograph of an endosperm cell wall at 16 DPP, stained with uranyl acetate-lead citrate: higher magnification of Figure 25a. The cell wall contains numerous plasmodesmata (pD). Electron-dense material (arrowheads) lines the periphery of the vacuoles. 1 cm scale bar = 0.538μm.

Figure 26. Electron micrograph of the endosperm-inner integument interface at 16 DPP, stained with uranyl acetate-lead citrate. No plasmodesmata are evident in the embryo sac wall (ESW). II inner integument; eS endosperm. 1 cm scale bar = 0.645μm.

Figure 27. Electron micrograph of the inner integument at 16 DPP, stained with uranyl acetate-lead citrate. The inner integument cell contains both starch grains (SG), and electron-opaque grains (arrowheads) that contain electron-lucent inclusions. 1 cm scale bar = 1.84μm.

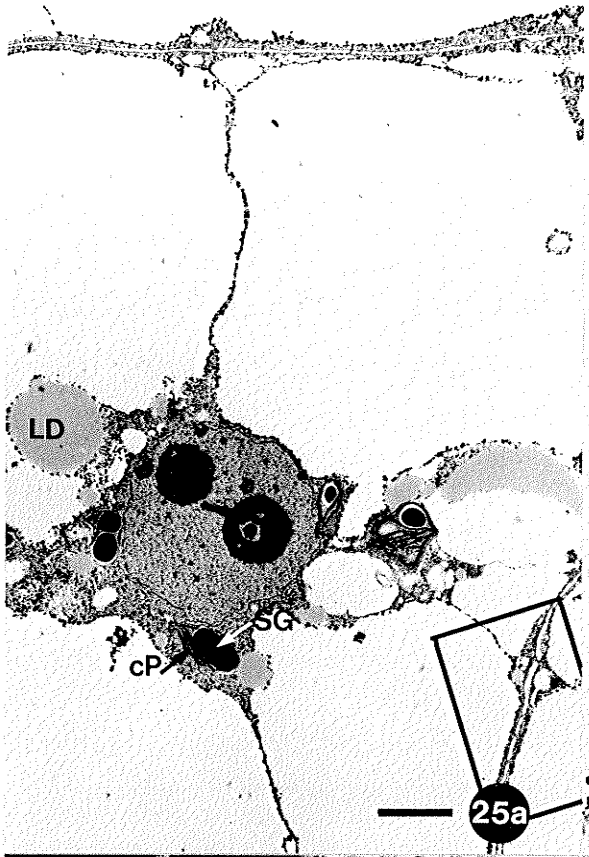
LD
SG
cP
25a

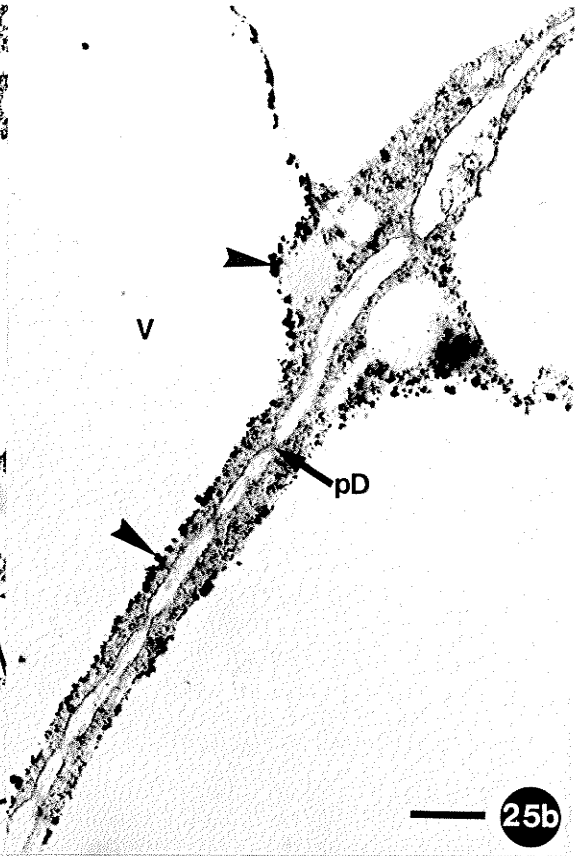
V
pD
25b

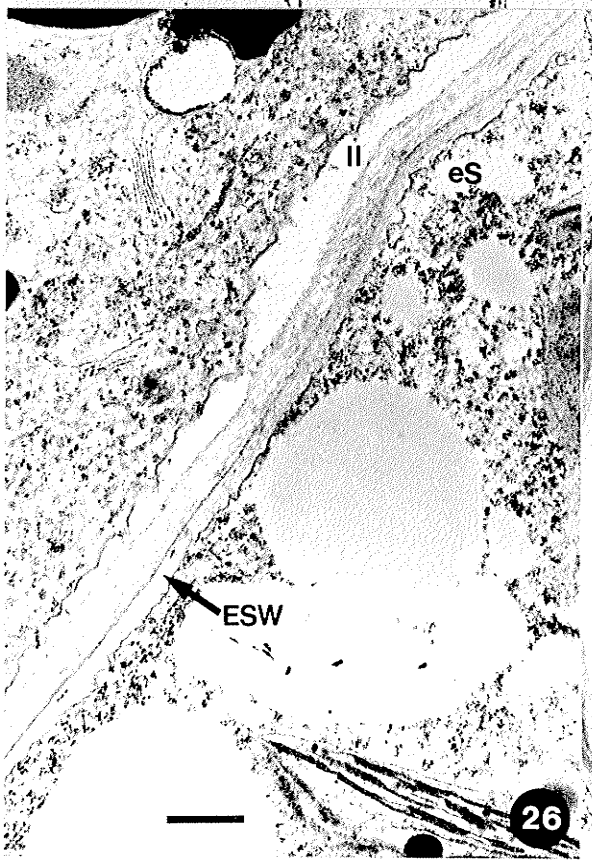
II
eS
ESW
26


SG
27

Figure 28. Light micrograph of the endosperm and testa at 18 DPP, stained with crystal violet. The cytoplasmic configuration of the endosperm cells is no longer astroid-shaped (compare to Figure 18). The outermost cells of the endosperm (eS) are smaller and contain more storage reserves than the more vacuolate cells of the inner endosperm. The inner integument (II) cells are collapsing, except for the outermost layer of large cells. Enlargement of boxed area is in Figure 30. 1 cm scale bar = 38.9μm.

Figure 29. Light micrograph of the endosperm and testa at 18 DPP, stained with PAS: semi-adjacent section to Figure 28. The starch grains (arrowheads) of the endosperm (eS) are smaller than those of the testa (T). The cells of the palisade layer contain small starch grains. 1 cm scale bar = 38.9μm.

Figure 30. Light micrograph of the endosperm and testa at 18 DPP, stained with crystal violet: higher magnification of Figure 28. The cytoplasm of the endosperm cells is no longer astroid-shaped (compare to Figure 12). Nuclei (N), starch grains (SG), and lipid droplets (LD) are visible in the endosperm cells. The cells of the pigment layer (PigL) stain more densely than at 16 DPP. 1 cm scale bar = 9.74μm.

Figure 31a. Fluorescent micrograph of the endosperm at 18 DPP, embedded in Historesin and stained with acridine orange and viewed under blue excitation: higher magnification of Figure 31b. Arrow indicates a metaphase figure of a dividing endosperm cell. 1 cm scale bar = 10.2μm.

Figure 32a. Fluorescent micrograph of the endosperm at 18 DPP, embedded in Historesin and stained with Hoechst dye #33342 and viewed under UV excitation: higher magnification of Figure 32b. Arrow indicates an anaphase figure of an outermost endosperm cell. 1 cm scale bar = 10.2μm.

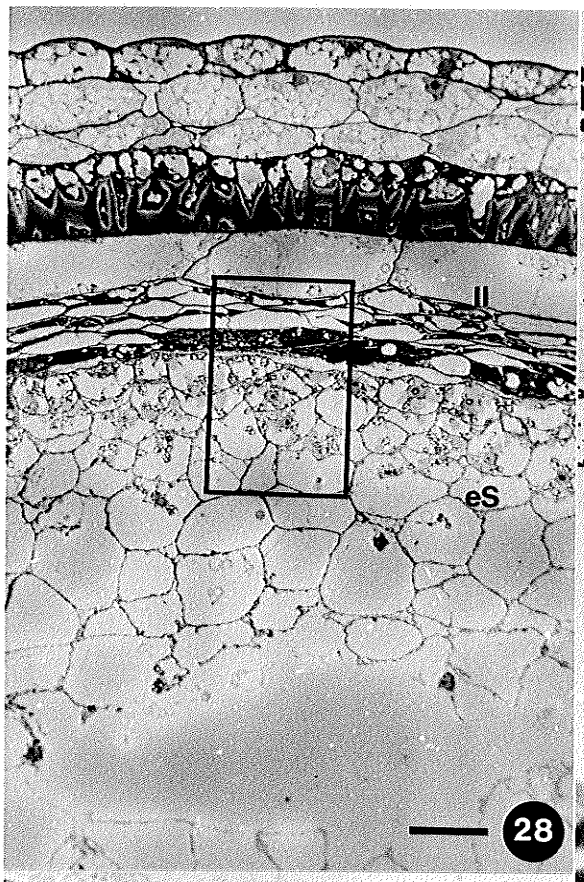
eS
28

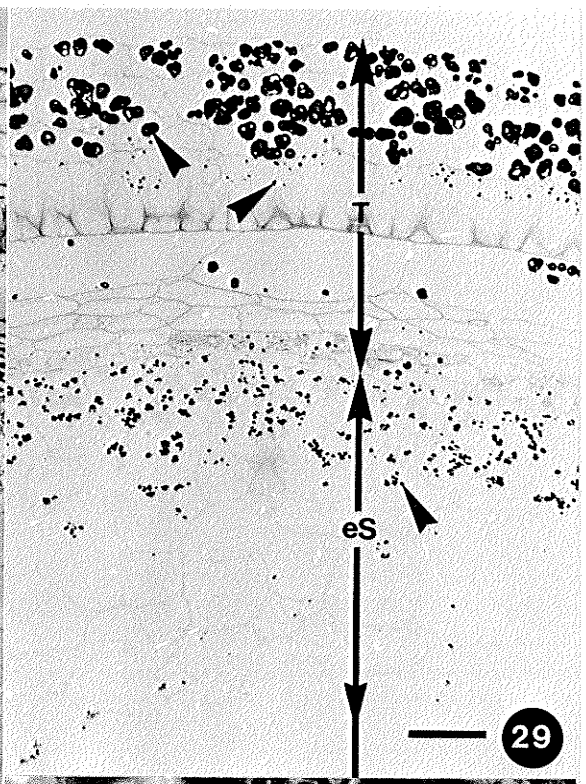
eS
29


PigL
SG
LD
N
30

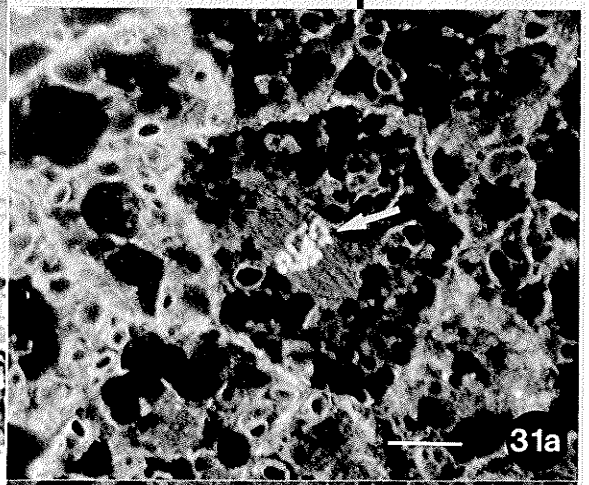
31a

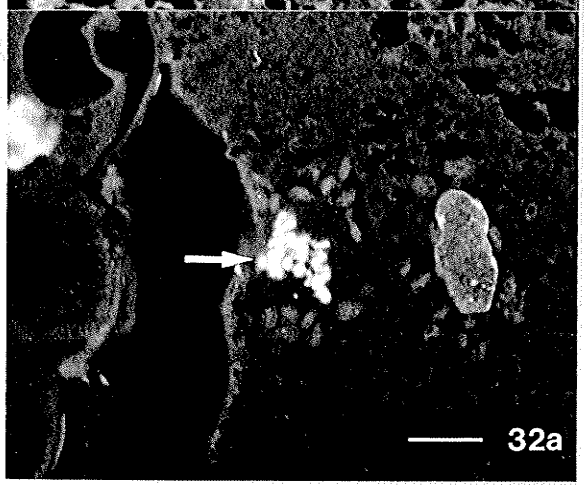
32a

Figure 31b. Fluorescent micrograph of the endosperm and testa at 18 DPP, embedded in Historesin and stained with acridine orange and viewed under blue excitation. Sagittal section of the seed reveals the inner integument (II), the endosperm (eS), and a mitotic figure (arrowhead). 1 cm scale bar = 40.8μm.

Figure 32b. Fluorescent micrograph of the endosperm and testa at 18 DPP, embedded in Historesin and stained with Hoechst dye #33342 and viewed under UV excitation. Sagittal section of the seed reveals the inner integument (II), the endosperm (eS), and mitotic figures (arrowheads). A cross section of the micropyle (Mi) is also visible. 1 cm scale bar = 40.8μm.

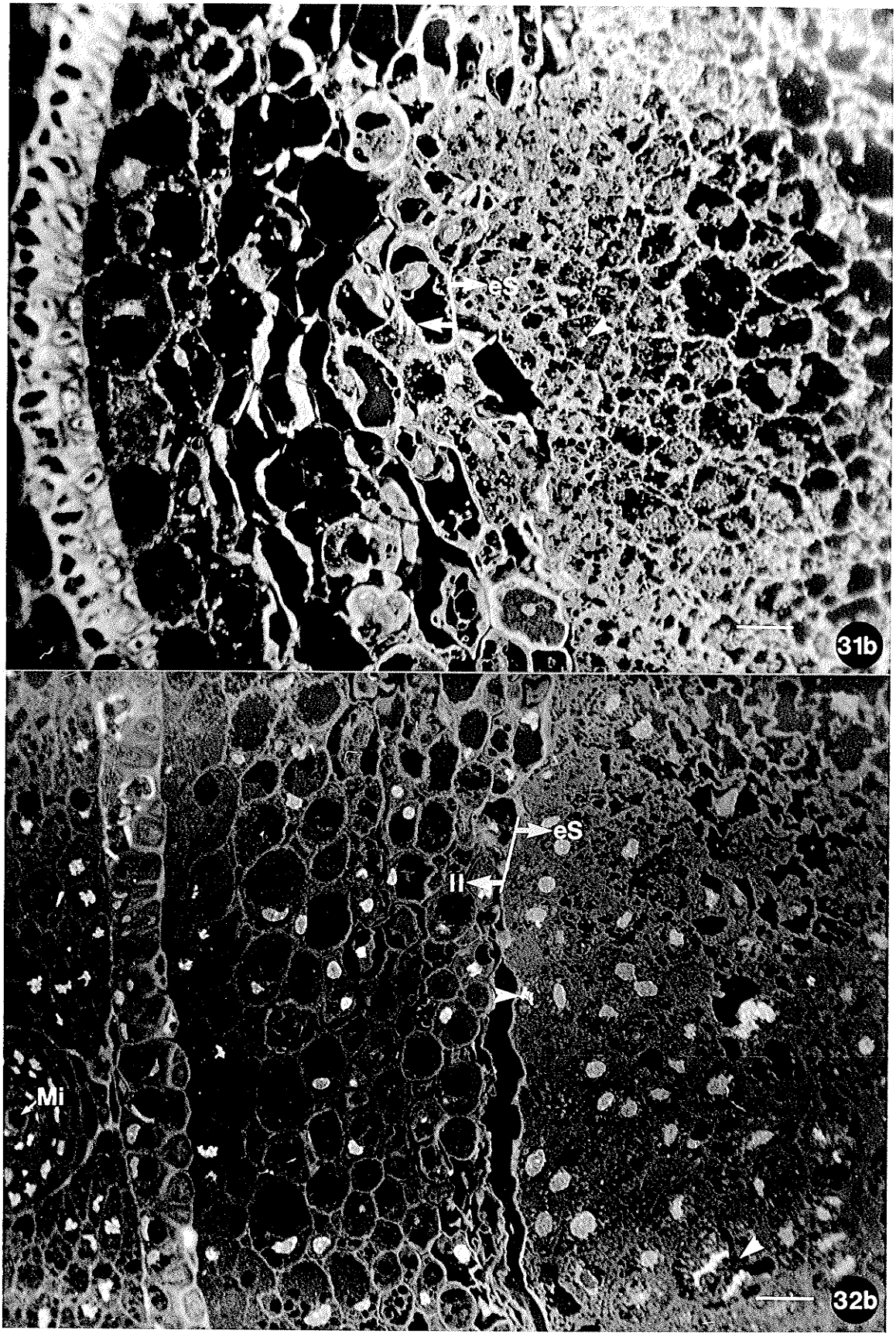
eS
31b
eS
II
Mi
32b

Figure 33. Electron micrograph of the outer endosperm and inner integument at 18 DPP, stained with uranyl acetate-lead citrate. The chloroplasts (cP) of the endosperm (eS) contain multiple starch grains (SG). Each starch grain is bounded by an electron-lucent region (arrowheads). 1 cm scale bar = 3.23μm.

Figure 34. Electron micrograph of a chloroplast in the endosperm at 18 DPP, stained with uranyl acetate-lead citrate: higher magnification of Figure 33. Long profiles of RER (arrowheads) associate with the periphery of chloroplasts (cP), which contain starch grains (SG). 1 cm scale bar = 0.645μm.

Figure 35. Electron micrograph of lipid droplets in the endosperm at 18 DPP, stained with uranyl acetate-lead citrate: higher magnification of Figure 33. Electron-dense particles (large arrowheads) encircle the lipid droplets (LD). Electron-opaque globules (small arrowheads) are visible in the mitochondria (M). A portion of a nucleus (N), and rough endoplasmic reticulum (RER) are also visible. 1 cm scale bar = 0.430μm.

Figure 36. Electron micrograph of inclusions in the endosperm at 18 DPP, stained with uranyl acetate-lead citrate. Many of the small vacuoles contain an electron-opaque astroid-shaped inclusion (arrowheads). 1 cm scale bar = 0.806μm.

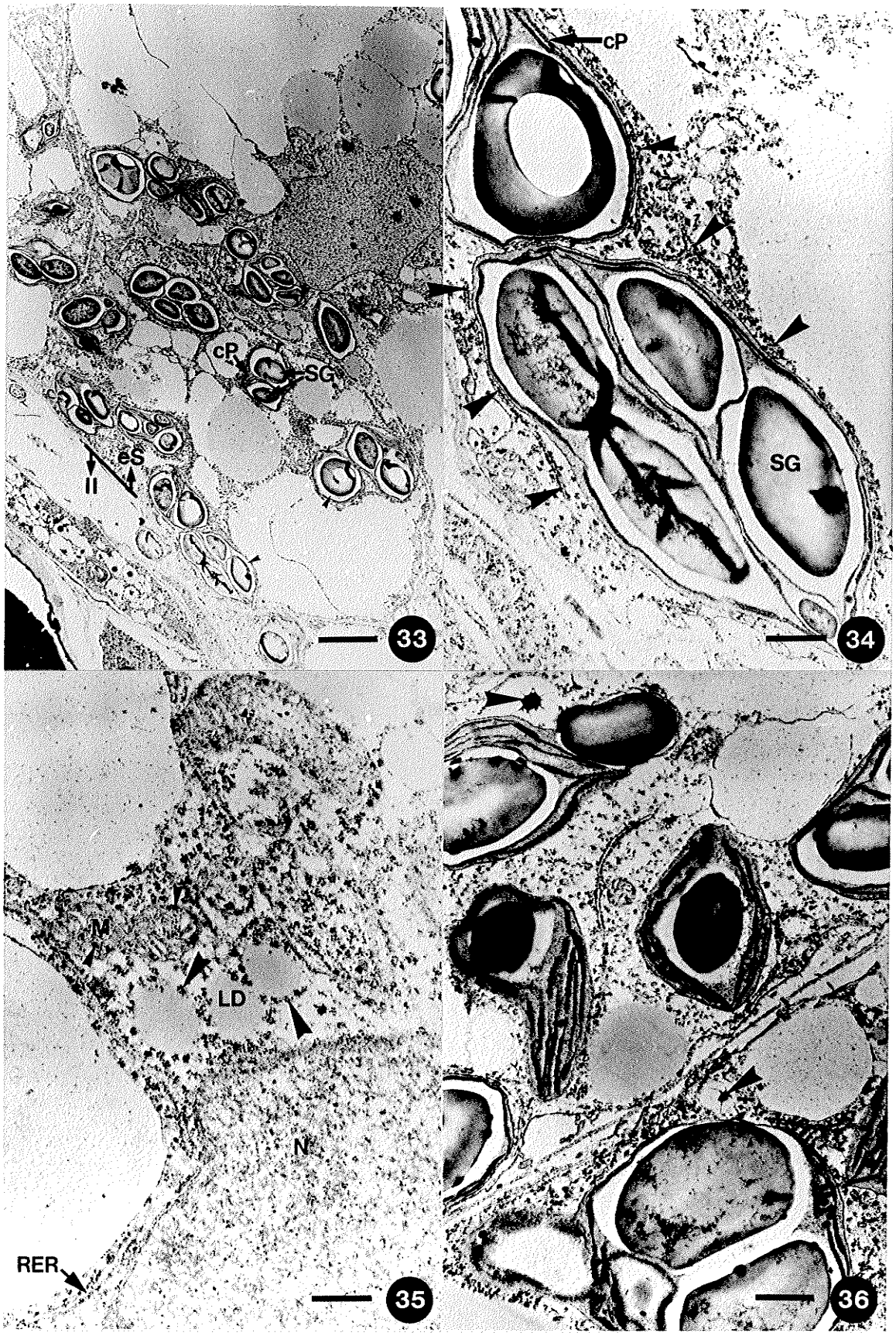
cP
SG
eS
II
33
cP
SG
34
M
LD
N
RER
35
36

Figure 37. Electron micrograph of an inclusion in the endosperm at 18 DPP, stained with uranyl acetate-lead citrate. A vacuole containing an electron-opaque inclusion (arrowhead) appears to be associated with dictyosomes (dS) that are producing dictyosome vesicles (DV). A portion of a nucleus (N) is also visible. 1 cm scale bar = 0.430μm.

Figure 38. Electron micrograph of an inclusion in the endosperm at 18 DPP, stained with uranyl acetate-lead citrate. Strands of an electron-opaque inclusion appear to be associated with particles (arrowhead) that border the tonoplast. 1 cm scale bar = 0.430μm.

Figure 39. Electron micrograph of the inner integument at 18 DPP, stained with uranyl acetate-lead citrate: higher magnification of Figure 33. Vacuoles with astroid inclusions (arrowheads) are present in the inner integument. 1 cm scale bar = 0.380μm.

Figure 40. Light micrograph of a portion of the seed at 22 DPP, stained with crystal violet. The aleurone layer (AL) has differentiated from the outermost layer of the endosperm tissue (eS). The inner integument (II) is collapsing, but the outer integument (OI) is still intact. A cotyledon (Cot) of the embryo is also visible. 1 cm scale bar = 38.9μm.

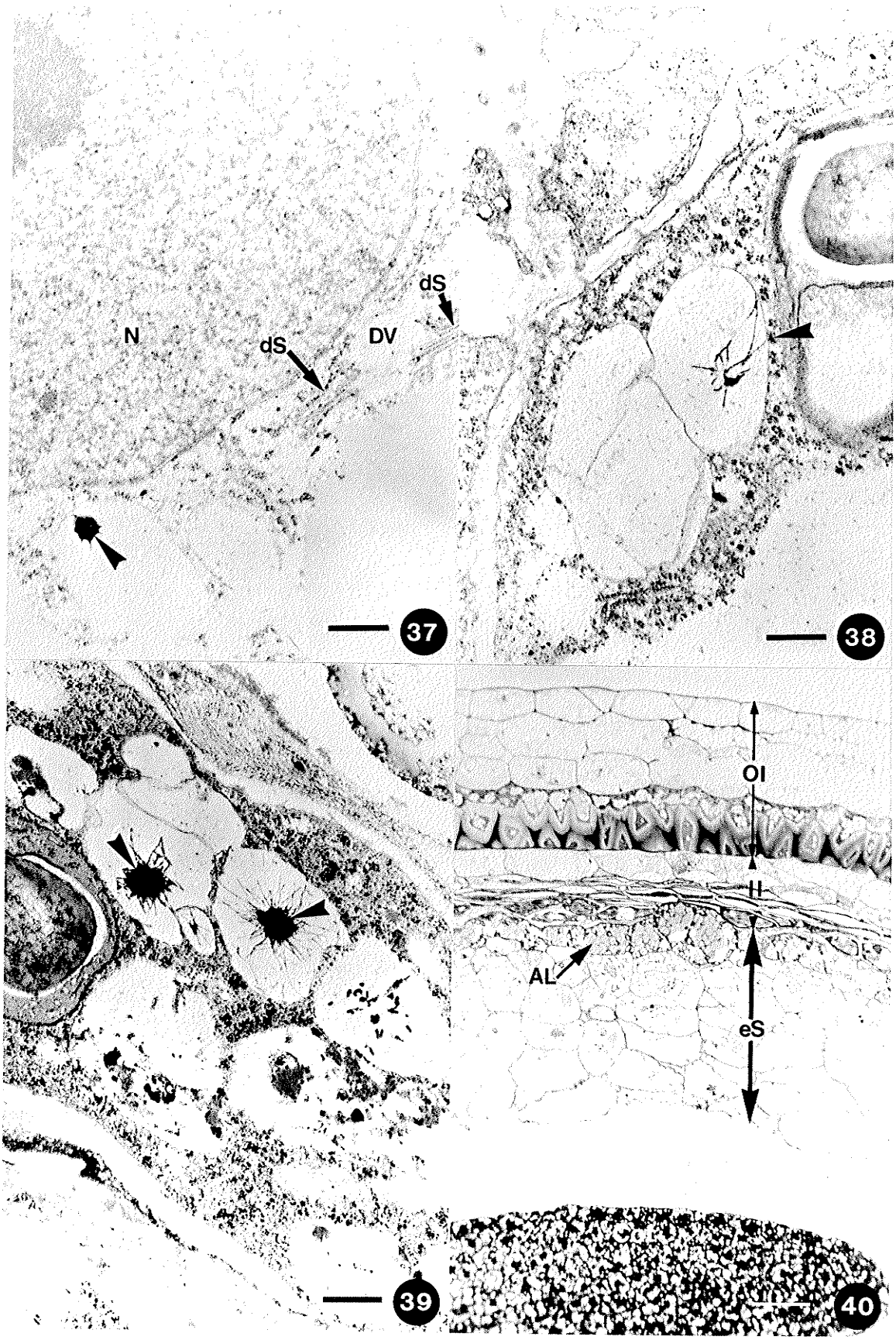
N
dS
DV
dS
37
38
OI
II
AL
eS
39
40

Figure 41a. Light micrograph of the endosperm and testa at 22 DPP, stained with Sudan black B: higher magnification of Figure 41b. The aleurone layer (AL) contains denser accumulations of lipid droplets (arrowheads) than that of the underlying endosperm (UeS). The cytoplasm of inner integument (II) and of palisade layer cells (arrow) are sudanophilic. 1 cm scale bar = 9.74μm.

Figure 41b. Light micrograph of a portion of the seed at 22 DPP, stained with Sudan black B: semi-adjacent section to Figure 40. Lipid droplets (arrowheads) are absent from both the inner integument (II) and the outer integument (OI), but are present in the endosperm (eS) and the cotyledon (Cot). The cotyledon appears to have a denser accumulation of lipid droplets than that of the aleurone layer (AL). 1 cm scale bar = 38.9μm.

Figure 42a. Light micrograph of the endosperm and testa at 22 DPP, stained with PAS: higher magnification of Figure 42b, and semi-adjacent section to Figure 41a. The aleurone layer (AL) contains smaller amyloplasts (arrowheads) than those of the underlying endosperm (UeS) and of the inner integument (II). 1 cm scale bar = 9.74μm.

Figure 42b. Light micrograph of a portion of the seed at 22 DPP, stained with PAS: semi-adjacent section to Figure 41b. Starch grains (arrowheads) are present in the outer integument (OI), the endosperm (eS), and the cotyledon (Cot), but the inner integument (II) is virtually devoid of starch grains. The cotyledon appears to contain denser accumulations of starch than that of the aleurone layer (AL). 1 cm scale bar = 38.9μm.

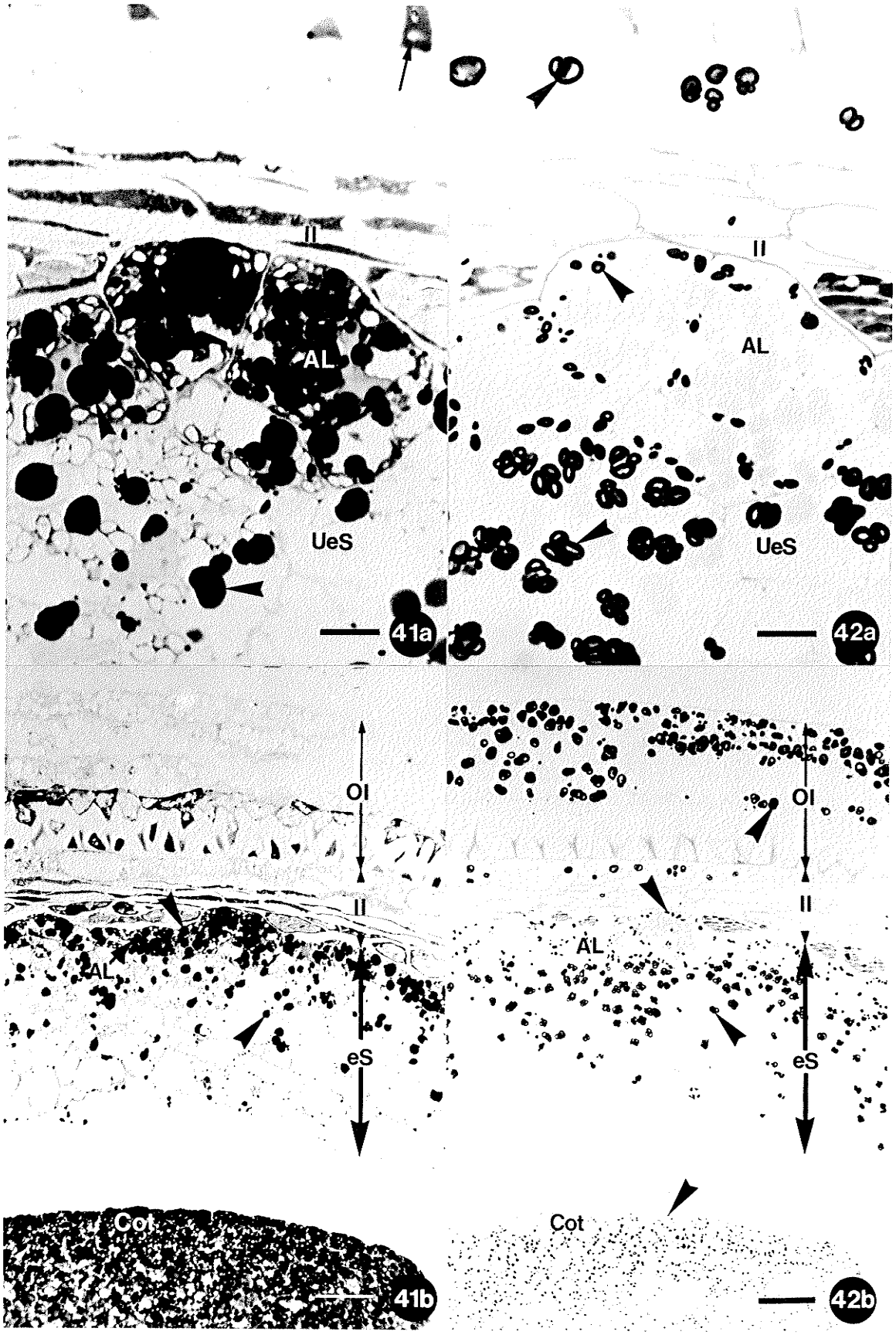
II
AL
UeS
41a
II
AL
UeS
42a
OI
II
AL
eS
OI
II
AL
eS
Cot
41b
Cot
42b

Figure 43. Light micrograph of the endosperm and testa at 22 DPP, stained with crystal violet: higher magnification of Figure 40. The aleurone layer (AL) contains denser accumulations of lipid droplets and starch grains than those of the underlying endosperm (UeS). The outermost cells (arrow) of the inner integument (II) are degenerating. The remainder of the inner integument is at an advanced stage of degeneration. 1 cm scale bar = 9.74μm.

Figure 44. Electron micrograph of lipid droplets in the endosperm at 22 DPP, stained with uranyl acetate-lead citrate. The lipid droplets (LD) are encircled with electron-dense particles (arrowheads). 1 cm scale bar = 0.538μm.

Figure 45. Electron micrograph of the endosperm and pigment layer at 22 DPP, stained with uranyl acetate-lead citrate. The aleurone cells (AL) contain fewer starch grains per chloroplast (cP) than those of the underlying endosperm cells (UeS). The anticlinal cell walls of the aleurone layer are broken (black arrowheads), and some of the lipid droplets appear to be coalescing (asterisks). The cells of the pigment layer lack starch grains, but contain electron-opaque grains (white arrowheads) that lack inclusions. 1 cm scale bar = 6.45μm.

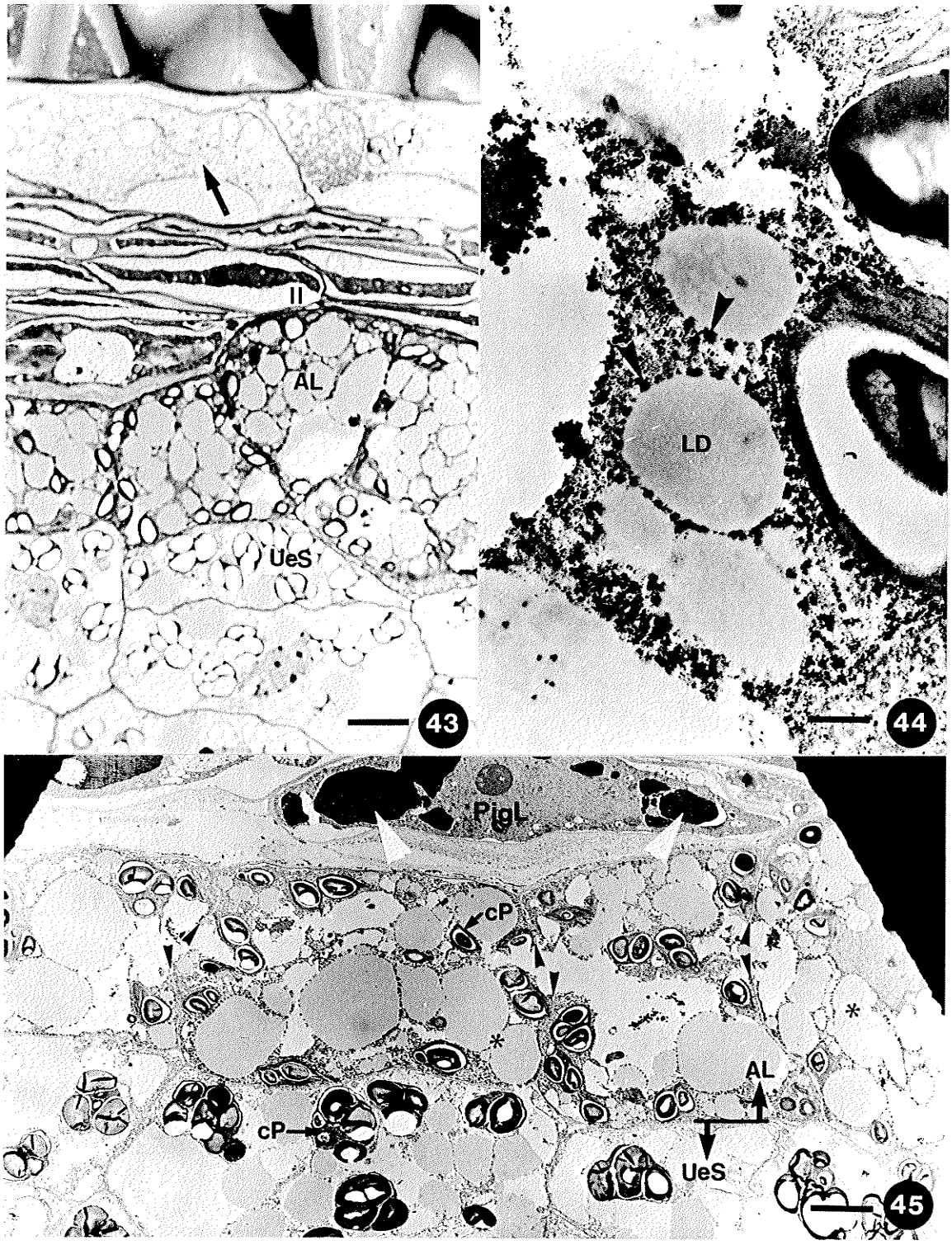
II
AL
UeS
43
LD
44
PigL
cP
cP
AL
UeS
45

Figure 46. Electron micrograph of chloroplasts in the endosperm at 22 DPP, stained with uranyl acetate-lead citrate. Rough endoplasmic reticulum (arrowheads) is associated with chloroplasts (cP) of both the aleurone layer (AL) and the underlying endosperm (UeS). 1 cm scale bar = 1.08μm.

Figure 47a. Light micrograph of the endosperm and inner integument at 22 DPP. The inner integument (II) has collapsed, leaving only the pigment layer (PigL) intact. Most of the plastids (P) in the endosperm have flattened profiles. The aleurone layer (AL) shows a denser accumulation of storage reserves, while the underlying endosperm shows a corresponding loss of storage reserves (compare to Figure 43). The underlying endosperm is beginning to collapse. 1 cm scale bar = 9.74μm.

Figure 47b. Light micrograph of the endosperm and inner integument at 22 DPP, stained with PAS: semi-adjacent section to Figure 47a. Virtually no starch grains (arrowheads) are left in the underlying endosperm (UeS) and in the pigment layer, and there are less starch grains in the aleurone layer (AL) than previously (compare to Figure 42a). 1 cm scale bar = 9.74μm.

Figure 47c. Light micrograph of the endosperm and inner integument at 22 DPP, stained with Sudan black B: semi-adjacent section to Figure 47a. Lipid droplets (arrowhead) are densely packed in the aleurone layer (AL). Plastids (P) also stain positively with Sudan black B. 1 cm scale bar = 9.74μm.


cR
UeS
AL
46

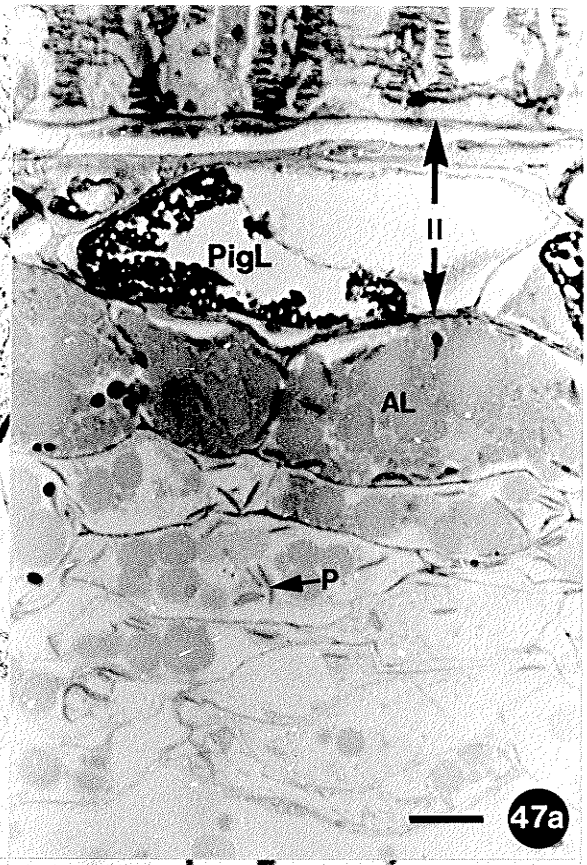
PigL
II
AL
P
47a

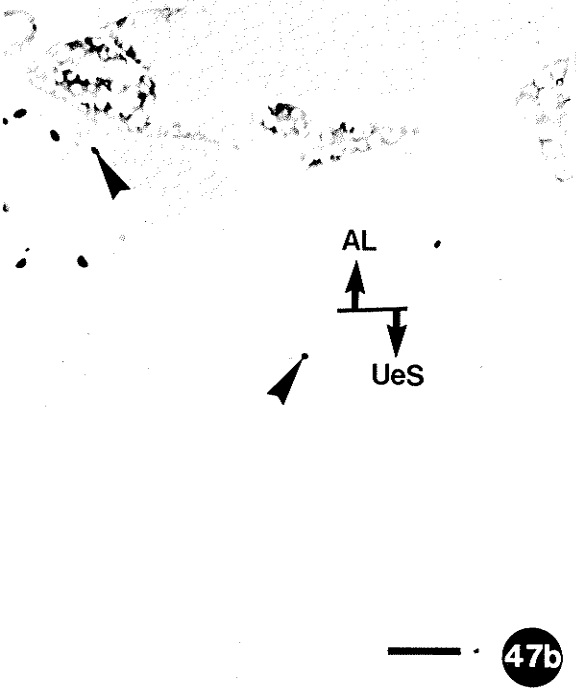
AL
UeS
47b

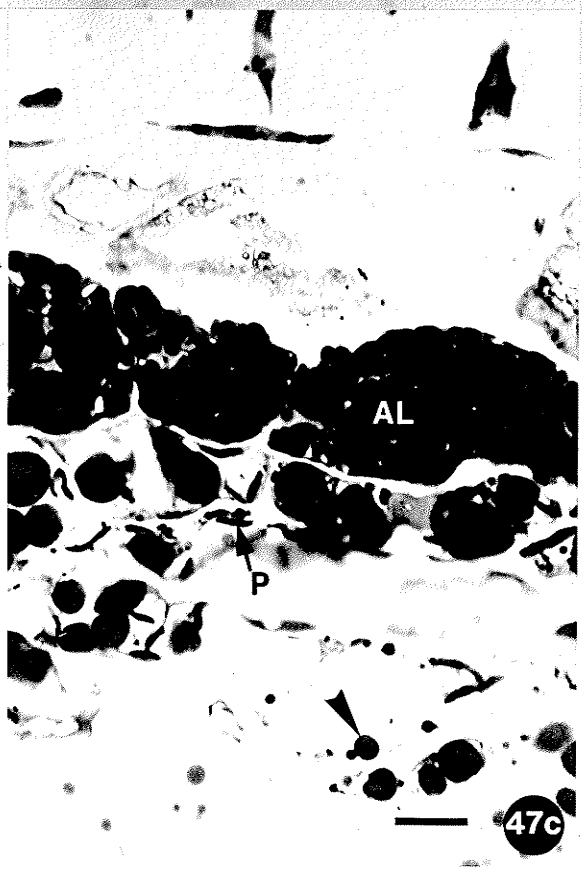
AL
P
47c

Figure 48. Electron micrograph of the endosperm at 22 DPP, stained with uranyl acetate-lead citrate. The cell walls (CW) of the aleurone layer (AL) are markedly thicker at the outer periclinal wall, where the protoplast has pulled away (asterisk). The chloroplasts (cP) of the aleurone layer are biconvex in section, but many of those in the underlying endosperm (UeS) that lack starch are flattened. The degenerating cells of the underlying endosperm are plasmolyzed, contain amoeboid nuclei (N), and have cell wall thickenings at the vertices (arrowheads). 1 cm scale bar = 5μm.

Figure 49. Electron micrograph of chloroplasts in the aleurone layer at 22 DPP, stained with uranyl acetate-lead citrate. Grana (arrowheads) are visible in the chloroplasts (Cp). 1 cm scale bar = 0.806μm.

Figure 50. Electron micrograph of the underlying endosperm at 22 DPP, stained with uranyl acetate-lead citrate. Electron-translucent globules (arrowheads), but not internal membranes, are visible in the plastids (P). The mitochondria (M) have electron-lucent cristae, and the nucleus (N) is amoeboid. 1 cm scale bar = 1.29μm.

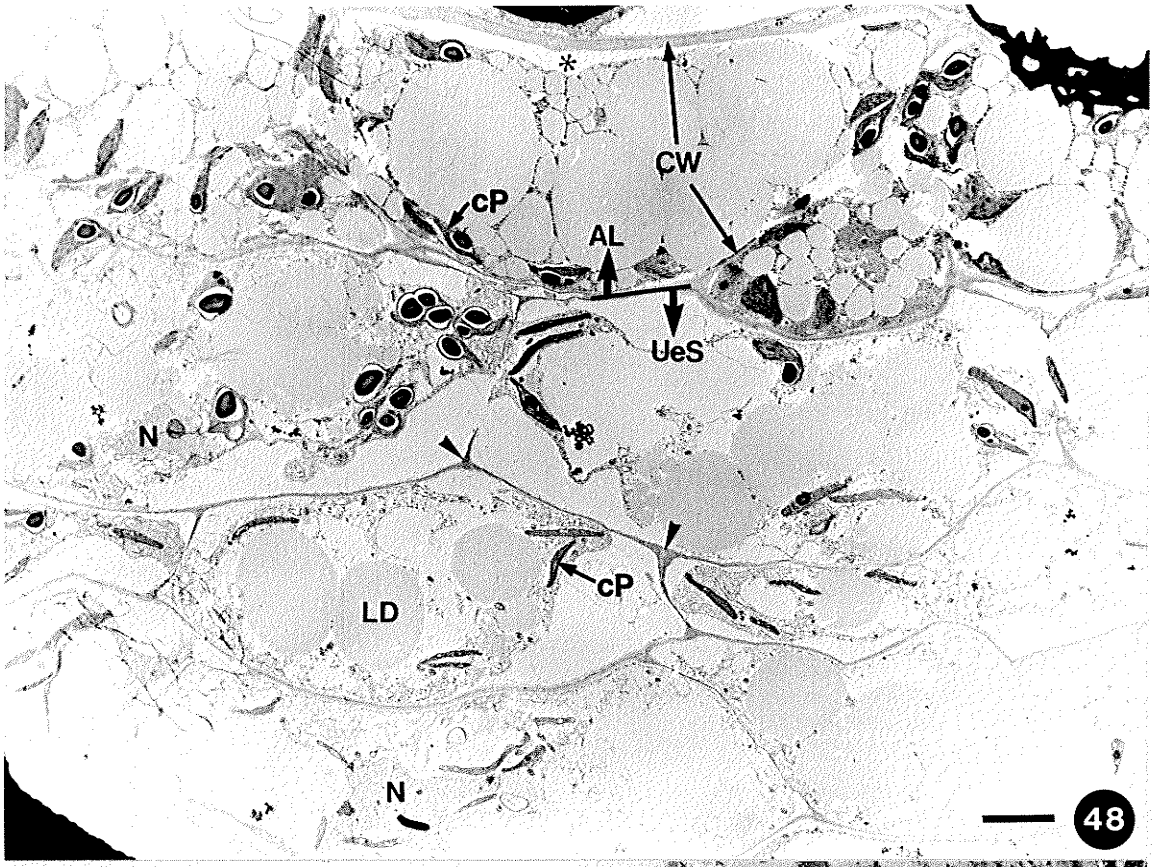
CW
cP
AL
UeS
N
cP
LD
N
48


cp
49


P
M
N
50

Figure 51. Electron micrograph of an aleurone cell at 22 DPP, stained with uranyl acetate-lead citrate. The thickening outer periclinal cell wall (CW) has alternating dark (arrowheads) and light layers. The chloroplast (cP) lacks starch, but contains grana (white arrowhead). Endoplasmic reticulum (ER) and a mitochondrion (M) are visible. 1 cm scale bar = 0.922μm.

Figure 52a Light micrograph of the endosperm and testa at 30 DPP, stained with crystal violet. The cell walls of the endosperm are thickening (arrowheads). The aleurone layer (AL) contains a dense accumulation of storage reserves, but the underlying endosperm cells stain lightly and are collapsing. 1 cm scale bar = 9.74μm.

Figure 52b. Light micrograph of the endosperm and testa at 30 DPP, stained with Sudan black B: semi-adjacent section to Figure 52a. The protoplast of the aleurone layer (AL) is sudanophilic. The underlying endosperm contains small lipid droplets (arrowhead) and plastids (P) that stain positively. 1 cm scale bar = 9.74μm.

Figure 52c. Light micrograph of the endosperm and testa at 30 DPP, stained with PAS: semi-adjacent section to Figure 52a. Starch grains (arrowhead) are present in the aleurone layer (AL), but not in the underlying endosperm. 1 cm scale bar = 9.74μm.

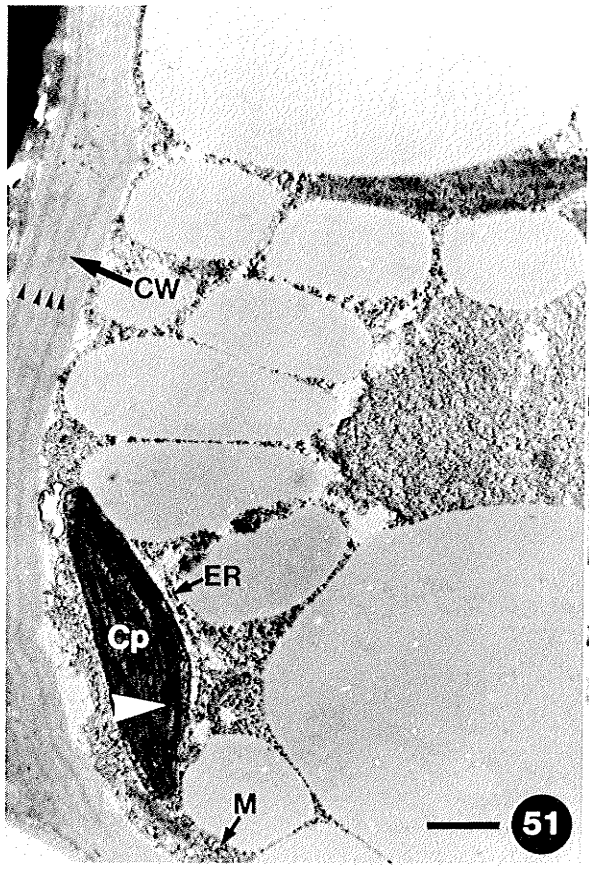

51

52a

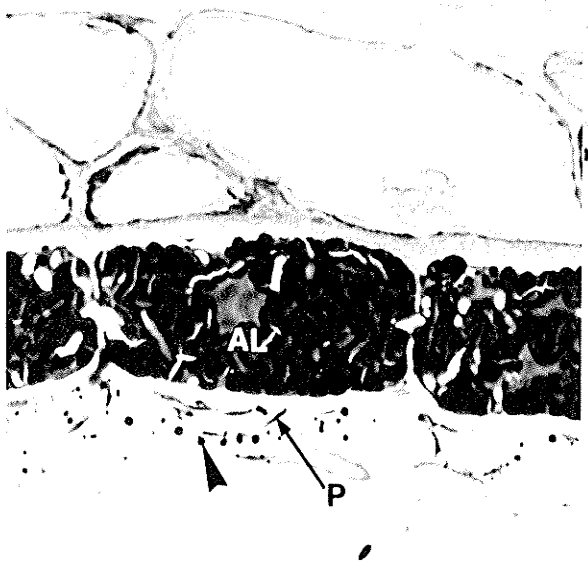

52b

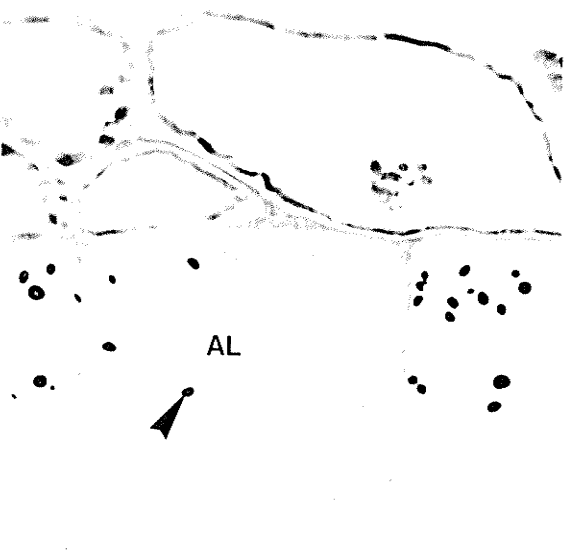

52c

Figure 53. Electron micrograph of the endosperm and pigment layer at 30 DPP, stained with uranyl acetate-lead citrate. The cell walls of the endosperm are thicker at the corners (arrowheads). Lipid droplets (LD) are present in both the aleurone layer (AL) and the underlying endosperm, but chloroplasts with starch grains (SG) are present only in the aleurone layer. A nucleus (N) is visible in the underlying endosperm. The cells of the pigment layer (PigL) contain a large vacuole (V) lined with electron-opaque material (arrows). 1 cm scale bar = 3.33μm.

Figure 54. Electron micrograph of the endosperm at 30 DPP, stained with uranyl acetate-lead citrate. The nucleus (N) of the underlying endosperm is flattened, and electron-opaque deposits (arrowheads) are visible between the plasmalemma and the cell wall. AL aleurone layer. 1 cm scale bar = 1.29μm.

Figure 55. Electron micrograph of the endosperm at 30 DPP, stained with uranyl acetate-lead citrate. Electron-translucent globules (arrowheads) are present in the chloroplasts (cP) of the underlying endosperm. AL aleurone layer. 1 cm scale bar = 0.538μm.

Figure 56. Electron micrograph of the underlying endosperm at 30 DPP, stained with uranyl acetate-lead citrate. The cisternae of the rough endoplasmic reticulum (RER) appears to be collapsed at regions (arrowheads) lack ribosomes. 1 cm scale bar = 0.430μm.

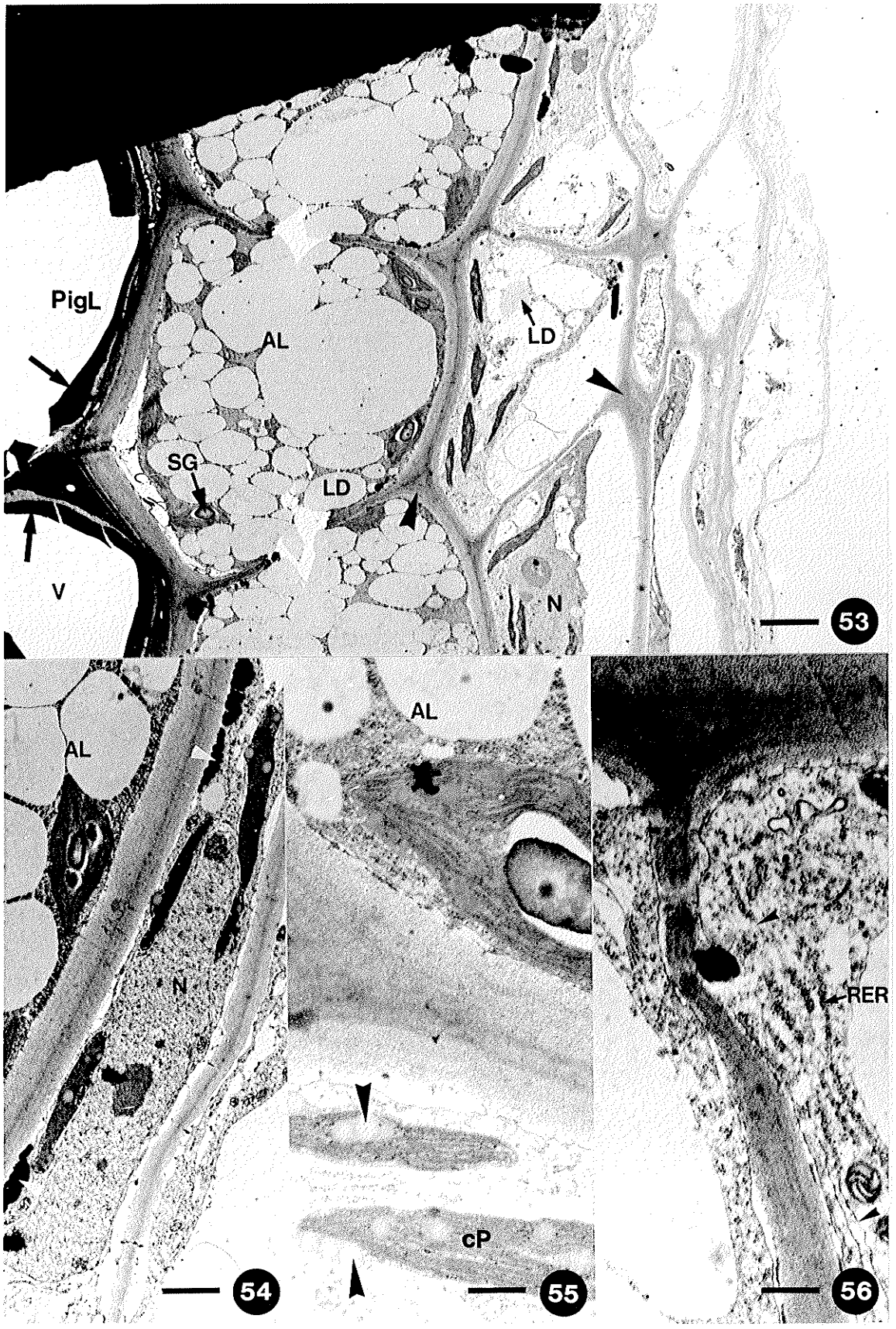
PigL
AL
LD
SG
LD
V
N
53
AL
AL
N
cP
54
55
RER
56

Figure 57. Electron micrograph of the aleurone layer at 30 DPP, stained with uranyl acetate-lead citrate. The appressed lipid droplets (LD) appear not to fuse, and they have an electron-dense layer where they contact one another. The spaces at the breaks of the anticlinal cell wall and between the protoplast and the outer periclinal cell wall (asterisks) are an artefact of specimen preparation. 1 cm scale bar = 1.08μm.

Figure 58. Electron micrograph of the lipid droplets of the aleurone layer at 30 DPP, stained with uranyl acetate-lead citrate. Electron-dense material (asterisk) found among the lipid droplets (LD) appears similar in texture and electron density to that of the particles (arrowheads) that encircle the lipid droplets. 1 cm scale bar = 0.430μm.

Figure 59a. Light micrograph of the endosperm and testa at 34 DPP, stained with crystal violet. The underlying endosperm (UeS) has collapsed completely. Intensely-staining protein bodies (arrowhead) are evident in the aleurone layer (AL). 1 cm scale bar = 9.74μm.

Figure 59b. Light micrograph of the endosperm and testa at 34 DPP, stained with coomassie brilliant blue: semi-adjacent section to Figure 59a. Protein bodies (arrowhead) of the aleurone layer (AL) and the portion of the plastids enclosing each starch grain (SG) stain positively. 1 cm scale bar = 9.74μm.

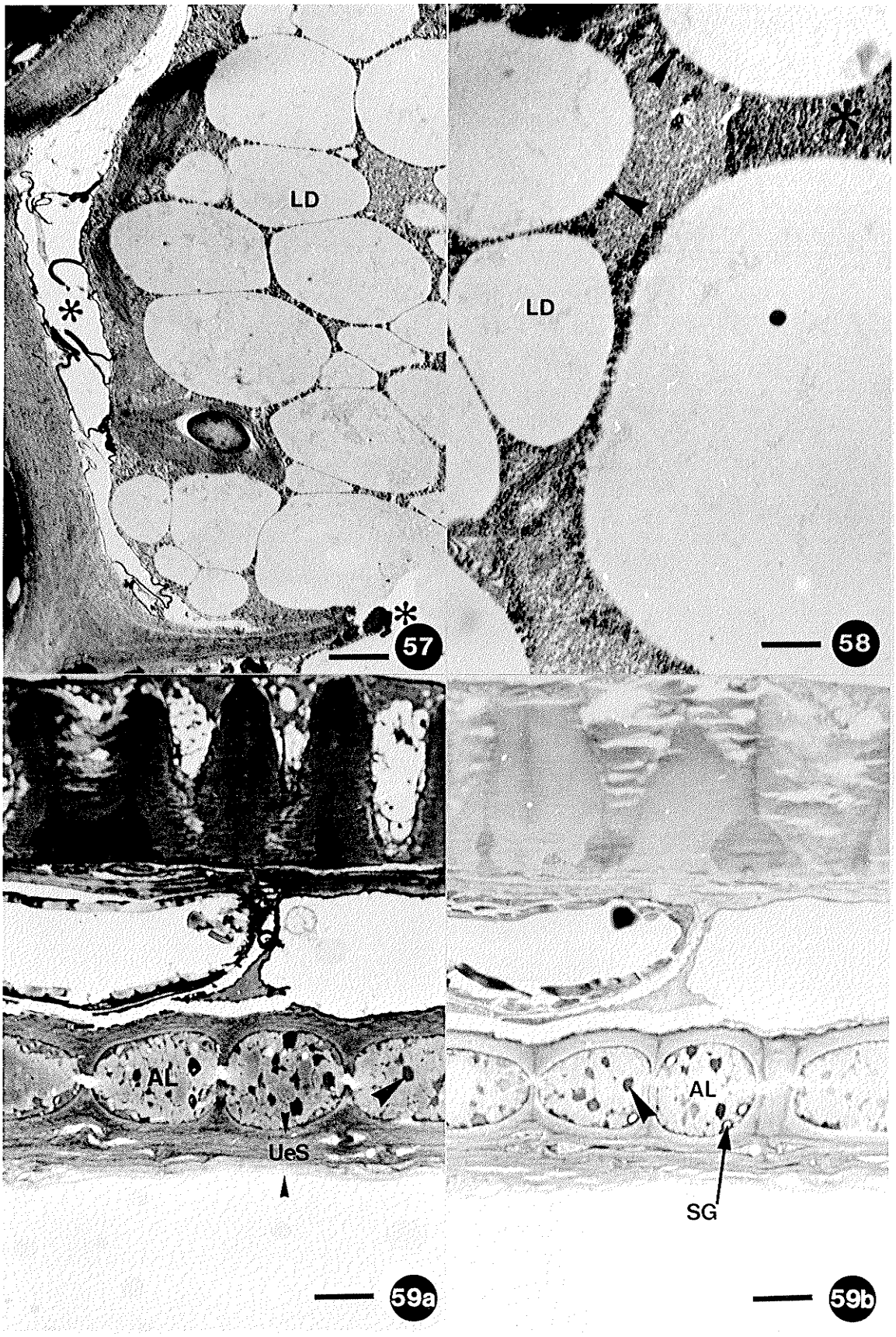
LD
LD
AL
UeS
AL
SG
57
58
59a
59b

Figure 59c. Light micrograph of the endosperm and testa at 34 DPP, stained with PAS: semi-adjacent section to Figure 59a. Starch grains (arrowhead) are present in the aleurone layer (AL). 1 cm scale bar = 9.74μm.

Figure 59d. Light micrograph of the endosperm and testa at 34 DPP, stained with Sudan black B: semi-adjacent section to Figure 59a. The protoplasts of the aleurone layer (AL) and of the palisade layer (PalL) are sudanophilic. The cell walls of the palisade layer are weakly sudanophilic, appearing tan in colour. 1 cm scale bar = 9.74μm.

Figure 60. Electron micrograph of an aleurone cell at 34 DPP, stained with uranyl acetate-lead citrate. The aleurone cell contains protein bodies (PB), lipid droplets (LD), plastids (P), and a nucleus (N). Some of the plastids contain a starch grain (SG). The breakages (asterisks) at the anticlinal cell walls are an artefact of specimen preparation. Above the aleurone cell is the inner integument (II) and below it is the collapsed underlying endosperm (UeS). 1 cm scale bar = 1.78μm.

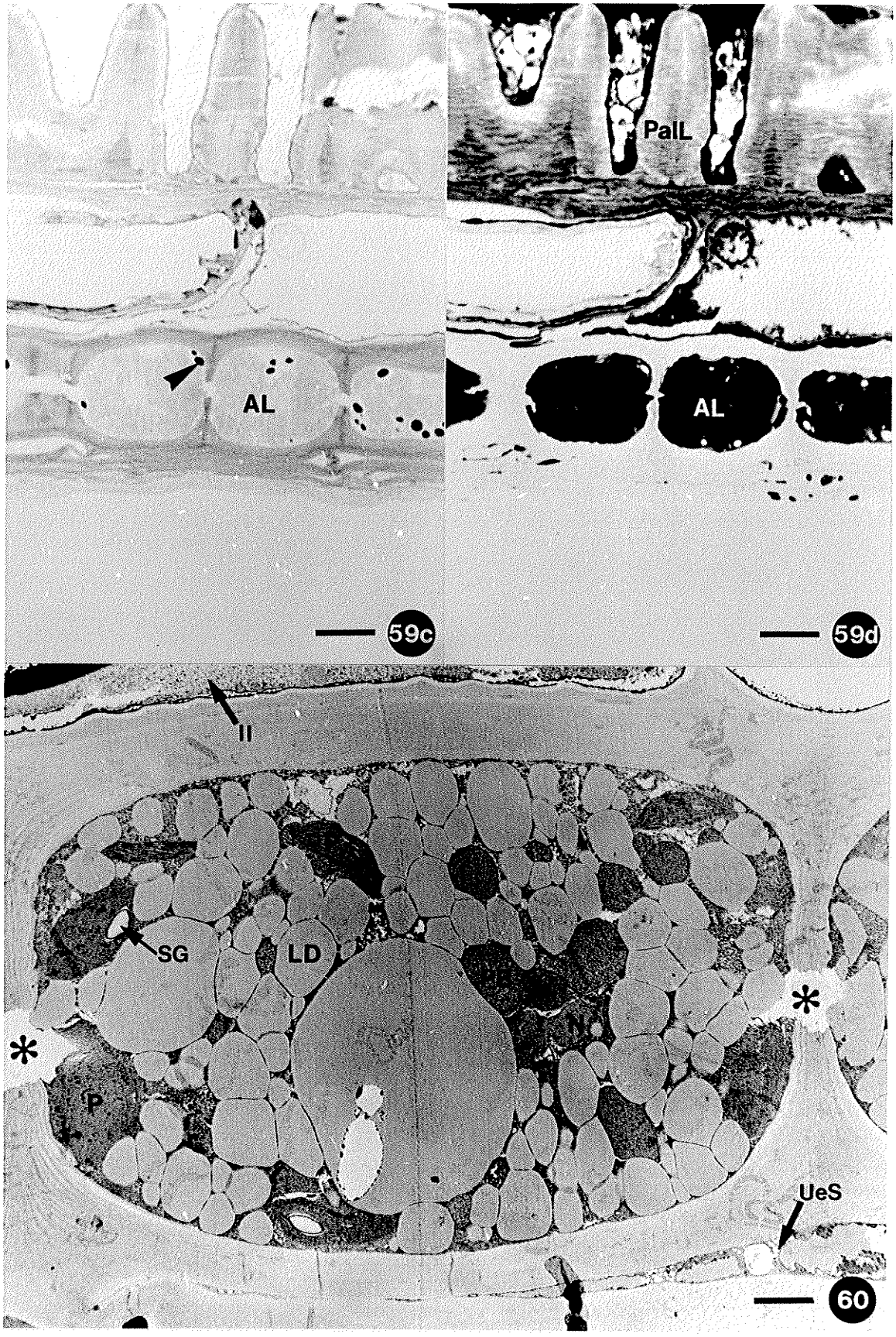
AL
PalL
AL
59c
59d
II
SG
LD
P
UeS
60

Figure 61. Electron micrograph of a protein body in the aleurone layer at 34 DPP, stained with uranyl acetate-lead citrate. The protein body (PB) contains a granular matrix and it appears to be bounded by a unit membrane (white circle). 1 cm scale bar = 0.215μm.

Figure 62. Electron micrograph of a nucleus in the aleurone layer at 34 DPP, stained with uranyl acetate-lead citrate. The nucleus (N) contains a fine pattern of condensed chromatin, and its outline is deformed by adjacent lipid droplets (LD). 1 cm scale bar = 0.922μm.

Figure 63. Electron micrograph of a chloroplast in the aleurone layer at 34 DPP, stained with uranyl acetate-lead citrate. The chloroplast (cP) contains a starch grain (SG), and electron-dense globules (arrowheads). 1 cm scale bar = 0.380μm.

Figure 64. Electron micrograph of the aleurone cytoplasm at 34 DPP, stained with uranyl acetate-lead citrate. Chloroplasts (Cp), and endoplasmic reticulum (small arrowheads) are found among the lipid droplets (LD). The lipid droplets have an electron-dense border where they contact (large arrowheads). 1 cm scale bar = 0.430μm.

Figure 65. Electron micrograph of the aleurone cell wall at 34 DPP, stained with uranyl acetate-lead citrate. A fibrillar, herringbone pattern (arrowheads) is evident in a section of the cell wall (CW). 1 cm scale bar = 0.380μm.

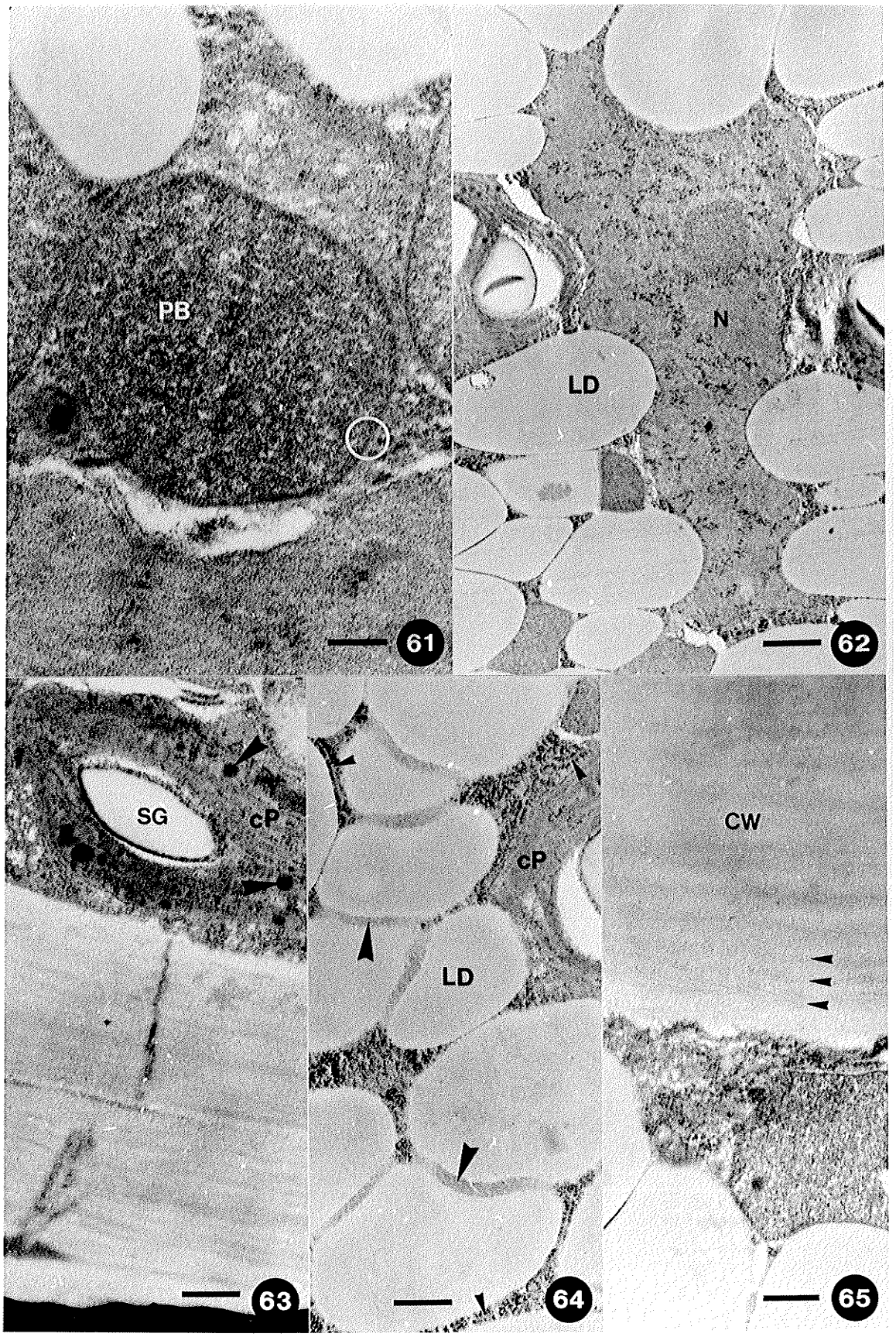
PB
61
N
LD
62
SG
cP
63
cP
LD
64
CW
65

Figure 66a. Light micrograph of the testa and aleurone layer at 38 DPP, stained with crystal violet. The testa consists of the outer integument (OI) and the inner integument (II). The outer integument consists of an epidermis (eD), two cell layers of subepidermis (SeD), and a palisade layer (PalL). The cells of the testa appear empty, except for deposits appressed to the outer periclinal wall of the epidermal cells (arrowheads). All that remains of the inner integument is the pigment layer. Appressed to the inner face of the testa is the aleurone layer (AL). 1 cm scale bar = 38.9μm.

Figure 66b. Light micrograph of the aleurone layer and testa at 38 DPP, stained with crystal violet: higher magnification of Figure 66a. Intensely staining deposits (arrowheads) are found in the pigment layer. The aleurone layer has thickened cell walls, and the anticlinal walls are intact. Appressed to the inner face of the aleurone layer is the crushed remains of the underlying endosperm. 1 cm scale bar = 9.74μm.

Figure 66c. Light micrograph of the aleurone layer and testa at 38 DPP, stained with PAS: semi-adjacent section to Figure 66b. Starch grains (arrowhead) are present in the aleurone layer. 1 cm scale bar = 9.74μm.

Figure 66d. Light micrograph of the aleurone layer and testa at 38 DPP, stained with Sudan black B: semi-adjacent section to Figure 66b. Lipid droplets (arrowhead) are revealed in the aleurone layer. The aleurone cell wall is non-sudanophilic, but the cell walls of the palisade layer (PalL) are weakly sudanophilic and stain tan in colour. 1 cm scale bar = 9.74μm.

Figure 66e. Light micrograph of the aleurone layer and testa at 38 DPP, stained with coomassie brilliant blue: semi-adjacent section to Figure 66b. Densely staining protein bodies (arrowheads) are evident in the aleurone layer. 1 cm scale bar = 9.74μm.

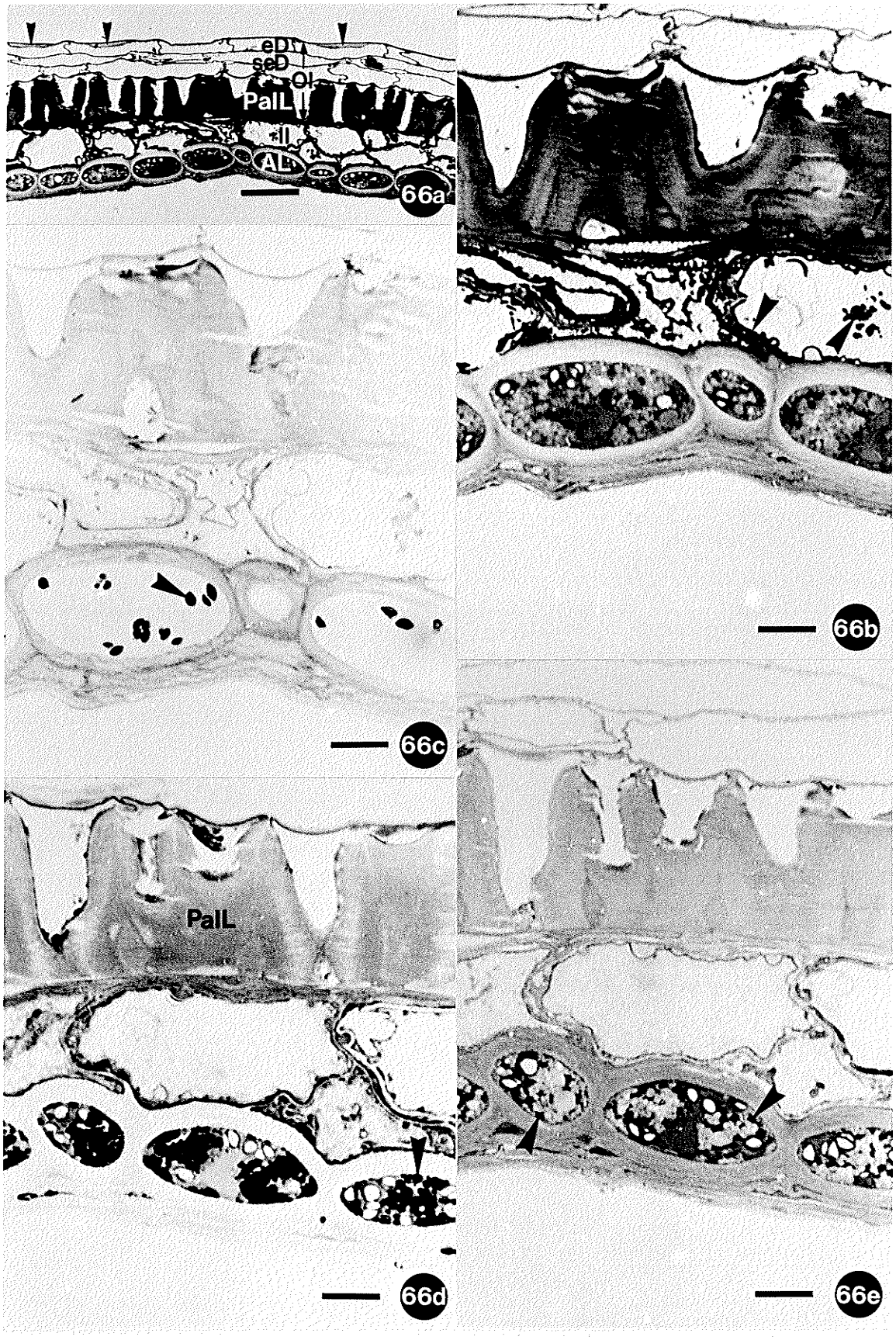
eD
seD
Ol
PalL
AL
66a
66b
66c
PalL
66d
66e

Figure 67. Electron micrograph of an aleurone cell at 38 DPP, stained with uranyl acetate-lead citrate. The lipid droplets (LD) have polygonal outlines. Protein bodies (PB) and chloroplasts (cP) that contain starch grains (SG) are also evident in the aleurone layer. The thickened cell wall (CW) has a banded appearance. 1 cm scale bar = 1.84μm.

Figure 68. Electron micrograph of the aleurone cytoplasm at 38 DPP, stained with uranyl acetate-lead citrate: higher magnification of Figure 67. The chloroplast (cP) contains starch grains (SG) and electron-dense globules (large arrowhead). Part of a protein body (PB) is evident. Among the organelles are profiles of endoplasmic reticulum (small arrowheads). 1 cm scale bar = 0.430μm.

Figure 69. Electron micrograph of a chloroplast in the aleurone layer at 38 DPP, stained with uranyl acetate-lead citrate: higher magnification of Figure 67. The chloroplast (cP) contains electron-translucent globules (arrowhead). 1 cm scale bar = 0.215μm.

Figure 70a. Light micrograph of isolated, mature aleurone layer at approx. 50 DPP, stained with crystal violet. Appressed to one face of the aleurone layer (AL) is the crushed remains of the underlying endosperm (UeS). 1 cm scale bar = 9.74μm.

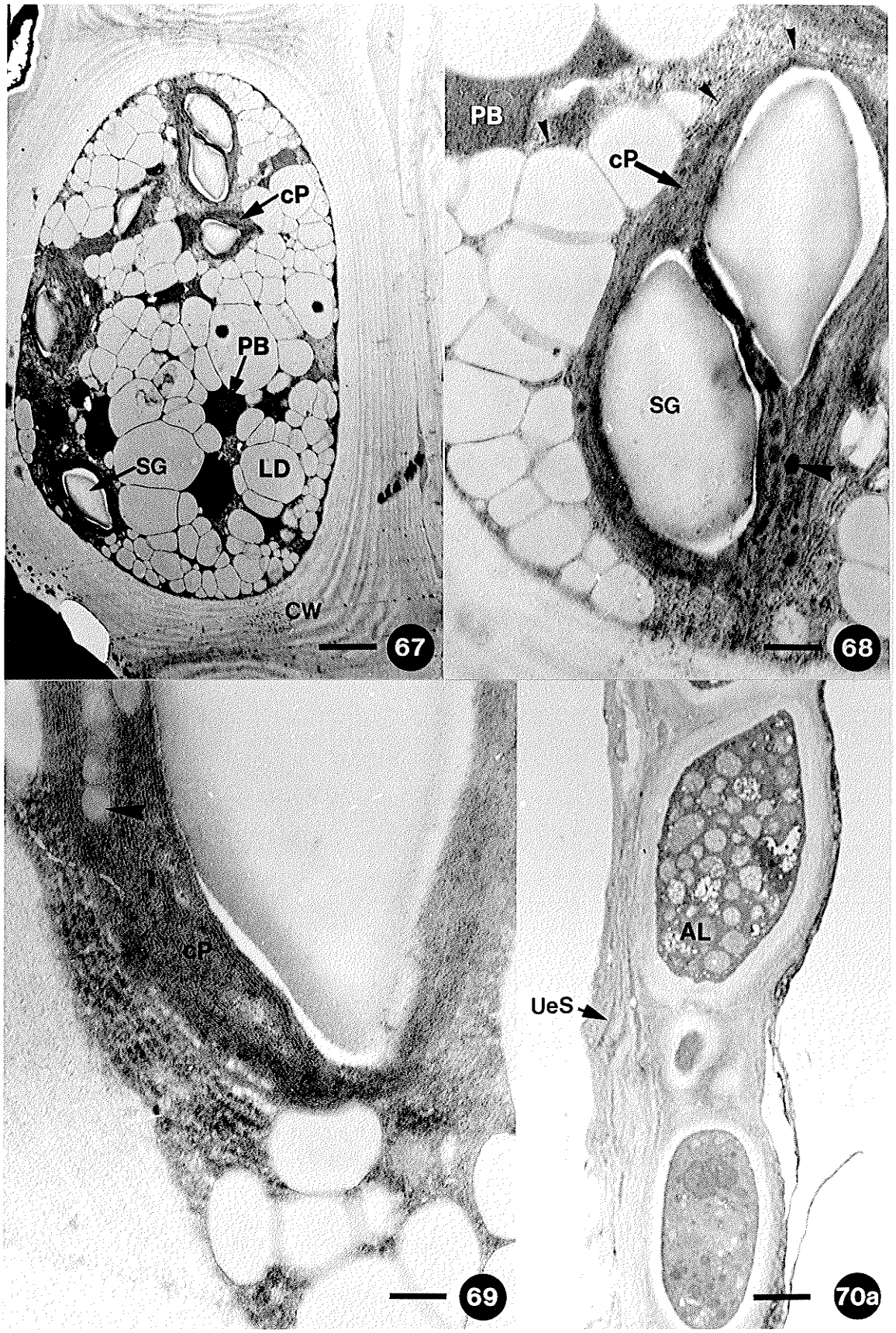
cP
PB
SG
LD
CW
67
PB
cP
SG
68
cP
69
AL
UeS
70a

Figure 70b. Light micrograph of isolated, mature aleurone layer at approx 50 DPP, stained with PAS: semi-adjacent section to Figure 70a. The aleurone protoplast lacks PAS-positive starch grains at this stage. 1 cm scale bar = 9.74μm.

Figure 70c. Light micrograph of isolated, mature aleurone layer at approx 50 DPP, stained with Sudan black B: semi-adjacent section to Figure 70a. Non-sudanophilic protein bodies (asterisk) are embedded in a matrix of sudanophilic material (black arrowhead). One cell contains large lipid droplets (white arrowhead). 1 cm scale bar = 9.74μm.

Figure 70d. Light micrograph of isolated, mature aleurone layer at approx 50 DPP, stained with coomassie brilliant blue: semi-adjacent section to Figure 70a. Protein bodies (asterisk) and the nucleus in the centre of the lowermost cell stain positively. 1 cm scale bar = 9.74μm.

Figure 71. Electron micrograph of an aleurone cell at maturity (approx 50 DPP), stained with uranyl acetate-lead citrate. Protein bodies (PB) and plastids (P) are embedded in a matrix of lipid droplets (LD). Small lipid droplets line the plasmalemma and the organelles. Two giant lipid droplets are evident in the centre of the cell. The protein bodies contain both electron-lucent and electron-opaque inclusions (arrowheads). The cell wall (CW) is greatly thickened. 1 cm scale bar = 1.78μm.

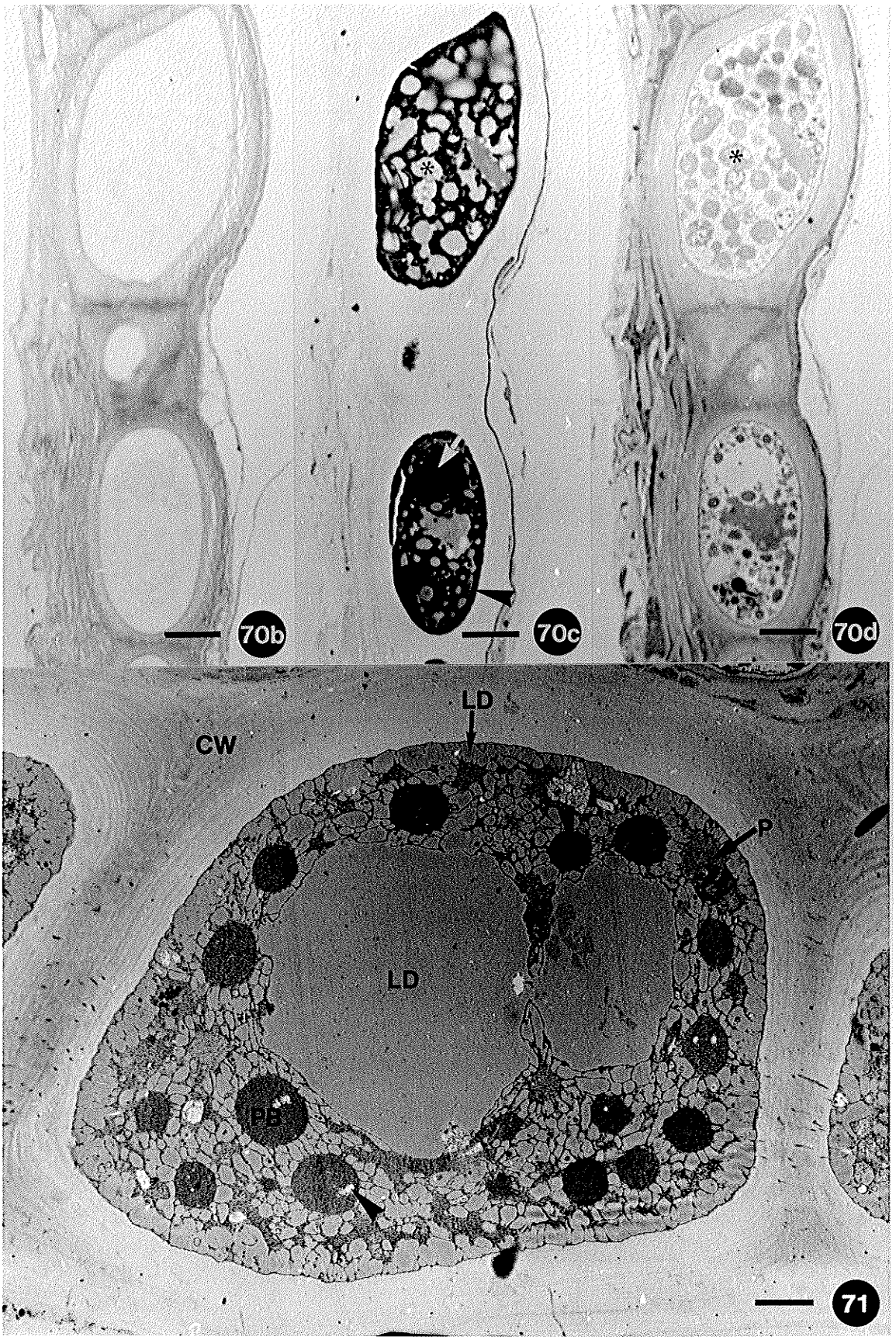
70b
70c
70d
LD
CW
P
LD
PB
71

Figure 72. Electron micrograph of the cytoplasm in an aleurone cell at maturity, stained with uranyl acetate-lead citrate. The plastid (P) contains electron-opaque globules, and lacks internal membranes. PB protein body. 1 cm scale bar = 0.430μm.

Figure 73a. Median section of a seed at 34 DPP, stained with crystal violet. The aleurone layer (AL) is continuous, except at the chalazal region (Ch). The underlying endosperm (UeS) appears thicker at the chalazal region than at the end opposite the chalaza. The micropyle (Mi) is also visible. Compare to Figure 1. 1 cm scale bar = 199μm.

Figure 73b. Light micrograph of the raphe of a seed at 34 DPP, stained with crystal violet: higher magnification of Figure 73a. The suspensor (S) interrupts the aleurone layer (AL) at the micropyle (Mi). The basal body (BB) is found between the micropyle and the chalaza (Ch). Cells of the endosperm (eS) contain starch grains in the inner layers, and plastids (black circle) near the chalaza. 1 cm scale bar = 54.7μm.

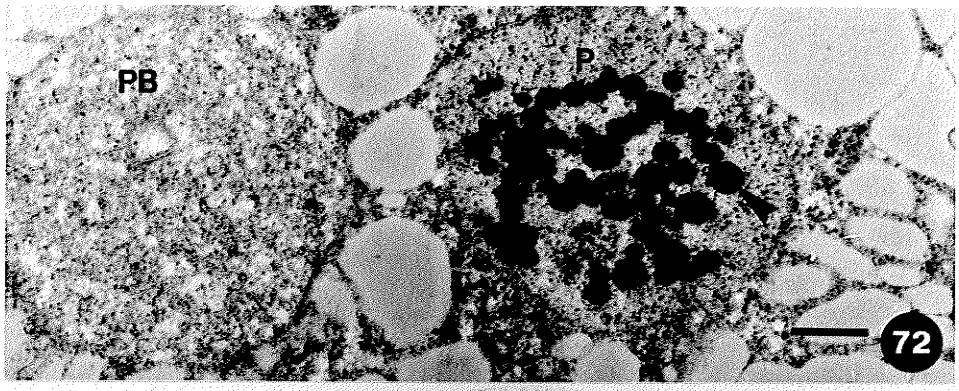

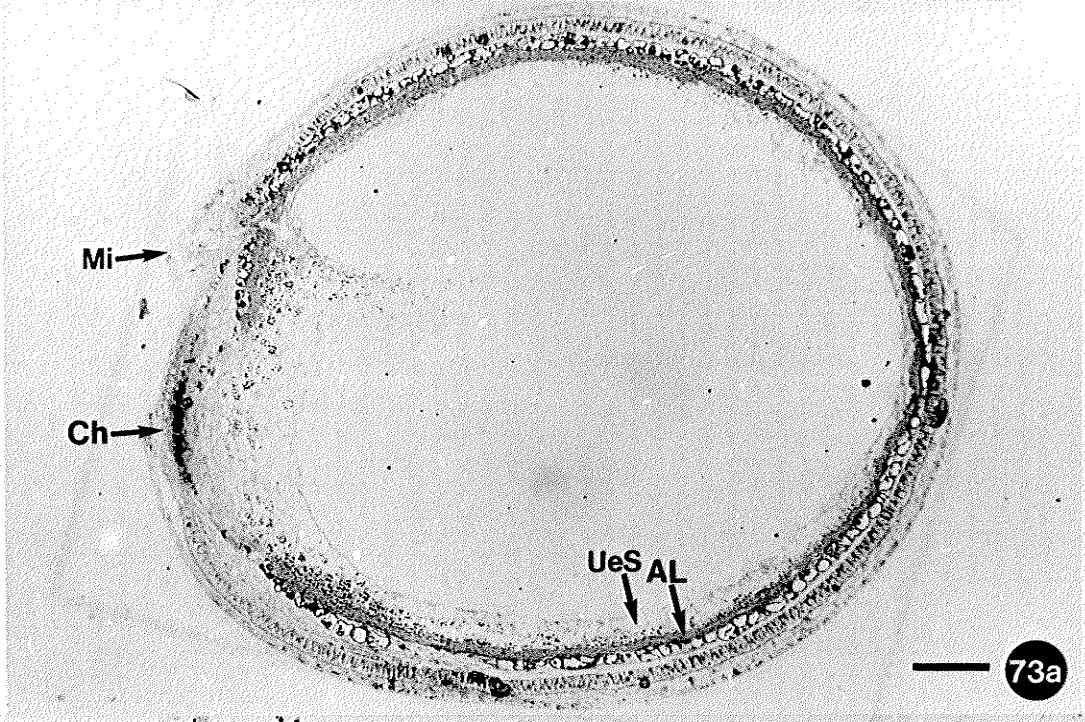

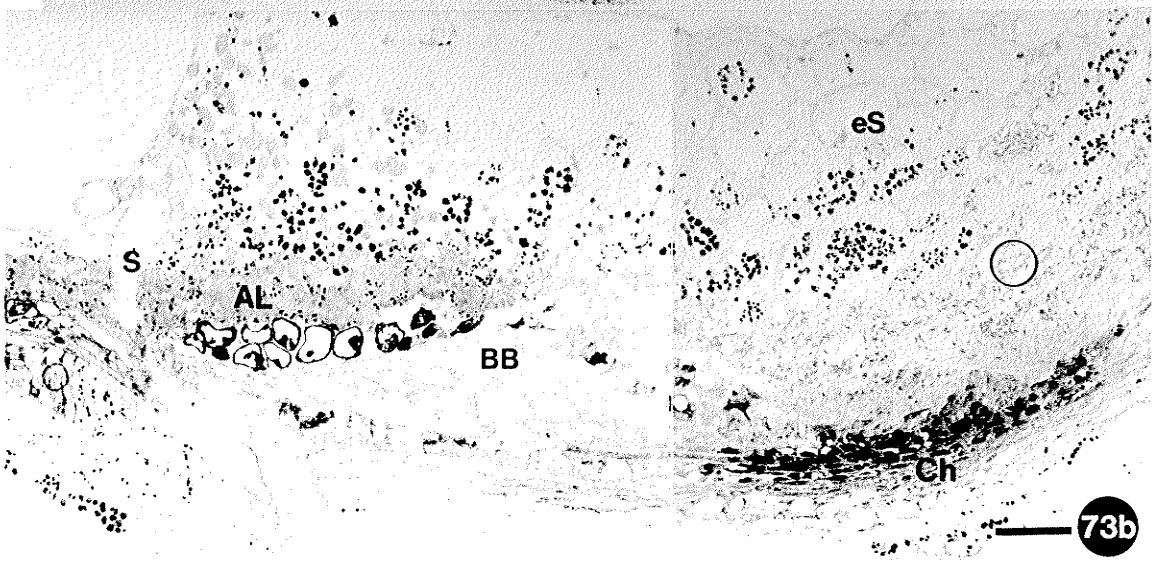

Mi

Figure 74. Fluorescent micrograph of free nuclear endosperm at 12 DPP, stained with Hoechst dye #33342 and viewed under UV excitation. The nuclei (N) are ovoid to round in outline. A telophase mitotic figure (arrow) and pinpoints of fluorescence (arrowhead) are evident. 1 cm scale bar = 9.74μm.

Figure 75. Fluorescent micrograph of embryo nuclei of a mature seed, stained with Hoechst dye #33342 and viewed under UV excitation. The nuclei (N) have an irregular outline and they contain prominent nucleoli (Nl). Pinpoints of fluorescence (arrowhead) are evident. 1 cm scale bar = 9.74μm.

Figure 76. Fluorescent micrograph of an aleurone nucleus of a mature seed, stained with Hoechst dye #33342 and viewed under UV excitation. The nucleus (N) is irregular in outline. Pinpoints of fluorescence (arrowhead) are evident. 1 cm scale bar = 9.74μm.

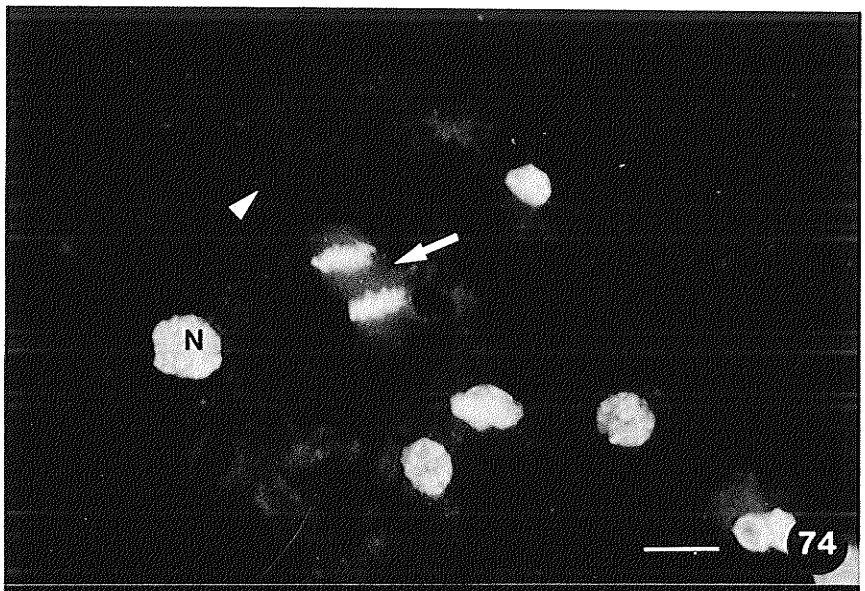
N
74

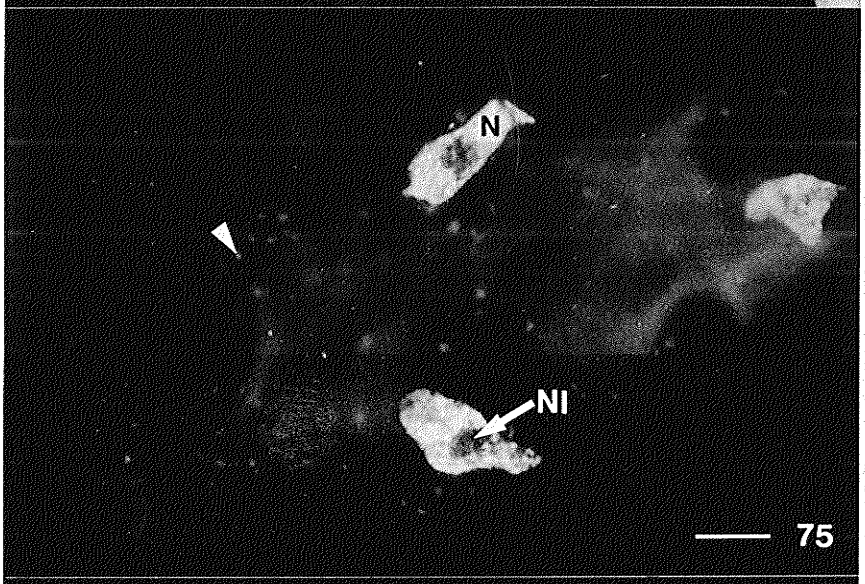
N
NI
75

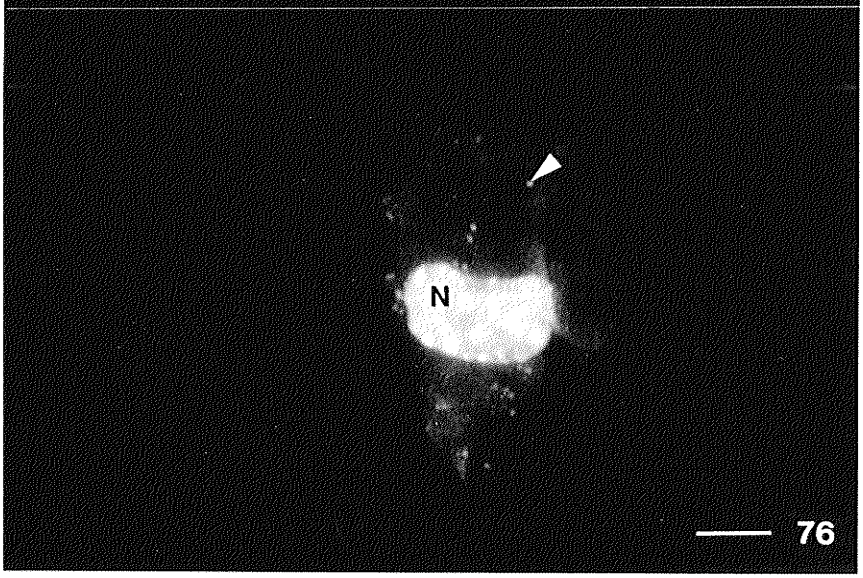
N
76

Figure 77. Comparison of total fluorescence of samples of nuclei. The total fluorescence (relative units) data of diploid (2), triploid (3), and aleurone layer (AL) populations of nuclei is visualized using a box plot. The box is the central 50% of the data and it is bisected at the median value. The vertical bars represent the upper and lower 25% of the data.

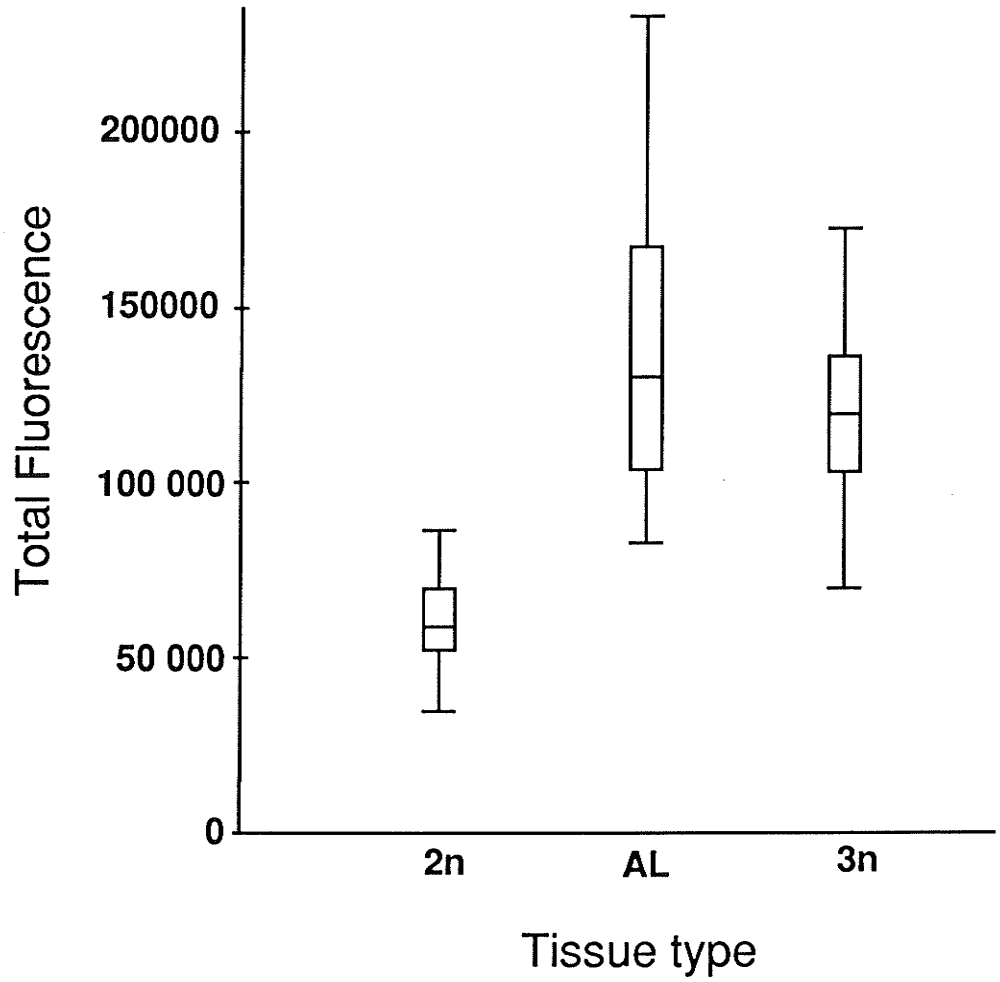
Total Fluorescence
200000
150000
100 000
50 000
0
2n
AL
3n
Tissue type

DISCUSSION

Origin of the aleurone layer

Histology

The histogenetic interpretation of the aleurone layer in *Brassica napus* (canola), an endosperm origin, is contrary to the integumentary origin proposed in *Sinapis alba* by Bergfeld and Schopfer (1986). The free nuclear endosperm in canola does cellularize, and the nascent cellular endosperm contains the biconvex chloroplasts characteristic of the free nuclear endosperm, in contrast to the amyloplasts of the neighbouring inner integument tissue (Fig. 12). As the endosperm accumulates both lipid droplets and starch grains, the innermost cell layer of the inner integument differentiates to the pigment layer, and it serves as a marker for the border between the inner integument and the endosperm (Figs. 18 and 30). The accumulation of starch and lipid in the endosperm is polarized, so that the outermost layer accumulates more starch and lipid than the innermost layer (Fig. 28). By 22 DPP, the polarization is marked enough so that the aleurone layer is distinguishable as the outermost cell layer of the endosperm (Fig. 40).

Cytology

Proof of the endosperm origin of the aleurone layer in canola relies on ploidy as a cytological marker to differentiate endosperm tissue from maternal tissues; e.g., inner integument. The choice of tissues representing standard and unknown ploidies is based on the ease and purity of their isolation. Pure

aleurone tissue (the unknown ploidy) is easily stripped from the testas of mature seeds. The cotyledons of the same seeds provide a source of diploid standard to represent maternal tissues, because pure, living integumentary tissue is difficult to isolate at any age. Pure endosperm tissue, representing the triploid standard, is easily isolated at the free nuclear stage, because it can be withdrawn by a micropipette. Autofluorescence of the cell walls interfered with fluorometric measurement of the nuclei. This necessitated isolation of the nuclei from the cells before staining.

The method of analysis used in this study differs from that of other photometric determinations of DNA levels (Mellerowicz *et al.* 1989, Kamo and Griesbach 1989) because the goal of the experiment is not to quantify the amount of DNA, but to compare amounts of DNA among seed tissues. The quantitative studies require an internal standard, such as chicken erythrocyte nuclei, but this study requires external standards of known ploidy to compare to that of the aleurone. This study also uses computerized image analysis to measure the total staining of the nuclei. This has an advantage over the plug method (Berlyn and Miksche 1976, page 250) because the embryo and aleurone nuclei of mature canola seeds are irregular in shape and some contain prominent nucleoli. The plug method requires homogenously staining nuclei that have a simple geometric shape. Computerized image analysis is much more flexible in this respect because the numerical methods enable both area and total staining to be computed for nuclei of arbitrary shape.

When the results of total fluorescence are graphically compared, the diploid and triploid data are symmetrical about their respective means, but the aleurone data shows an uneven spread in the upper 50 percent (Fig. 77). The upper limit of the aleurone data is almost twice that of the mean of the triploid

standard. This could be an indication of endopolyploid nuclei present in the population of aleurone nuclei. In spite of the asymmetry of the aleurone data, a t-test shows that the total fluorescence of aleurone nuclei is significantly similar to that of the triploid standard, but significantly different from that of the diploid standard; therefore, the aleurone layer is indeed derived from the endosperm (Table 1).

The free endosperm nuclei were ellipsoidal (Fig. 74), but the nuclei of the embryo and of the aleurone from mature seed had irregular shapes (Figs. 75 and 76). The irregular shape of the latter nuclei is probably due to deformation by the densely packed cellular contents. This deformation of the nucleus is visible in electron micrographs of the aleurone layer at 34 DPP (Fig. 62). Since nucleoli contain RNA and protein, in addition to DNA, they fluoresce less intensely than the chromatin of the remainder of the nucleus (Fig. 75). Pinpoints of fluorescence are visible in the cytoplasm among the nuclei, especially in the embryo and aleurone preparations (Figs. 75 and 76). These pinpoints presumably indicate the DNA-containing organelles: chloroplasts and mitochondria.

Aleurone layer development

Organization of the testa

The organization of the developing canola testa is typical of that in most of the Brassicaceae. Bouman (1975) provides a generalized histogenetic interpretation of the strata found in the testa of a mature seed of the Brassicaceae. The four strata are the epidermis, the subepidermis, and the palisade , which constitute the outer integument, and several layers of compressed cells, which

constitute the inner integument. It is important to note that up to 18 DPP, in the developing seed of canola, the inner integument cells are in their original, expanded state. Increase in size of the developing seed occurs mainly by expansion of the adaxial end (Fig. 1). This process of expansion in *Diplotaxis erucoides* seeds is illustrated diagrammatically by Pacini *et al.* (1975).

Cellular configurations of the endosperm

At 14 DPP, free nuclear endosperm lines the inner surface of the testa (Fig. 5). Even though the free nuclear endosperm appears tenuous, it contains motifs of cellular organization. The nuclei are spaced, rather than grouped, and the chloroplasts are arranged around each nucleus in a tangential orientation to the testa (Fig. 5).

The tangential orientation of the chloroplasts does not appear to be controlled by directional illumination as reviewed by Haupt (1982). He observed that, under low illumination, chloroplasts of *Marchantia* orient their broad surface towards the source, but under intense illumination, the profile faces the source. The free nuclear endosperm chloroplasts in canola appear to present their broad surface to the testa throughout the circumference of the embryo sac, rather than to the source of the illumination.

The chloroplast orientation could be controlled by a combination of turgor pressure and microtubular arrays. The microtubular arrays of wheat free nuclear endosperm radiate from the nuclei, and bend parallel with the tonoplast of the embryo sac central vacuole and with the embryo sac wall (Van Lammeren 1988). The pattern of chloroplast orientation in canola closely resembles that of the microtubular arrays described in wheat. Turgor pressure exerted by the central

vacuole compresses the free nuclear endosperm against the embryo sac wall, and probably causes the bending of microtubular arrays observed by Van Lammeren (1988). Free nuclear endosperm in the chalazal cavity is not subjected to this constriction. Indeed, many of the chloroplasts in the chalazal cavity are radially oriented to their respective nuclei. Van Lammeren (1988) states that the microtubular arrays probably stabilize the position of the free nuclei, so that they are regularly spaced, apparently in preparation for cellularization.

Perinuclear organization of plastids has been observed in the free nuclear endosperm of *Capsella* (Schulz and Jensen 1974), and in the central cell of *Alyssum maritimum* (Vijayaraghavan and Prabhakar 1984). Clustering of organelles is also observed during microsporogenesis in many species, but no mechanisms are offered (Rodkiewicz *et al.* 1989). The perinuclear position of the chloroplasts in the free nuclear endosperm of canola could function as the shortest route of energy, building blocks, and reducing power for DNA synthesis and division of free nuclei. The canola chloroplasts could either be "anchored" to the nuclei via microfilaments, or they could be channeled into their relative positions by arrays of microtubules. Fluorescent immunolabelling techniques could be used to visualize such structures.

The vacuolar system that develops around free nuclei about to cellularize may function to counteract the turgor of the embryo sac (Fig. 21). Upon cellularization, the developed turgor pressure appears to cause the inner tangential wall to bulge towards the central vacuole (Fig. 13). The chloroplasts are now oriented radially, rather than tangentially, around the nucleus (Fig. 12), a configuration similar to that of the microtubular arrays observed in nascent cellular wheat endosperm (Van Lammeren 1988). The astroid configuration of the

endosperm cytoplasm is also evident in light micrographs of wheat endosperm (Fineran *et al.* 1982) and in *Capsella* (Raghavan 1986, page 21).

At 18 DPP, the endosperm cytoplasm loses its astroid configuration (Figs. 28 and 30), especially in the outermost cell layer, which will later differentiate to the aleurone layer. This loss of cellular organization may be similar to that in wheat where Van Lammeren (1988) observes that the microtubular arrays of incipient aleurone cells no longer radiate from the nucleus, but they are concentrated in bands associated with the anticlinal walls. Even though the organelles of the incipient canola aleurone layer appear randomly distributed, the nucleus remains in a central position through maturation of the seed (Fig. 70d). The role of microtubules in the cellular configurations of endosperm is interesting, and it could be a subject for a subsequent study in the development of canola seed.

Endosperm nutrition

The presence of chloroplasts, mitochondria, and ribosomes in the free nuclear endosperm indicates a metabolically active state. Since the plastids contain grana and the free nuclear endosperm is visibly green, autotrophy is possible in this tissue, which may contribute more towards its nutrition than from the parent plant via the funiculus. Well-developed chloroplasts were noted in the uninucleate central cell of *Brassica campestris* (Sumner and Van Caeseele 1990) and of *Capsella* (Schulz and Jensen 1973). The central cell of *Capsella* lacked wall ingrowths and it was presumed that nutrition of the central cell was derived largely from autotrophy, rather than from the integuments. Chlorophyll has been measured in the endosperm of other members of the Brassicaceae (Vijayaraghavan and Prabhakar 1984), and in the seed coat (including the

aleurone layer) of *Sinapis alba* (Bergfeld and Schopfer 1986). In the developing seed of *Sinapis alba*, the chlorophyll content increases until the inception of the aleurone layer, after which, it decreases. The increase of chlorophyll in *Sinapis alba* coincides with the proliferation of cellular endosperm in canola. After the inception of the canola aleurone layer, the number of integumentary plastids decreases, and the chloroplasts of the underlying endosperm degenerate, which agrees with the decrease in chlorophyll content in *Sinapis alba*. Finally, the chloroplasts of the aleurone layer are converted to rudimentary plastids in the mature seed (Fig. 72).

Endosperm-embryo relations

It is generally believed that the endosperm functions as a tissue to nourish the developing embryo in exalbuminous seeds, and to nourish the germinating embryo in albuminous seeds. This interpretation is upheld by studies on endosperm development in *Capsella* (Schulz and Jensen 1974) and in *Diplotaxis* (Pacini *et al.* 1975). They view the seeds of these species of the Brassicaceae as strictly exalbuminous because the developing embryo consumes the cellular endosperm, leaving only a micropylar and a chalazal remnant. Canola appears not to be strictly exalbuminous because the endosperm-derived aleurone layer survives in the mature seed. Furthermore, the nutritive function of the endosperm appears able to operate only between 18 and 30 DPP, the period from cessation of endosperm cellularization to the collapse of the endosperm underlying the aleurone layer. Even though the majority of the endosperm cells lyse in advance of the embryo (Fig. 11), the lysed cells contain a minority of endosperm storage reserves. It appears that the amount of endosperm storage reserves from the lysed cells is insufficient to sustain the energy requirement for

embryo expansion; therefore, the majority of energy required may emanate from autotrophy, rather than from endosperm breakdown. The majority of the endosperm reserves are concentrated in the aleurone layer and in the underlying four layers of endosperm, which are resistant to lysis (Fig. 40). Between 22 and 30 DPP the underlying endosperm layers lose most of their storage reserves, but the aleurone layer attains a denser accumulation during the same period (Figs. 47a and 52a); therefore, the embryo and the aleurone layer may compete for the remaining storage reserves of the underlying endosperm, which is eventually crushed. These observations of canola endosperm development cause its nutritive function to be unclear. Incisive physiological experiments would clarify the role of the endosperm during embryo development in exalbuminous seeds, and may elucidate a function of the aleurone layer in the developing canola seed.

Structural features of the free nuclear endosperm

The embryo sac wall during the free nuclear stage pulls away from the inner integument in places (Figs. 3 and 7). This shows that there is a weak bond between the walls of the two tissues, and that the embryo sac wall is quite elastic. Turgor pressure may be important in keeping the embryo sac wall appressed to the inner integument. Slitting the seed for easier penetration of fixative would release this necessary turgor and cause parts of the embryo sac wall to collapse inwards. Indeed, when the seed is slit, a drop of fluid oozes from the cut.

At 14 DPP, the mitochondria of the free nuclear endosperm have saccular cristae and a proportionally small amount of matrix volume (Fig. 7). The matrix is electron dense and neither nucleoid regions nor ribosomes are evident in the sections that were surveyed. This internal organization contrasts with that of earlier stages in *Capsella* (Schulz and Jensen 1974), and of the central cell in

Brassica campestris (Sumner and Van Caeseele 1990). Generally, mitochondria that they observed contain tubular cristae separated from one another by the matrix. In *Capsella*, nucleoid regions are present, as well as mitochondrial ribosomes. Canola mitochondria at 14 DPP probably represent a non-proliferating state. The mitochondria of the inner integument, a tissue about to senesce at this stage, contain the similar arrangement of appressed cristae, reinforcing the idea that they are not proliferating (Fig. 10). Douce (1985, page 13) states that saccular cristae and an electron-dense matrix could represent a state of active respiration. Since the membrane of the crista contains enzymes for oxidative phosphorylation, and the matrix contains enzymes for the citric acid cycle, then the large crista to matrix ratio may also represent an adaptation for operation in low oxygen concentration. This could power anabolic processes in the dark; a time when the chloroplasts are evolving the least amount of oxygen. The significance of the occasional elongate mitochondrion (Fig. 8) is unknown, but it could be an intermediate in the dynamic form of mitochondria. Time-lapse cinematography has revealed that mitochondria move and rapidly change in shape (Alberts *et al.* 1989, page 342).

Mode of endosperm cellularization

The free nuclear endosperm of canola cellularizes centripetally, but in *Diplotaxis* Pacini *et al.* (1975) note that cellularization is centrifugal, proceeding from the tonoplast to the integument and the embryo. In canola, the mode of endosperm celluluarization is similar to the model developed from observations of wheat endosperm cellularization (Fineran *et al.* 1982). In wheat, cellularization begins by partitioning of free nuclei by anticlinal cell walls to form compartments that are open at the embryo sac central vacuole (Fineran *et al.* 1982). The anticlinal

cell walls are formed with a phragmoplaset, as opposed to the free-wall formation theory of Morrison and O'Brien (1976). The endosperm then proliferates by karyokinesis and division of the open compartments by periclinal cell walls (Fineran *et al.* 1982). This first round of division is the earliest stage observed so far in canola and it results in a peripheral cellular layer and an inner layer of open compartments (Fig. 12). A periclinally oriented cell plate is also observed in one of the open compartments (Figs. 13 and 24a). In wheat, the sequential karyokinesis and periclinal division of the inwardly growing compartments continue until opposite compartments meet and seal at the centre of the embryo sac. The compartments in canola seeds do not appear to meet, but leave a central vacuole (Fig. 11). This probably occurs because the canola embryo sac is much larger than that of wheat at the stage of endosperm cellularization. Nascent endosperm cells of both wheat (Fineran *et al.* 1982) and canola (Fig. 12) display an astroid configuration of the cytoplasm. Radial files of cells appear two days after initiation of endosperm cellularization in canola (Fig. 14), and they are probably a result of mitosis in the cellular endosperm (Fig 32b). Fineran *et al.* (1982) also notes mitoses in the peripheral endosperm during later stages of cellularization. These similarities observed between wheat and canola suggest that the nuclear endosperm of both monocots and dicots may share a common mode of cellularization.

Senescence of seed tissues

Part of the development of the canola seed involves the selective senescence and lysis of tissues. Senescence is an active, endogenous process involving the organized loss of normal function, and leading to cell "death" (Noodén 1988, page 6). Lysis is observed in the vacuolate cells of the inner

endosperm (Fig. 11), and senescence is observed in the testa (Figs. 40 and 66a) and in the underlying endosperm cells (Fig. 52a). In the testa, the inner integument is the first tissue to senesce. At 14 DPP, electron microscopy reveals plasmolysis of the inner integument cells (Fig. 10). Plasmolysis is at an advanced state at 18 DPP, and the cells begin to collapse. Except for the pigment layer, which accumulates a lining of electron-opaque material, collapse continues until only the pigment layer and cell wall debris remains (Fig. 47a). The term "pigment layer" for the remnant of the inner integument is a misnomer in canola, because microdissection reveals that the palisade layer imparts the red-brown colour to the seed coat. Edwards (1968) notes that the purple-black colour of the seed coat of *Sinapis arvensis* is found in the palisade layer, but he mentions that the pigment layer also contributes to the colour. The cells of the outer integument do not collapse in canola, but they gradually lose their starch and protoplasmic content, so that they appear empty by 38 DPP (Fig. 66a).

A second disintegration event is the lysis of the vacuolate cells of the inner endosperm in advance of the embryo (Fig. 11). In cereals such as wheat, the nascent, inner endosperm is also quite vacuolate (Evers 1970), but comparatively little of it is invaded by the expanding embryo. These cells in wheat become the starchy endosperm, and are non-living at maturity (Brenchley 1909). The five outermost layers of the canola endosperm appear to contain the majority of the storage reserves, and from 18-22 DPP they are resistant to lysis in advance of the embryo (Figs. 28 and 40). After the inception of the aleurone layer, the underlying endosperm begins to senesce and collapse. Ultrastructure of the underlying endosperm during this stage supports the concept of senescence as an active process (Noodén 1988, page 6) because mitochondria, lipid droplets, starch, and nuclei are still intact (Fig. 48). The first signs of senescence are

plasmolysis, amoeboid nuclei, and flattened chloroplasts that contain electron-translucent globules. The cytoplasm is also less dense than that of the aleurone layer, which may be indicative of fewer ribosomes in the underlying endosperm. A gradient of senescence is observed in the underlying endosperm, with the outer layers showing fewer and less marked signs of senescence than that of the inner layers. At 30 DPP, the cell walls have thickened. At this stage, the outer layers still have nuclei, plastids, mitochondria, and RER. The inner layers lack plastids and nuclei, have less cytoplasm than the outer layers, and they are collapsing (Fig. 53). The RER of the outer layers lack ribosomes in some places, and in other places they are collapsed (Fig. 56). Other signs, noted by Noodén (1988, pages 6-12) as that of senescence, are also present; e.g., whorls of membranous material (Fig. 53), and electron-opaque deposits between the plasmalemma and the cell wall (Fig. 54). These electron-opaque deposits could be a product of membrane lipid breakdown. At 34 DPP the underlying endosperm has collapsed, and little cellular material remains (Fig. 59a).

Meanwhile, the aleurone layer not only survives this neighbouring degeneration, but storage material accumulation becomes denser. Up to 38 DPP, the anticlinal cell walls of the aleurone layer tend to break (Fig. 53). The breakage of the cell walls is not due to fixation in a hypotonic medium because a higher molarity (0.75M) of phosphate buffer did not reduce the problem. The breakage is probably due to handling or by stress from slitting the seed to facilitate penetration of fixative. At 34 DPP, the aleurone layer is one cell layer thick, and is continuous except at the chalazal area and at the suspensor (Figs. 73a and 73b). In the chalazal area it intergrades into a region that is several cell layers thick. The cells in this region appear larger, have thinner cell walls, clearer cytoplasm, and contain flattened plastids rather than dense storage reserves. The aleurone layer

appears to contain a factor that protects it from senescence. One reason for its survival may originate from hormones, because the underlying endosperm displays a gradient of senescence. Senescence appears to proceed from the inner layers towards the outer layers (Fig. 53), and collapse appears to proceed from the adaxial end of the seed towards the abaxial end (Fig. 73a). Another reason for the survival of the aleurone layer could be its action as a competitive sink, so that nutrients are diverted to it rather than to the underlying endosperm; therefore, the underlying endosperm would have a lower net synthesis of essential macromolecules and eventually senesce. A hormone that could account for this behavior of the aleurone is cytokinin. Excised leaves treated with cytokinins exhibit a delayed senescence, and treated areas absorb nutrients from other parts that have less cytokinins (Salisbury and Ross 1992, page 335). Another such candidate could be abscisic acid (ABA). This hormone is normally found in maturing seeds, and it prevents premature germination in the pod (vivipary) and induces storage protein accumulation in embryos (Salisbury and Ross 1992, page 346). In *Sinapis alba* seeds, exogenous ABA reversibly inhibits water uptake during germination (Schopfer *et al.* 1979).

Lipid and starch accumulation

Lipid, and then starch accumulation in the endosperm commences after cellularization. This indicates a shift of energy use from that of tissue proliferation to that of anabolic processes. The mode of lipid droplet formation is unclear from this study, and it is also a topic currently under controversy (Murphy and Cummins 1989). An ultrastructural study by Wanner and Theimer (1978) proposes that the lipid droplets are derived from budding ER vesicles. In canola, the lipid droplets appear in cellularizing endosperm at 16 DPP, but are

naked and show no association with ER, which is sparse at this stage (Figs. 19 and 23). An ultrastructural study of developing *Sinapis alba* embryos by Bergfeld *et al.* (1978) proposes a cytoplasmic origin of lipid droplets, that later become associated with RER cisternae during "osmiophilic coat" formation. The lipid droplet synthesis in canola does appear to be cytoplasmic, but subsequent association with RER is not observed. Instead, at 18 DPP, profiles of RER are associated with the chloroplasts (Fig. 34), and electron-dense particles are associated with the lipid droplets (Fig. 35). The particles that encircle the lipid droplets are composed of multiple subunits, but it is unknown whether they are either polysomes or multienzyme assemblies. Fatty acids are known to be synthesized in the chloroplast (Bewley and Black, 1985, pages 45-48); therefore, a hypothetical pathway of lipid droplet formation consistent with the observations in canola would be the synthesis of diacylglycerols from chloroplast fatty acids by the RER that surrounds the chloroplasts, triacylglycerol synthesis by the particles that encircle the lipid droplets, and then incorporation of triacylglycerols into the lipid droplets themselves. Murphy (1988) showed that diacylglycerol acyl-transferease activity was present in the lipid body fraction of developing canola seed; therefore, this pathway could operate in canola.

The aleurone layer is demarcated at 22 DPP by the greater concentration of lipid droplets (Fig. 41a) and the lesser amount of starch per chloroplast (Fig. 42a), than that of the underlying endosperm. The smaller amount of starch in the aleurone layer may reflect the role of the chloroplasts in the synthesis of the acyl components of triacylglycerols, the major component of lipid droplets (Bewley and Black 1985, pages 15-17). The particles that encircle the lipid droplets persist until 34 DPP, the stage of greatest concentration of lipid in the aleurone cells (Fig. 59d). At 34 DPP, the lipid droplets have an electron-dense coat, similar to the

osmiophilic coat reported by Bergfeld *et al* (1978) (Fig. 64). The mode of loss of the particles that encircle the lipid droplets and that of the gain of the electron dense coat is unknown. The protein of this coat, oleosin, has been isolated and it is believed to be responsible for the stable emulsification of large lipid droplets into the small lipid droplets of the mature seed (Murphy and Cummins 1989). In canola, the lipid droplets of the aleurone become smaller between 34 DPP and the mature state, but some aleurone cells of the mature state contain giant central lipid droplets (Fig. 73).

Protein body deposition

The aleurone cells of the mature canola seed do not contain any starch, but they do contain lipid droplets and protein bodies. Membrane-bound protein bodies are not evident until 34 DPP, late in the development of the aleurone cells (Fig. 60). At 18 DPP, vacuoles are visible that contain an electron-opaque, astroid inclusion (Fig. 36), but at 22 DPP they are absent. The mode of formation of the inclusions is unknown, but electron micrographs suggest that they may originate from coalesced dictyosome vacuoles (Fig. 37) or from particles associated with the tonoplast (Fig. 38). These vacuoles appear similar to the initial stage of protein body development in cereals, where inclusions of electron-opaque phytin is deposited into vacuoles prior to deposition of the protein matrix (Peterson *et al.* 1985), but their disappearance in canola endosperm negates their role in protein body formation. In *Diplotaxis*, Pacini *et al.* (1975) noted astroid inclusions in the degenerating nucellus, and they were attributed to lysosomes. These inclusions are also found in the pigment layer of canola at 18 DPP (Fig 39), but they probably contribute to the formation of the electron-opaque grains, visible at 22 DPP (Fig. 45), rather than to degeneration of the cells. The electron-opaque grains

of the pigment layer may be composed of myrosin because they resemble those of the myrosin cells in the cotyledon of mature *Sinapis alba* seeds (Rest and Vaughan 1972).

The protein bodies of mature canola aleurone cells are simpler than the aleurone grains of the Gramineae aleurone, which have two types of inclusions: phytin globoids, and protein crystalloids (Jacobsen *et al.* 1971). In canola, the protein bodies contain an electron-dense, granular matrix, and some contain electron-opaque and electron-lucent inclusions (Fig. 71). The electron-opaque inclusions are irregular in section, but the inclusions of cereal protein bodies are round in section. There are aleurone grains in *Sinapis alba*, but they contain many globoids (Rest and Vaughan, 1972). The electron-lucent inclusions have an indistinct outline, which is unlike the globoid cavities of cereal protein bodies (Peterson *et al.* 1985) and of *Sinapis alba* cotyledon protein bodies (Bergfeld *et al.* 1980). The development of aleurone protein bodies in canola is rapid. They are absent at 30 DPP, but present at 34 DPP. Lipid may be utilized in the synthesis of protein bodies because lipid and protein staining reveal that the protein content appears to increase at the expense of the lipid (compare Figs. 59b and 59d, 66d and 66e, and 70c and 70d). The mechanism of protein body formation was not studied in canola, but, like the protein bodies of cereal aleurone, they are bounded by a unit membrane, and at maturity each is surrounded by a layer of lipid droplets (Morrison *et al.* 1975).

Conclusion

Definition of the aleurone layer

The aleurone layer of canola resembles that of the archetype in the Gramineae in the majority of possible aspects. These similarities are reflected in histogenesis, location, storage reserves, cell wall thickening, and intracellular organization and configuration. Most of the differences are of minor detail, such as the presence of simple protein bodies in canola, rather than aleurone grains, and the lack of clearly defined plasmodesmata in the mature canola seed. There is one major difference: that the canola seed is more or less exalbuminous; therefore, it cannot share with the Gramineae the major function of endosperm digestion. The problem of classification of this tissue in canola reduces to whether one maintains a functional definition, or a structural definition of an aleurone layer. An anatomist would choose a structural definition with functional subtypes. Thus, an aleurone layer is the outermost, specialized and living layer of the endosperm, a definition echoed by other researchers (Bergfeld and Schopfer 1986; Reid and Meier 1972). Its structural specialization presumes that it has a particular function different from that of the underlying endosperm. An aleurone layer is present when this definition is applied to canola.

Function

An aleurone layer of a functional subtype different from that in the Gramineae is present in canola seeds. The aleurone layer in the Brassicaceae must have a function during germination because Bergfeld and Schopfer (1986) report that the aleurone layer of *Sinapis alba* resumes metabolic activity during this period. Even though the aleurone resembles storage tissue, it probably does not

provide nutrients, hormones, or other factors necessary for growth of the seedling. Edwards (1968) reports that excised seeds of the Brassicaceae can germinate under many conditions, and Bergfeld and Schopfer (1986) discount a nutritive function because the cotyledons contain sufficient storage reserves. A clearer understanding of the aleurone layer would likely be obtained from observations of its chemical and physiological properties. The aleurone layer could secrete antimicrobial agents that protect the seedling as it emerges from the soil. Two other possible functions in this respect are mentioned by Edwards (1968) and by Bergfeld and Schopfer (1986). Firstly, the metabolic activity of the aleurone layer may be very high and control germination by affinity for oxygen, a function investigated in rice aleurone layer by Roberts (1964). Secondly, the aleurone layer could control water uptake or leakage by the embryo, a function investigated in the *Avena fatua* aleurone layer by Raju and Walther (1988).

Further studies

The results of this study provide many opportunities for research in canola seed development and germination. A detailed EM investigation of the canola aleurone layer during germination is a direct follow up to this study. This may uncover signs of secretion such as stacked ER radiating from the nucleus towards the cell wall and dissolution of the cell wall matrix (Jones 1969a; Jones 1969b; Jones and Price 1970). Experiments ought to be undertaken in canola to determine the function(s) of the aleurone layer during germination. During development, elucidation of the pathways of endosperm and embryo nutrition and possible interdependencies could clarify the enigmatic nature of the exalbuminous state in seeds. How the aleurone layer is able to survive intact, while the underlying endosperm lyses and degenerates is an interesting problem.

Finally, the living aleurone layer of canola, an easily isolable tissue, could be cultured for regeneration of triploid plants, or for physiological experiments on endosperm.

Critique of previous research

The aleurone layer lies appressed to the inner face of the testa, but it is not derived from it. Contrary to the most recent histogenetic study of the Brassicaceae aleurone layer (Bergfeld and Schopfer 1986), the series of developmental events observed in this study implies an endospermal origin of the aleurone layer (Table 2). Measurement of nuclear DNA proves this indication by showing that the aleurone layer has about the same amount of nuclear DNA as that of the free nuclear endosperm, but it has significantly more nuclear DNA than embryo nuclei (Fig. 77).

In this study, the free nuclear endosperm cellularized and began to accumulate starch and lipid. The cells of the inner integument plasmolyzed and gradually collapsed, except for the pigment layer. The aleurone layer was discernible as the outermost layer of the endosperm by 22 DPP. After the inception of the aleurone layer, the cells of the underlying endosperm tissue plasmolyzed and gradually collapsed.

A similar study in *Sinapis alba*, by Bergfeld and Schopfer (1986), arrived at an integumentary origin of the aleurone layer. The free nuclear endosperm never cellularized, and it disappeared within about three weeks after pollination. Concomitantly, the outermost and the innermost few cell layers of the inner integument collapsed, leaving a few middle cell layers intact. The middle layers of the inner integument developed thick walls, and by 14 DPP, the outermost

layer was recognized as the aleurone layer. The thick-walled cells underlying the aleurone layer lost their cellular contents and became crushed by the embryo.

Table 2. Chronology of major events during the histogenesis of the aleurone layer.

Age (DPP)	*Brassica napus*	*Sinapis alba* *	Age (DPP)
14	Free nuclear endosperm.	Nucellus nearly dissolved.	7
16	Endosperm cellularization; lipid and starch accumulates.		
22	Aleurone layer discernible.	Aleurone layer discernible.	14
		Inner layers of inner integument collapsed.	16
30	Endosperm cell walls thicken. Starch absent from testa. Inner integument collapsed, except for pigment layer.	Inner integument middle layer cell walls thicken. Outer layers of inner integument collapsed. Endosperm absent.	21
34	Protein bodies in aleurone. Underlying endosperm crushed.	Protein bodies in aleurone. Underlying thick-walled cells crushed.	28
38	Near-mature aleurone layer.	Near-mature seed.	40
56	Mature aleurone layer.	Mature seed.	50

*Data from Bergfeld and Schopfer (1986).

Assuming that the histogenesis of the aleurone layer in *Sinapis alba* and in canola are similar, it seems likely that Bergfeld and Schopfer (1986) have mistaken the identity of certain cell layers in the stages of development they observed. A comparison of their photographs to that of this study reveals these possible misinterpretations. Their photographs at 14 DPP and at 21 DPP correspond in canola to the stage of inner integument collapse (Fig. 28) and the

stage of aleurone cell wall thickening (Fig. 52a), respectively. Also, what they describe as the lysing of "the inner epidermis of the inner integument and the adjacent 5-7 cell layers" resembles the lysing of the innermost layers of the endosperm in this study. These cells are highly vacuolate, and they appear to dissolve in advance of the embryo (Fig. 11). What they describe as the collapsing of the "outer epidermis of the inner integument and the adjacent 1-2 cell layers" resembles the collapsing of the cells of the inner integument at 18 DPP (Fig. 28). The tissue they describe as the "thick-walled layer" distinctly resembles the endosperm underlying the aleurone layer at 30 DPP (Fig. 52a). The difficulty in identifying tissue types by visual examination alone is probably the reason for the differing histogenetic interpretations of the aleurone layer in this study and in that of Bergfeld and Schopfer (1986).

Other researchers have presumed a nucellar origin of the aleurone layer (Thompson 1933), but this view is discredited. The nucellus cannot be a likely candidate as a progenitor of the aleurone layer because it rapidly disintegrates following fertilization in developing seeds of the Brassicaceae (Pacini *et al.* 1975; Bergfeld and Schopfer 1986). Thompson (1933) implies, through his camera lucidas, that the aleurone layer is a remnant of the nucellus, but he was probably not aware of its significance, because the layer is labeled nucellus, rather than aleurone. Because of this designation of the aleurone layer, he also reports that the cabbage seed lacks endosperm at maturity. Edwards (1968), though he states that the free nuclear endosperm absorbs the adjacent nucellus soon after fertilization, mistakenly describes the outer nucellus as continuing to divide with the embryo until it is crushed at maturity. It is obvious that what is identified as the nucellus in one photo is the inner integument minus its outermost layer of large parenchyma cells.

The original study of testa development in the Brassicaceae (Guignard 1893) reports that the aleurone layer is endospermal; therefore, this investigation brings the controversy a full circle to rest on the endosperm once again. In the introduction to his work, he not only stresses the importance of studying the tissues of the seed as a whole, but also to follow the full course of development from fertilization to maturity. The comment is well grounded, but, in addition, for histogenetic studies, developing seeds should be harvested every day (Brenchley 1909) since some histological events occur rapidly. For example, the cellularization and expansion of the endosperm in canola appears to take only two days. In fact, the initial stage of anticlinal wall formation in endosperm cellularization had been missed because harvests were two days apart. The aforementioned researchers who had mistaken the identity of certain tissues harvested developing seeds once each week; a flaw that can be corrected by daily harvests.

REFERENCES

Alberts, B., Bray, D., Lewis, J, Raff, M., Roberts, K., and Watson, J.D. 1989. Molecular biology of the cell, 2nd ed. Garland Publishing, Inc., New York.

Arndt-Jovin, D.J. and Jovin, T.M. 1989. Fluorescence labeling and microscopy of DNA. *In* Methods in cell biology vol. 30. *Edited by* D.L. Taylor and Y. Wang. Academic Press, Inc., San Diego.

Ashford, A.E., Allaway, W.G., and McCully, M.E. 1972. Low temperature embedding in glycol methacrylate for enzyme histochemistry in plant and animal tissues. J. Histochem. Cytochem. **20**:986-990.

Bates, L.S., Bender, M., and Jackson, W. 1981. Eastern gama grass. Seed structure and protein quality. Cereal Chem. **58**:138-141.

Bechtel, D.B. and Pomeranz, Y. 1977. Ultrastructure of the mature ungerminated rice (*Oryza sativa*) caryopsis. The caryopsis coat and the aleurone cell. Am. J. Bot. **64**:966.

Bechtel, D.B. and Pomeranz, Y. 1981. Ultrastructure and cytochemistry of mature oat (*Avena sativa* L.) endosperm. The aleurone layer and starchy endosperm. Cereal Chem. **58**:61-69.

Bergfeld, R., Hong, Y.N., Kühnl, T., and Schopfer, P. 1978. Formation of oleosomes (storage lipid bodies) during embryogenesis and their breakdown during seedling development in cotyledons of *Sinapis alba* L. Planta **143**:297-307.

Bergfeld, R., Kühnl, T., and Schopfer, P. 1980. Formation of protein storage bodies during embryogenesis in cotyledons of *Sinapis alba* L. Planta **148**:146-156.

Bergfeld, R. and Schopfer, P. 1986. Differentiation of a functional aleurone layer within the seed coat of *Sinapis alba* L. Ann. Bot. **57**:25-33.

Berlyn, G.P. and Miksche, J.P. 1976. Botanical microtechnique and cytochemistry. The Iowa State University Press, Ames, Iowa.

Bewley, J.D. and Black, M. 1978. Physiology and biochemistry of seeds in relation to germination. Vol. 1: Development, germination, and growth. Springer-Verlag, New York.

Bewley, J.D. and Black, M. 1985. Seeds: physiology of development and germination. Plenum Press, New York.

Bouman, F. 1975. Integument initiation and testa development in some Cruciferae. Bot. J. Linn. Soc. **70**:213-229.

Bradbury, S.J. 1989. Micrometry and image analysis. *In* Light microscopy in biology: a practical approach. *Edited by* A.J. Lacey. *Series* The practical approach series. *Series edited by* D. Rickwood and B.D. Hames. IRL Press, New York.

Brenchley, W.E. 1909. On the strength and development of the grain of wheat (*Triticum vulgare*). Ann. Bot. **23**:117-142.

Buckhout, T.J., Gripshover, B.M., and Morré, D.J. 1981. Endoplasmic reticulum formation during germination of wheat seeds. Plant Physiol. **68**:1319-1322.

Coutos-Thevenot, P, Jouanneau, J.P., Brown, S., Petiard, V., and Guern, J. 1990. Embryogenic and non-embryogenic cell lines of *Daucus carota* cloned from meristematic cell clusters: relation with cell ploidy determined by flow cytometry. Plant Cell Reports **8**:605-608.

Cutter, E.G. 1978. Plant anatomy: Part 1: Cells and tissues, 2nd ed. Edward Arnold Ltd., London.

Douce, R. 1985. Mitochondria in higher plants. Structure, function, and biogenesis. Academic Press, Inc., Toronto.

Edwards, M.M. 1968. Dormancy in seeds of charlock. I. Developmental anatomy of the seed. J. Exp. Bot. **19**:575-582.

Esau, K 1977. Anatomy of seed plants, 2nd ed. John Wiley and Sons, Inc., New York.

Evers, A.D. 1970. Development of the endosperm of wheat. Ann. Bot. **34**:547-555.

Fineran, B.A., Wild, D.J.C., and Ingerfeld, M. 1982. Initial wall formation in the endosperm of wheat, *Triticum aestivum*: a reevaluation. Can. J. Bot. **60**:1776-1795.

Fulcher, R.G., O'Brien, T.P., and Lee J.W. 1972. Studies on the aleurone layer. I. Conventional and fluorescence microscopy of the cell wall with emphasis on phenol-carbohydrate complexes in wheat. Aust. J. Biol. Sci. **25**:23-34.

Gahan, P.B. 1984. Plant histochemistry and cytochemistry. An introduction. Experimental botany series vol. 18. *Edited by* J.F. Sutcliffe and J. Cronshaw. Academic Press, Toronto.

Gerhardt, P., Murray, R.G.E., Costilow, R.N., Wood, W.A., Krieg, N.R., and Phillips, G.B. 1981. Manual of methods for general bacteriology. American Society for Microbiology, Washington, D.C.

Guignard, L. 1893. Recherches sur la développement de la graine et en particulier du tégument séminal. J. Bot., Paris **7**:1-14, 21-34.

Haupt, W. 1982. Light-mediated movement of chloroplasts. Ann. Rev. Plant Physiol. **33**:205-233.

Jacobsen, J.V., Knox, R.B., and Phyliotis, N.A. 1971. The structure and composition of aleurone grains in the barley aleurone layer. Planta **101**:189-209.

Jones, R.L. 1969a. Gibberellic acid and the fine structure of barley aleurone cells. I. Changes during the lag-phase of alpha-amylase synthesis. Planta **87**:119-133.

Jones, R.L. 1969b. Gibberellic acid and the fine structure of barley aleurone cells. II. Changes during the synthesis and secretion of alpha-amylase. Planta 88:73-86.

Jones, R.L. and Price, J.M. 1970. Gibberellic acid and the fine structure of barley aleurone cells. III. Vacuolation of the aleurone cell during the phase of ribonuclease. Planta **94**:191-202.

Jones, S.B. and Luchsinger, A.E. 1986. Plant systematics. McGraw-Hill Book Company, Toronto.

Kamo, K.K. and Griesbach, R.J. 1989. Determination of ploidy level in "Mitchell" *Petunias*. Plant Sci. **65**:119-124.

Laguna-Hernandez, G., Marquez-Guzman, J., and Engleman, E.M. 1984. Ultrastructure of the aleurone cells of mature seeds of Turbina corymbosa (Convolvulaceae). J. Plant Anat. Morph. **1**:39-44.

Leica. 1992. Quantimet 500 image processing and analysis system. Leica Cambridge Ltd., Cambridge.

Lyshede, O.P. 1984. Seed structure and germination in Cuscuta pedicellata with some notes on C. campestris. Nordic Journal of Botany **4**:660-674.

Márquez-Guzmán, J. and Laguna-Hernández, G. 1982. Anatomía de la semilla y germinación de *Turbina corymbosa* (L.) Raf., Convolvulaceae. Phyton **42**:1-8.

Mellerowicz, E.J., Riding, R.T., and Little, C.H.A. 1989. Genomic variability in the vascular cambium of *Abies balsamea*. Can. J. Bot. **67**:990-996.

Morrison, I.N., Kuo, J, and O'Brien, T.P. 1975. Histochemistry and fine structure of developing wheat aleurone cells. Planta **123**:105-116.

Morrison, I.N. and O'Brien, T.P. 1976. Cytokinesis in the developing wheat grain; division with and without a phragmoplast. Planta **130**:57-67.

Murphy, D.J. 1988. A highly active soluble diacylglycerol synthesizing system from developing rapeseed, *Brassica napus* L. Lipids **23**:157-163.

Murphy, D.J. and Cummins, I. 1989. Seed oil-bodies: isolation composition and role of oil-body apolipoproteins. Phytochem. **28**:2063-2069.

Netolitzky, F. 1926. Anatomie der angiospermen-samen. Handbuch der pflanzenanatomie, Band 10. *Edited by* K. Linsbauer. Gebrüder Borntraeger, Berlin.

Noodén, L.D. 1988. The phenomena of senescence and aging. *In* Senescence and aging in plants. *Edited by* L.D. Noodén and A.C. Leopold. Academic Press Inc., New York.

Obata, T. 1979. Fine structural changes in barley aleurone cells during gibberelic acid-induced enzyme secretion. Ann. Bot. **44**:333-337.

O'Brien, T.P. and McCully, M.E. 1981. The study of plant structure. Principles and selected methods. Termarcarphi Pty. Ltd., Melbourne.

Ogawa, M., Tanaka, K., and Kasai, Z. 1979. Accumulation of phosphorous, magnesium, and potassium in developing rice grains: followed by electron microprobe X-ray analysis focusing on the aleurone layer. Plant and Cell Physiol. **20**:19-27.

Oparka, K.J. and Gates, P. 1981. Transport of assimilates in the developing caryopsis of rice (Oryza sativa L.). Ultrastructure of the pericarp vascular bundle and its connections with the aleurone layer. Planta **151**:561-573.

Pacini, E., Simoncioli, C., and Cresti, M. 1975. Ultrastructure of nucellus and endosperm of *Diplotaxis erucoides* during embryogenesis. Caryologia **28**:525-538.

Peterson, D.M., Saigo, R.H., and Holy, J. 1985. Development of oat aleurone cells and their protein bodies. Cereal Chem. **62**:366-371.

Raghavan, V. 1986. Embryogenesis in angiosperms. A developmental and experimental study. Ser. 17, Developmental and cell biology series. *Edited by* P.W. Barlow, P.B. Green, and C.C. Wylie. Cambridge University Press, New York.

Raju, M.V.S., and Walther, A. 1988. Heterogeneity and behavior of aleurone cells in the caryopsis of wild oats (*Avena fatua*). Flora **180**:417-427.

Randolph, L.F. 1936. Developmental morphology of the caryopsis in maize. J. Agric. Res. **53**:881-916.

Reid, J.S.G. and Meier, H. 1972. The function of the aleurone layer during galactomannan mobilization in germinating seeds of fenugreek (*Trigonella foenum-graecum* L.), crimson clover (*Trifolium incarnatum* L.), and lucerne (*Medicago sativa* L.): a correlative biochemical and ultrastructural study. Planta **106**:44-60.

Reid, J.S.G. and Meier, H. 1973. Enzymic activities and galactomannan mobilization in germinating seeds of fenugreek (*Trigonella foenum-graecum* L., Leguminosae). Secretion of alpha-galactosidase and beta-mannosidase by the aleurone layer. Planta **112**:301-308.

Rest, J.A. and Vaughan, J.G. 1972. The development of protein and oil bodies in the seed of Sinapis alba L. Planta **105**:245-262.

Reynolds, E.S. 1963. The use of lead citrate at high pH as an electron opaque stain in electron microscopy. J. Cell Biol. **17**:208-212.

Roberts, E.H. 1964. The distribution of oxidation-reduction enzymes and the effects of respiratory inhibitors and oxidising agents on dormancy in rice seed. Phys. Plant. **17**:14-29.

Rodkiewicz, B., Duda, E., and Bednara, J. 1989. Organelle aggregations during microsporogenesis in Nymphaea. Flora **183**:397-404.

Salisbury, F.B. and Ross, C.W. 1985. Plant physiology, 3rd ed. Wadsworth Publishing Company, Belmont, CA.

Schopfer, P., Bajracharya, D., and Plachy, C. 1979. Control of seed germination by abscisic acid. I. Time course of action in *Sinapis alba* L. Plant Physiol. **64**:822-827.

Schultz, S.R. and Jensen, W.A. 1973. *Capsella* embryogenesis: The central cell. J. Cell Sci. **12**:741-763.

Schultz, S.R. and Jensen, W.A. 1974. *Capsella* embryogenesis: the development of the free nuclear endosperm. Protoplasma 80:183-205.

Silcock, D.J., Francis, D., Bryant, J.A., and Hughes, S.G. 1990. Changes in nuclear DNA content, cell and nuclear size, and frequency of cell division in the cotyledons of *Brassica napus* L. during embryogenesis. J. Exp. Bot. **41**:401-407.

Sumner, M.J. and Van Caeseele, L.A. 1990. The development of the central cell of *Brassica campestris* prior to fertilization. Can. J. Bot. 68:2553-2563.

Thompson, R.C. 1933. A morphological study of flower and seed development in cabbage. J. Agric. Res. **47**:215-232.

Van Lammeren, A.A.M. 1988. Structure and function of the microtubular cytoskeleton during endosperm development in wheat: an immunofluorescence study. Protoplasma **146**:18-27.

Vaughan, J.G. 1970. The structure and utilization of oil seeds. Chapman and Hall, London.

Vijayaraghavan, M.R. and Prabhakar, K. 1984. The endosperm. *In* Embryology of angiosperms. *Edited by* B.M. Johri. Springer Verlag, New York.

Wanner, G. and Theimer, R.R. 1978. Membranous appendices of spherosomes (oleosomes). Possible role in fat utilization in germinating oil seeds. Planta **140**:163-169.

Werker, E. and Vaughan J.G. 1974. Anatomical and ultrastructural changes in aleurone and myrosin cells of *Sinapis alba* during germination. Planta **116**:243-255.